

**DEVELOPMENT OF BETA-TRICALCIUM PHOSPHATE
BASED INJECTABLE SYNTHETIC BONE GRAFT
MATERIALS**

**BETA-TRİKALSİYUM FOSFAT BAZLI ENJEKTE
EDİLEBİLİR SENTETİK KEMİK GREFT
MATERYALLERİNİN GELİŞTİRİLMESİ**

DENİZ SARP

ASSOC. PROF. HALİL MURAT AYDIN
Supervisor

Submitted to Graduate School of Science and Engineering of Hacettepe University
as a Partial Fulfillment to the Requirements for the Award of the Master of Science
in Bioengineering

2018

This work named " **Development of Beta-Tricalcium Phosphate Based Injectable Synthetic Bone Graft Materials**" by **DENİZ SARP** has been approved as a thesis for the Degree of **MASTER OF SCIENCE IN BIONEENGINEERING** by the below mentioned Examining Committee Members.

Assoc. Prof. Dr. Sedat ODABAŞ
Head



Assoc. Prof. Dr. Halil Murat AYDIN
Supervisor



Assoc. Prof. Dr. Eda Ayşe AKSOY
Member



Assoc. Prof. Dr. Murat BARSBAY
Member



Assist. Prof. Dr. Batur ERCAN
Member



This thesis has been approved as a thesis for the Degree of **MASTER OF SCIENCE IN BIONEENGINEERING** by Board of Directors of the Institute for Graduate School of Science and Engineering.

Prof. Dr. Menemşe GÜMÜŞDERELİOĞLU
Director of the Institute of
Graduate School of Science and Engineering

To you...

YAYINLAMA VE FİKRİ MÜLKİYET HAKLARI BEYANI

Enstitü tarafından onaylanan lisansüstü tezimin tamamını veya herhangi bir kısmını, basılı (kağıt) ve elektronik formatta arşivleme ve aşağıda verilen koşullarla kullanıma açma iznini Hacettepe Üniversitesine verdiğimi bildiririm. Bu izinle Üniversiteye verilen kullanım hakları dışındaki tüm fikri mülkiyet haklarım bende kalacak, tezimin tamamının ya da bir bölümünün gelecekteki çalışmalarda (makale, kitap, lisans ve patent vb.) kullanım hakları bana ait olacaktır.

Tezin kendi orijinal çalışmam olduğunu, başkalarının haklarını ihlal etmediğimi ve tezimin tek yetkili sahibi olduğumu beyan ve taahhüt ederim. Tezimde yer alan telif hakkı bulunan ve sahiplerinden yazılı izin alınarak kullanılması zorunlu metinlerin yazılı izin alınarak kullandığımı ve istenildiğinde suretlerini Üniversiteye teslim etmeyi taahhüt ederim.

Yükseköğretim Kurulu tarafından yayınlanan “**Lisansüstü Tezlerin Elektronik Ortamda Toplanması, Düzenlenmesi ve Erişime Açılmasına İlişkin Yönerge**” kapsamında tezim aşağıda belirtilen koşullar haricinde YÖK Ulusal Tez Merkezi / H. Ü. Kütüphaneleri Açık Erişim Sisteminde erişime açılır.

- o Enstitü / Fakülte yönetim kurulu kararı ile tezimin erişime açılması mezuniyet tarihinden itibaren 2 yıl ertelenmiştir. ⁽¹⁾
- o Enstitü / Fakülte yönetim kurulunun gerekçeli kararı ile tezimin erişime açılması mezuniyet tarihinden itibaren Ay ertelenmiştir. ⁽²⁾
- o Tezimle ilgili gizlilik kararı verilmiştir. ⁽³⁾

06 /09/2018


Deniz SARP

“Lisansüstü Tezlerin Elektronik Ortamda Toplanması, Düzenlenmesi ve Erişime Açılmasına İlişkin Yönerge”

- (1) Madde 6. 1. Lisansüstü teze ilgili patent başvurusu yapılması veya patent alma sürecinin devam etmesi durumunda, tez danışmanının önerisi ve enstitü anabilim dalının uygun görüşü üzerine enstitü veya fakülte yönetim kurulu iki yıl süre ile tezin erişime açılmasının ertelenmesine karar verebilir
- (2) Madde 6. 2. Yeni teknik, materyal ve metodların kullanıldığı, henüz makaleye dönüşmemiş veya patent gibi yöntemlerle korunmamış ve internetten paylaşılması durumunda 3. Şahıslara veya kurumlara haksız kazanç imkanı oluşturabilecek bilgi ve bulguları içeren tezler hakkında tez danışmanının önerisi ve enstitü anabilim dalının uygun görüşü üzerine enstitü ve fakülte yönetim kurulunun gerekçeli kararı ile altı ayı aşmamak üzere tezin erişime açılması engellenebilir.
- (3) Madde 7. 1. Ulusal çıkarları veya güvenliği ilgilendiren, emniyet, istihbarat, savunma ve güvenlik, sağlık vb. konulara ilişkin lisansüstü tezlerle ilgili gizlilik kararı, tezin yapıldığı kurum tarafından verilir*. Kurum ve kuruluşlarla yapılan işbirliği protokolü çerçevesinde hazırlanan lisansüstü tezlere ilişkin gizlilik kararı ise, ilgili kurum ve kuruluşun önerisi ile enstitü veya fakültenin uygun görüşü üzerine üniversite yönetim kurulu tarafından verilir. Gizlilik kararı verilen tezler Yükseköğretim Kuruluna bildirilir.
Madde 7. 2. Gizlilik kararı verilen tezler gizlilik süresince enstitü veya fakülte tarafından gizlilik kuralları çerçevesinde muhafaza edilir, gizlilik kararının kaldırılması halinde Tez Otomasyon Sistemine yüklenir.

* Tez danışmanının önerisi ve enstitü anabilim dalının uygun görüşü üzerine enstitü veya fakülte yönetim kurulu tarafından karar verilir.

ETHICS

In this thesis study, prepared in accordance with the spelling rules of Institute of Graduate Studies in Science of Hacettepe University,

I declare that

- all the information and documents have been obtained in the base of the academic rules
- all audio-visual and written information and results have been presented according to the rules of scientific ethics
- in case of using other Works, related studies have been cited in accordance with the scientific standards
- all cited studies have been fully referenced
- I did not do any distortion in the data set
- and any part of this thesis has not been presented as another thesis study at this or any other university.

06/08/2018


Deniz Sarp

ÖZET

BETA-TRİKALSİYUM FOSFAT BAZLI ENJEKTE EDİLEBİLİR SENTETİK KEMİK GREFT MATERYALLERİNİN GELİŞTİRİLMESİ

Deniz SARP

Master, Biyomühendislik Bölümü

Danışman: Doç. Dr. Halil Murat AYDIN

Eylül 2018, 149 sayfa

Dünyanın yaşlanan nüfusu ile birlikte travma, dejeneratif hastalıklar veya cerrahi müdahale sonucu kemik dokusu kaybı ile karşılaşan hasta sayısı da artmaktadır. Kemik doku malzemelerine olan talebi karşılamak adına sentetik kemik malzemeleri üretilmiştir. Kritik-boyutlu veya zorlu şekillerden oluşan kemik defektleri karşısında enjekte edilebilir kemik greftleri, halihazırda sunulan blok veya granül tipi malzemelerden daha fazla kullanılabilirlik sunmaktadırlar. Set etmeyen enjekte edilebilir sentetik kemik malzemeleri yük taşımayan bölgelerde ('puti'ler) kemik dolgusu görevi görürler. Enjekte edilebilir kemik malzemeleri ortopedi, kozmetik, rekonstrüktif veya dental cerrahisi gibi birçok tıbbi alanda kullanılmaktadırlar. Klinikte başarılı olacak enjekte edilebilir sentetik kemik malzemesi kolayca kullanılan ve uygulanan, kemiği uyaran, erken bozunmayan, standartlaştırılmış kaliteye sahip, sterilize edilebilen ve makul raf ömrü olan bir malzemedir. Bu çalışmanın amacı, poli(etilen glikol)-gliserol içerisine karışacak β -trikalsiyum fosfat

(β -TCP)-biyoaktif cam partiküllerinden oluşan ideal enjekte edilebilir sentetik kemik greft oluşturmaktır. Kızılötesi (IR) Absorbans Spektroskopisi ile sterilizasyonda kullanılan gama ışımalarının (25 kGy) malzemenin kimyasal yapısını etkilemediği görülmüştür. Taramalı elektron mikroskobu (SEM) ve bilgisayarlı tomografi (mikro-CT) analizleri ile malzemelerde homojen faz dağılımı görülmüştür. Malzeme kompozisyonunun termal davranışı üzerindeki etkisini izlemek için termogravimetrik analiz kullanılmış, 1:1 ve 2:3 taşıyıcı:seramik oranlarında hazırlanan malzemelerde yaklaşık %50 ağırlık kaybı kaydedilmiştir. Yine kompozisyon ve gama ışınması ile sterilizasyonun malzemenin reolojik özellikleri üzerindeki etkisi araştırılmıştır. Numuneler, farklı PEG miktarları ve gama ile ışınlanmış/ışınlanmamış olarak çeşitli kombinasyonlarla hazırlanmış, şırınga basma testinde ise en yüksek enjeksiyon gücü (73 N) gerektiren malzemenin yüksek PEG oranı içeren steril numunelerin olduğu görülmüştür. Viskozite çalışmasında malzemenin viskoelastisitesinin PEG oranı ile arttığı görülmüştür ($\tan \delta$ değeri 0.38'den 0.31'e düşmüştür). Malzemelerin yıkanma-direnci ile kohezyonları su içerisindeki ağırlık kaybı ve Ca^{2+} iyonu salınımı ile, ayrı ayrı ölçülmüştür. PEG ve gliserol'in ortak etkileri ile bu özelliklerin değiştiği görülmüştür. Kalsiyum salınım profillerinden iyon seramik partiküllerin iyon emilimi/salınımının dinamik bir proses olduğu anlaşılmıştır. Malzemelerin sitotoksosite testleri MEM elüsyon yöntemi ile L929 fare fibroblastları kullanılarak gerçekleştirilmiştir. Hücre canlılık oranı 3-(4,5-dimetiltiazol-2-yl)-2,5-difeniltetrazolyum bromit analiz kiti ile elde edilmiştir. 10 kGy ve 25 kGy ile sterilize edilmiş malzemelerin 24-saatlik ekstraktları %22.94 ve %56.53 olarak ayrı ayrı kaydedilmiştir. Ekstrat inkübasyon süresi ile hücre canlılığı arasında bir ilişki kurulamamıştır. 10 kGy ile sterilize edilmiş numunelerin ekstrat seyreltilerinde hücre canlılığı önemli bir şekilde artmıştır, %63.40'tan %86.17'ye %50 seyreltili ile ulaşılmıştır. Bulgular, tez konusu malzemeler için *in vitro* testlerinin limitasyonları ve *in vitro* toksisite ile *in vivo* sağlıklı kemik oluşumu arasındaki farkı açısından literatürle uyum sağlamaktadır.

Anahtar Kelimeler: enjekte edilebilir kemik grefti, beta-trikalsiyum fosfat, polietilen glikol, gliserol, biyoaktif cam

ABSTRACT

DEVELOPMENT OF BETA-TRICALCIUM PHOSPHATE BASED INJECTABLE SYNTHETIC BONE GRAFT MATERIALS

Deniz SARP

Master of Science, Department of Bioengineering

Supervisor: Assoc. Prof. Dr. Halil Murat AYDIN

September 2018, 149 pages

As the global population ages, the number of patients suffering from bone tissue loss due to trauma, degenerative diseases, or surgical intervention increases. To meet the demand for bone graft materials, synthetic substitutes have been developed. In cases of critical-sized or irregularly-shaped bone defects injectable bone substitutes (IBS) provide more utility over pre-fabricated blocks or granules. Non-setting IBSs (putties) act as bone void fillers in non-load-bearing areas. IBSs are employed in a range of medical fields including orthopaedic, cosmetic, reconstructive and dental surgeries. A clinically-successful IBS will be easy-to-handle and apply, have osteo-stimulatory properties, avoid premature degradation, have standardised quality, be sterilisable and have a viable shelf-life. The aim of this research was to develop an ideal IBS composed of β -tricalcium phosphate (β -TCP)-

bioactive glass particles in a poly(ethylene glycol) (PEG) – glycerol carrier. Fourier Transform Infrared Spectroscopy (FT-IR) spectroscopy verified that gamma sterilisation (25kGy) did not affect its chemical composition. Scanning electron microscopy (SEM) and micro-computerised tomography (μ -CT) revealed a homogenous phase distribution of the constituents with the sample preparation technique used. Compositional effects on IBS thermal properties were investigated with thermogravimetric analysis and an approximately 50% loss in weight was recorded in both 1:1 and 2:3 (%w) carrier-to-ceramic compositions. The effects of both varying IBS carrier composition and the gamma-sterilisation condition on the rheological properties of the biomaterial were evaluated. The highest peak injection force (73 N) recorded for any combination of poly(ethylene glycol) (PEG) content and sterility conditions in prepared samples was seen in sterile samples with high PEG content. Oscillatory viscosity measurements of the samples revealed an increase in IBS viscoelasticity ($\tan \delta$ changed from 0.38 to 0.31) with increased PEG concentration. The washout-resistance and cohesiveness of the IBS was examined according to weight loss in and Ca^{2+} ion release in dissolution media, respectively. Both PEG and glycerol were found to have competing effects on these two properties. Furthermore, calcium release profiles showed a dynamic ion release/uptake behaviour of the ceramic particles in water. Cytotoxicity testing of the IBSs were performed using the MEM elution method with L929 mouse fibroblasts. Cell viability was quantified with a 3-(4,5-Dimethylthiazol-2-yl)-2,5-diphenyltetrazolium bromide analysis kit. 24-hour extracts of IBS composites sterilised with gamma irradiation of 10 kGy and 25 kGy resulted in a cell viability value of 22.94 % and 56.53 %, respectively. No relationship between extract incubation times and cell viability could be established. A significant ($p < 0.0001$) increase in cell viability in extract dilutions of 10 kGy – treated samples was observed, increasing from 63.40 % (100 % extract concentration) to 86.17 % (50 % extract concentration). These results concur with literature regarding the limitations of *in vitro* testing for IBSs and the commonly reported discrepancy between *in vitro* cytotoxicity and *in vivo* successful healthy bone formation for similar materials.

Keywords: injectable bone substitute, beta-tricalcium phosphate, polyethylene glycol, glycerol, bioactive glass

ACKNOWLEDGEMENTS

I wish to deeply thank my advisor, Associate Professor HALİL MURAT AYDIN, for his strong encouragement, support and guidance through this research.

I would like to thank the Head of the Bioengineering Department Prof. Dr. MENEMŞE GÜMÜŞDERELİOĞLU as well as the entire department for their support. I wish to express my gratefulness to my committee members for their time, critique and helpful suggestions: Assoc. Prof. Dr. EDA AYŞE AKSOY, Assoc. Prof. Dr. MURAT BARS BAY, Assist. Prof. Dr. BATUR ERCAN and Assoc. Prof. Dr. SEDAT ODABAŞ.

To my colleagues: GÜLÇİN GÜNAL, thank you for your insight and contributions to this work, I couldn't have completed this work in time without you. PELİN DENİZ and DİLARA TÜRKEL your friendship and humour kept me moving through the thickest of times, thank you. PEZHMAN HOSSEİNİAN, SELCEN GÜLER, SAFA KARARMAZ, MELTEM AYDIN, BENGİSU TOPUZ thank you for your friendship and support during the completion of this thesis. ATAKAN TEVLEK, thank you for your contributions to this work.

I graciously acknowledge BMT Calsis Health Technologies Co., for providing the resources and facilities required for the completion of this project. To LEVENT METE ÖZGÜRBÜZ, thank you for your mentorship through the years.

To my family AYNUR ÖZDİL, MEHMET ÖZDİL, AHMET ÖZDİL and ENES ÖZDİL, you may never truly know how much I love and adore you, thank you.

MELİH SARP, thank you for your love, support and inspiration, through this thesis, and always.

And, BADE, you hold my hand for now, but my heart forever.

CONTENTS

	Page
ÖZET	i
ABSTRACT	iii
ACKNOWLEDGEMENTS.....	vi
LIST OF TABLES	ix
LIST OF FIGURES	x
1. INTRODUCTION	1
1.1. Thesis Objectives.....	2
1.2. Literature Review	4
1.2.1. Basics of Bone Biology	4
1.2.2. Orthobiologics	10
1.2.3. Injectable Bone Substitutes (IBS)	17
1.2.4. Design Considerations for Injectable Bone Grafts	34
1.3. Materials and Method	50
2. Results and Discussion	56
2.1. Morphological Analyses - SEM.....	56
2.2. Morphological Analyses - μ -CT.....	58
2.3. Chemical Analyses - FT-IR Analysis	59
2.4. Thermal Analyses - Thermogravimetric Analysis	62
2.5. Washout Study	66
2.6. Cohesion Study	74
2.7. Injectability Study.....	78
2.8. Viscosity Analysis	84
3.CONCLUSION.....	102
4. REFERENCES	103
5. APPENDIX	123

6. CURRICULUM VITAE 148

LIST OF TABLES

	<u>Page</u>
Table 1. Ca/P Ratios for Popular Calcium Phosphates.....	27
Table 2. List of commercially-available 'pre-mixed', 'to-be-mixed' and other injectable bone graft substitutes (adapted from Bohner [199] with permission	41
Table 3. Advantages and disadvantages of sterilisation techniques [242]	46
Table 4. Synthesised IBS Compositions	50
Table 5. L929 fibroblast cytotoxicity of IBSs.....	96

LIST OF FIGURES

	<u>Page</u>
Figure 1. Key components of the proposed IBS system	3
Figure 2. Cells and ligands of skeletal remodelling [18]	9
Figure 3. SEM images of IBS compositions B31 sterile, B31 unsterile, A31 sterile and A31 unsterile (groups left to right), at 50x, 250x, 1000x and 5000x magnification (top to bottom)	58
Figure 4. Micro -CT scans of sterile A31 (A), unsterile A31 (B), sterile B31 (C) and unsterile B31 (D)	59
Figure 5. FT-IR spectra of sterile and non-sterile IBS	62
Figure 6. TGA thermogram of Sterile A31 IBS Composition	64
Figure 7. TGA thermogram of non-sterile A31 IBS Composition	65
Figure 8. TGA thermogram of sterile B31 IBS Composition.....	65
Figure 9. TGA thermogram of non-sterile B31 IBS Composition	66
Figure 10. Image of sterile IBS samples in ultrapure water after 1 hour of incubation. B11(1), B11(2), B11(3), B12(1), B12(2), B12(3), B22(1), B22(2), B22(3), B21(1), B21(2) and B21(3) (from left to right)	67
Figure 11. Representative sample showing the amount of IBS remaining on gauze pad after 24 hours of incubation.....	68
Figure 13. Disintegration profile of unsterile samples over time. Error bars represent to standard deviation from the mean for each IBS group.....	69
Figure 14. Comparison of material loss in various IBS compositions in aqueous environment. Solid columns represent sterile IBS samples and striped columns represent non-sterile IBS samples	70
Figure 15. Calcium ion release from sterile and unsterile B11 samples over 48 hours	75
Figure 16. Amount of calcium release from sterile IBS samples. Light blue columns represent calcium release from sample at 1 hour, dark grey columns represent calcium release from sample at 24 hours.....	76
Figure 17. Experimental setup for mechanical testing machine and syringe apparatus during injectability tests	79
Figure 18. Representative graph (sample B11) graph of applied force vs plunger displacement	80

Figure 19. Average Peak Injection Forces for Sterile IBS Compositions. Dotted columns represent samples of LHMW PEG content	81
Figure 20. Peak injection forces for all groups. Light grey columns (including dotted-grey columns) represent gamma-sterilised samples of the same group. Dotted columns represent samples of LHMW PEG content	82
Figure 21. Change in G' , G'' with oscillatory frequency of representative IBS (B11)	88
Figure 22. Oscillatory frequency-dependent change in G' , G'' and η^*	91
Figure 23. G' (Pa), G'' (Pa) and Loss Factor of sterile IBS at angular frequency of 10 rad/s	92
Figure 24. Change in $\tan \delta$ with oscillatory frequency. Dotted lines represent non-sterile IBS samples. '+' denotes sterilised sample, '-' denotes non-sterile sample	93
Figure 25. The effect of gamma sterilisation on the viscoelasticity of IBS samples. In the legend '-' denotes non-sterile samples and '+' denotes gamma-sterilised samples	94

SYMBOLS AND ABBEVIATIONS

Symbols

β	Beta
μ	Micro
α	Alpha
γ	Gamma
ω	Omega, angular frequency
G'	Storage Modulus
G''	Loss Modulus
$\tan \delta$	Tan Delta or Dampening factor
η^*	Complex Viscosity
G'	Storage Modulus
G''	Loss Modulus

Abbreviations

ECM	Extracellular Matrix
MGP	Matrix Gla protein
RANKL	Receptor activator of nuclear $\kappa\beta$ ligand
BMP	Bone morphogenetic proteins
M-CFS	Macrophage colony stimulating factor
OPG	Osteoprotegerin
TGF- β	Transforming growth factor - β
IGF	Insulin-like growth factor
FGF	Fibroblast growth factor
PDG	Platelet-derived growth factor
bFGF	Basic fibroblast growth factor
PRP	Platelet-rich plasma
HUCMSCs	Human umbilical cord mesenchymal stem cells
IBS	Injectable bone substitute
CPC	Calcium phosphate cement
CSC	Calcium sulphate cement

PMMA	Poly(methyl methacrylate)
TTCP	Tetracalcium phosphate
DCPA	Dicalcium phosphate anhydrous
BCIS	Bone cement implantation syndrome
HPMC	Hydroxyl methylcellulose
PPF	Poly(propylene fumarate)
PEO	Poly(ethylene oxide)
Ca/P	Calcium-to-phosphate ratio
LSR	Liquid-to-Solid Ratio
HA	Hydroxyapatite
TCP	Tricalcium phosphate
OCP	Octacalcium phosphate
BG	Bioactive glass
HCA	Hydroxycarbonate apatite
CMC	Carboxymethyl cellulose
PEG	Poly(ethylene glycol)
Gly	Glycerol
CE	European Conformity
VHP	Vaporised hydrogen peroxide
EtO	Ethylene Oxide
E-beam	Electron-beam
HHMW	Higher high molecular weight
LHMW	Lower high molecular weight
SEM	Scanning Electron Microscopy
EDS	Energy-dispersive X-ray spectroscopy
FTIR	Fourier Transform Infrared
ATR-FTIR	Attenuated Total Reflectance Fourier Transform Infrared
μ -CT	Micro Computerised Tomography
TGA	Thermal Gravimetric Analysis
SD	Standard Deviation
IDT	Initial Disintegration Temperature
MTT	3-(4,5-Dimethylthiazol-2-yl)-2,5-diphenyltetrazolium bromide
UV	Ultraviolet
sc-CO ₂	Supercritical carbon dioxide

1. INTRODUCTION

Many tissues of the human body have self-repair capabilities, through complex and interwoven chemical and biological mechanisms. However, in some instances these mechanisms may become overwhelmed, and tissue repair or regeneration must be augmented with external intervention. The bone remodelling process is the naturally-occurring homeostatic mechanism in which cells of osteogenic lineage regulate anabolic and catabolic activity of bone cells, breaking down or producing new bone tissue according to the local need. However, defects in bone tissue that are of a 'critical' size, for instance, are generally beyond repair via the bone remodelling process alone. There are millions of patients each year who have acquired such critical defects through injury, disease or curettage of bone tumours. Treatment of these patients usually involve the use of a bone graft or bone graft substitute to accelerate and guide healing in such defects. In such cases, bone tissue engineering practices utilising biomaterials provide means for assisting the bone repair and regeneration efforts of the body. Without these bone tissue engineering options, a patient may have to face the numerous difficulties associated with a persistent non-repair of bone which may include pain and immobility. A large portion of orthopaedic research is dedicated to the development of materials capable of treating critical-sized bone defects. A critical size bone-defect is generally defined as one that is between 1 cm and 5 cm, as defects larger than this carry a serious risk of non-union and require more than a graft or biomaterials approach, such as the bone transport method designed by the Russian surgeon Ilizarov [1]. For bone defects appropriate for treatment via a grafting procedure, there are several options of material, both organic and synthetic, that the surgeon may choose from. Although the application site primarily dictates the type of material to be used, many other factors will influence the success of the available material options. These factors include the physical form in which the material is provided, the availability of the material, the proven clinical performance of the material and the delivery methods that need to be employed for its implantation. Furthermore, for synthetic grafting materials compatibility, functionality compared to biological alternatives, and manufacturability must all be tested and proven prior to presentation to market.

Although autografts, allografts and xenografts present the advantage of being more structurally, chemically and biologically aligned to natural bone tissue, they are weighed-down by issues that their synthetic alternatives by-pass. Considered the current gold standard of treatment, naturally-compatible autologous bone tissue taken from another bone site of the same patient, is limited by availability and donor site morbidity. Allogenic bone, tissue that is sourced from another person or cadaver, poses the risk of tissue rejection or disease transmission to the receiver. Even after surpassing ethical constraints, xenogeneic grafts, although may be more readily available, also pose the same risks of disease transmission and tissue incompatibility as allografts. It is at this point that clinicians opt for synthetic materials, which although lacking several features exhibited by natural tissues, are abundantly available, disease-free options. Moreover, most synthetic materials have an extensive history of clinical use and success to support their safety and effectiveness in indicated uses. In fact, with an ever-growing expansion in manufacturing technology, biomaterials can now be tailored to address the needs of the microenvironment of the defect site. They are also typically impregnated or functionalised with certain molecules or cells that drive healing mechanisms at the defect location. Synthetic materials can also be combined with autografts, to extend the amount of graft material used, preserving and presenting the key biological cues for bone repair.

1.1. Thesis Objectives

The broad aim of this research project is to develop a synthetic bone repair material in the form of an injectable paste indicated for the treatment of bone defects caused by sports injuries, degenerative diseases, surgical interventions or other cases resulting in defects in bone tissue. The injectable bone substitute (IBS) is designed to support the efforts of local endogenous bio-constituents in bone regeneration. As a biocompatible and biodegradable bone void filler, the composite IBS will augment the activity of anabolic or anti-catabolic agents at sites that are incapable of repair through natural mechanisms alone. The combination of polymer and ceramic has a long-standing history in biomaterials research and over 30 years of clinical use history. The development of an injectable bone graft substitute is intended to contribute, both scientifically and potentially commercially, to the need for viable

synthetic alternatives required by the growing number clinical cases that are under-sourced with natural grafting options.

The material composition of the IBS is a combination of a bioceramic, bioglass and polymeric gel matrix. An investigation into the effects of varying the amount of each component within the composition will be conducted as a means of developing the most optimised formulation with respect to chemical and rheological integrity, ease-of-handling and cytocompatibility. Figure 1 below visually summarises they key components of the proposed composite biomaterial to be investigated.

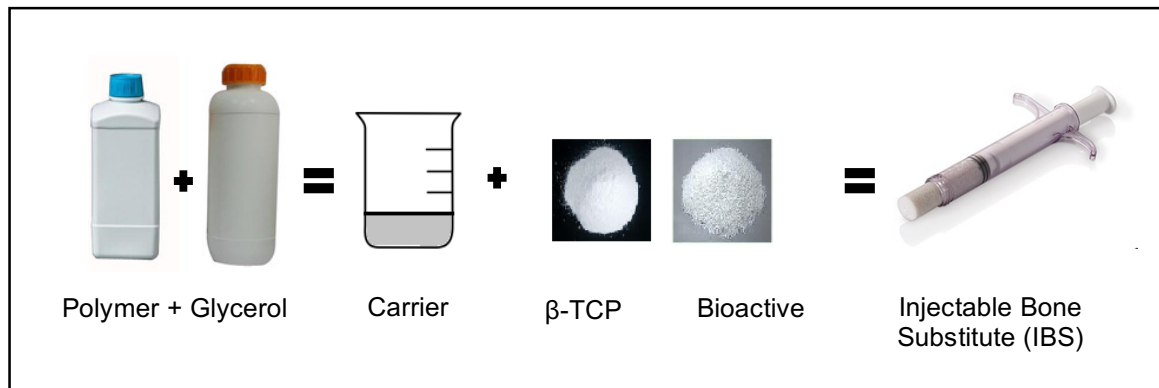


Figure 1. Key components of the proposed IBS system

We speculate that a successful combination of the carrier, β -TCP particles and bioactive glass particles via the manufacturing technique disclosed herein will produce an injectable bone paste with potential as a bone tissue repair material.

This broad objective can be narrowed down to the following specific research questions that the outcome of the research is intended to provide answers to:

- *Do the various constituents of the proposed IBS mix homogenously via a standardised and repeatable manufacturing method?*
- *What is the relationship between amount of constituent and IBS injectability?*
- *What is the relationship between amount of constituent and IBS viscosity?*
- *What is the relationship between amount of constituent and IBS washout property and cohesiveness?*
- *What is the effect of terminal sterilisation (gamma) on chemical, biological and rheological properties of the IBS?*
- *Is there an optimal formulation of the proposed biomaterial that satisfies the clinical criteria for the abovementioned properties?*
- *What is the degree of cytocompatibility of the optimal IBS formulation?*

1.2. Literature Review

1.2.1. Basics of Bone Biology

The aim for a bone repairing biomaterial is to enhance the rate and quality of bone healing at sites of bone fracture, tissue degeneration, implant loosening or surgical intervention. A clear understanding of the fundamentals of bone structure; its constituents; blood supply, cells and matrix; the mechanisms of bone formation; and methods for controlling the behaviour of bone cells, is thus essential for designing a bone repair material. The physical, chemical and biological features of bone repair biomaterials can orchestrate local cells and factors that drive the bone remodelling process. By knowing what the key players of the process are, as well as their mechanisms of action, an engineer can tailor specific material properties to influence when and how bone is turned over [2]. There are several basic facts that are critical to the success of a bone repair material. For porous, scaffold-type biomaterials, pore size and pore interconnectivity are crucial for the penetration of cells and development of vasculature in the newly formed tissue which is critical to cell survival. A pore size over 300 μm is cited in literature as ideal for osteoblast penetration [3]. For materials that will undergo compression, a Young's modulus similar to that of native bone [4] is important for providing a dynamically stable environment for migrated cells and for avoiding issues such as stress shielding or early material wear. Also, material degradation rates that are synced to the rate of bone formation by the body will ensure that the support provided by the material is available as necessary. Furthermore, materials that contain or elute stimulatory agents can directly influence and enhance activities such as cell migration, cell adherence, cell proliferation and formation of vasculature. Alternatively, materials may release anti-catabolic agents which inhibit the further breakdown of bone matter by bone resorbing cells, which again, in effect, supports generation of new bone tissue.

1.2.1.1. Constituents and Structure of Bone

Bone is a specialised connective tissue which has four specific functions in the human body: providing the body with a rigid structure, protecting vital internal organs, acting as a reservoir for marrow and fat storage, and regulating calcium and

phosphate levels within the body. Bone tissue is classified as a micro- and nano-composite tissue and is a complex mix of organic and inorganic architecture. Approximately 2/3 of the weight of calcified bone is made up of inorganic minerals that is composed mainly of carbonated apatite whilst the remaining 1/3 is formed by an organic matrix that is composed primarily of collagen. The organic phase gives bone its rigidity, viscoelasticity and toughness, the mineral phase provides structural reinforcement, stiffness and mineral homeostasis, and the remaining bone matter consists of cell-stimulatory non-collagenous proteins [5].

Initially, approximately 94% of bone (also known as osteoid) is Type 1 collagen and small amounts of non-collagenous protein. As minerals of the inorganic phase deposit on this network of collagen fibrils during the process known as mineralisation, a light-weight yet extremely strong material, bone, is created. The organic phase of bone consists of cells of the bone remodelling process - osteoclasts (bone resorbing cells), osteoblasts (bone depositing cells) and osteocytes (osteoblasts residing in the bone matrix). It is the number, availability and presence of relevant stimuli for these catabolic and anabolic cell types, respectively, that dictate whether existing bone is to be resorbed in an area or whether new bone is laid down.

On a chemical level, inorganic bone acts as a mineral reservoir that controls the concentrations of calcium, sodium, magnesium, phosphate and other ions. The interrelation between bone and the body's endocrine system, and its involvement in mineral and nutrient homeostasis, has been documented [6]. Physically, it provides the mechanical strength of skeletal bone. The inorganic phase of bone is mainly composed of hydroxyapatite ($\text{Ca}_{10}(\text{PO}_4)_6(\text{OH})_2$). New ions are introduced into the structure of hydroxyapatite through various substitution mechanisms which replace the Ca^{2+} or adsorb onto the crystal surface. Calcium, phosphate and carbonate are therefore the most abundant inorganic constituents of bone [7]. Other proteins of the extracellular matrix (ECM) include signalling proteins (such as bone morphogenetic proteins, cytokines, growth factors and adhesion molecules) and proteins involved in the mineralisation process (such as osteopontin (secreted by osteoblasts and mediates cell-matrix interactions), osteonectin (bonds calcium) and Matrix Gla protein (MGP, is a calcification inhibitor)) [8].

Like the different phases of bone, the structure of bone itself also falls into two categories - lamellar bone and woven bone. The local bone structure and

microarchitecture affects the choice, amount, form and method of application of a bone repair material. Whilst lamellar bone boasts strong, compacted layers of bone capable of supporting loads and fixation of orthopaedic hardware, other areas are highly porous, and whilst excellent for accommodating vascular networks and cells, they are also highly susceptible to fracture or damage.

The lamellar or compact bone is found on the outer regions of bone, has a porosity of 5-30% and makes up for about 80% of the total bone mass [9]. Lamellar bone in adults is formed by collagen fibrils that are arranged in parallel sheets (called lamellae) or concentric sheets. Lamellar bone in long bones form around blood vessels and nerves, forming Haversian systems or canals that run parallel to the surface of the bone, along its longitudinal axis.

Woven bone, also known as non-lamellar or trabecular bone, contains randomly dispersed, interlacing collagen fibrils covered in hydroxyapatite crystals deposited in a disorderly manner [10]. It is essentially an interwoven scaffold of rod and plate shaped trabeculae, that are spaced approximately 1 mm apart from each other. Trabecular bone forms in areas where bone is rapidly laid down, as in the case of fetal growth, fracture healing or hyperthyroidism. Trabecular bone has a 30-90% porosity and fills up the interior of the bone to allow for vascularisation and storage of marrow content [9]. Arranged as cross-braced interior struts, woven bone can provide maximum rigidity with the use of minimal material. Its formation can therefore be found to be aligned parallel with the major lines of compressive or tensile forces.

A bone defect may be restricted to a single structural phase of bone or may span both types of zones. A bone void filler or augmentation product must therefore address the structural conditions of the zones which the defect is covers. It must also provide incentive for bone cells to be involved in the bone healing effort. There are four main cells found in the mineralised bone matrix, namely, osteoblasts, osteoclasts, osteocytes and bone lining cells.

1.2.1.2. Bone Remodelling

Bone is a dynamic tissue that is constantly broken down and reformed in response to the needs of the body. The bone remodelling process refers to a natural mechanism of the human body where mature bone tissue is resorbed, and new

bone is formed (ossification) by specialised bone cells. Factors influencing the balance between resorption and formation range from the presence of vitamins (vitamin A, C, D), minerals (calcium, phosphate, magnesium), hormones (oestrogen/testosterone, parathyroid hormone) and signalling molecules (interleukin 1, receptor activator of nuclear factor kappa B ligand (RANKL)), to physical factors such as the presence or absence of mechanical loading on the bone itself. Bone remodelling factors act to either increase/decrease resorption and/or increase/decrease formation of bone through their effects on the cells of the bone remodelling process.

Cells of the bone turnover process are distinguished based on their morphology and characteristic locations in the bone matrix, and are involved in bone formation/resorption, mineral homeostasis and bone repair [11]. In the event of loss of bone matter in cases such as trauma or pathological conditions etc., the quick restoration of bone mass and prevention of further damage to surrounding tissue relies on the rapid and correct execution of these processes.

Two cell types which stem from hematopoietic stem cell line are responsible for the turnover of the bone matrix. The first is the osteoclast, which carries out catabolic activities involved in the resorption of bone tissue. The activity of the osteoclast is in fact regulated by the second cell type, the osteoblast. The osteoblastic lineage, itself, executes anabolic activities forming new bone tissue wherever it is needed and is responsible for the regulated production of mineralised bone matrix which is later removed by the osteoclast [12].

1.2.1.2.1. Osteoblasts

Osteoblasts are specialised connective tissue cells responsible for the synthesis of a matrix material called osteoid and its subsequent mineralisation through the deposition of inorganic salts throughout it. It produces a myriad of products including enzymes (e.g. alkaline phosphatase and collagenase), growth factors, hormones (e.g. osteocalcin) and Type I collagen. The reservoirs of osteogenic cells, that later differentiate into osteoblasts, are found in the periosteum (outer lining of bone) and endosteum of the marrow cavity. Through the interconnected network of bone marrow, periosteum, pericytic cells and invading vasculature, osteoprogenitors migrate to sites of bone damage and here they are stimulated by various growth

factors, in particular bone morphogenetic proteins (BMPs), which pushes their differentiation toward the osteoblastic lineage [13, 14].

Osteocytes are osteoblasts that have become trapped and isolated amongst calcified bone matrix that they have produced. From the pits they reside in, called lacunae, these cells support other osteoblasts in a paracrine manner and have some catabolic activity (they are slower than osteoclasts though). They also communicate with each other and bone surfaces via extensive filamentous protoplasmic processes that run along channels (canaliculi) in the bone matrix. With this network, osteocytes can sense areas of high loading or fracture and recruit osteoclasts to dissolve bone where needed. In fact, more than 90% of the bone cells in the mature human skeleton are osteocytes [2].

1.2.1.2.2. Osteoclasts

Osteoclasts are large multinucleated cells that break down bone matter through chemical, enzymatic or phagocytic attack. They are the only cell type capable of resorbing mineralised bone. It is the secretion of pro-osteoclastic factors (M-CSF, RANKL) by osteoblasts that drives osteoclast precursor cells from the hematopoietic lineage to differentiate into osteoclasts [15]. Osteoprotegerin (OPG) is another factor known to act as a decoy receptor that binds RANKL and prevents it from interacting with its receptor on osteoclast precursors, thereby inhibiting osteoclast differentiation and function. Together, M-CSF and the RANK-RANKL-osteoprotegerin system regulate osteoclast differentiation.

The main mechanism of bone tissue breakdown by the osteoclast is by binding to the surface of bone and secreting transport protons that reduce local pH and solubilise bone material, in conjunction with additional acid protease secretion which also degrades bone matter [11]. Osteoclasts release acid phosphatase which dissolves both the organic collagen and inorganic calcium phosphates of bone. As the osteoclast breaks down the mineralised bone matrix, it engulfs the small fragments formed and continues their breakdown within cellular vacuoles, eventually releasing the breakdown products like calcium and phosphorous back into the blood stream.

1.2.1.2.3. Osteoblast-Osteoclast Relationship in Bone Remodelling

Drivers of bone remodelling, osteoblasts and osteoclasts, have a direct relationships with each other. *In vitro* evidence has shown that cells of the osteoblastic lineage modulate the activity of osteoclasts through a number of cytokines and growth factors locally generated [16]. M-CSF and soluble RANK-L receptors are expressed on osteoclast precursors and play a major role in their differentiation into mature osteoclasts [17]. Under the influence of a combination of effectors (Vitamin D, parathyroid hormone and stimulation from osteocytes), osteoblasts secrete RANK-L and interleukin-6, of which RANK-L has been confirmed to be an absolute necessity for pro-osteoclastic activity [18, 19]. Whilst pre-osteoblasts secrete mainly RANK-L, mature osteoblasts express high levels of OPG [20]. The overall bone remodelling event, however, depends on the complex interplay between a cocktail of factors including cytokines (interleukins), growth factors, attachment factors, sex hormones (estrogen) and parathyroid hormone [21]. The figure below (Figure 2) is a graphic representation of the osteoblast-osteoclast interaction and the key elements involved.

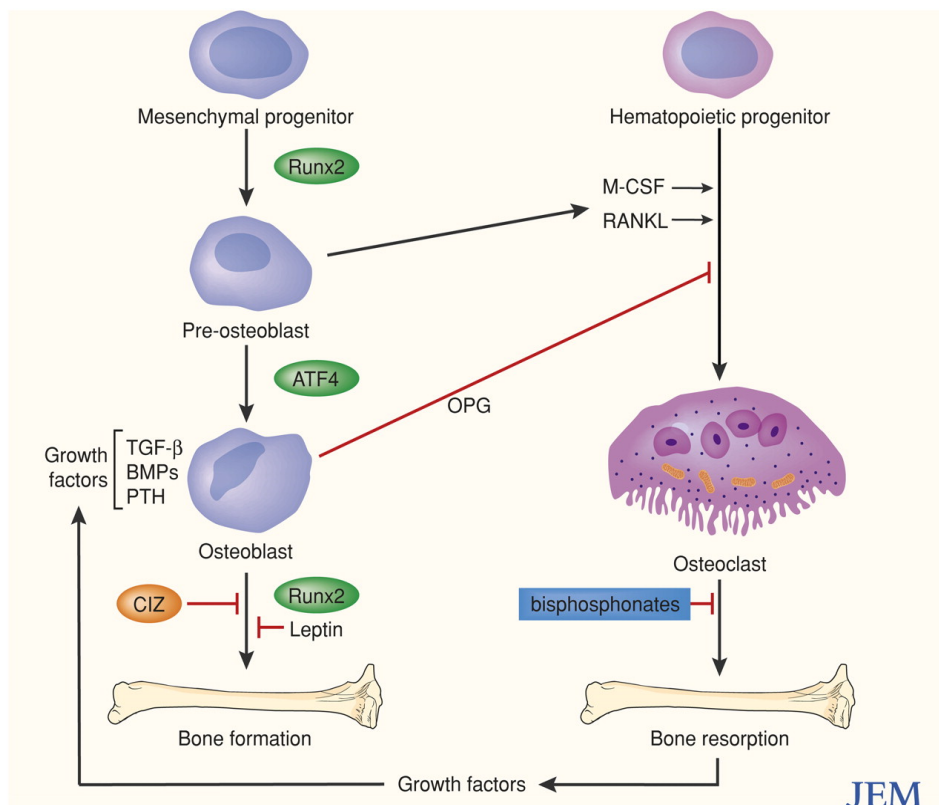


Figure 2. Cells and ligands of skeletal remodelling [18]

1.2.2. Orthobiologics

'Orthobiologics' refers to materials or substances used in orthopaedics to improve the healing of musculoskeletal injuries such as damaged bone, muscle, tendon or ligament tissue. They are generally constructed from substances found naturally in the body. Examples of orthobiologic substances used in regenerative medicine applications include bone grafts, platelet rich plasma, stem cells, growth factors, autologous conditioned serum etc. Orthobiologics are applied in cases of orthopaedic tissue trauma that overwhelms natural healing mechanisms. Some orthobiologic substances may also act on a systemic level, such as those used to treat degenerative diseases such as osteoporosis, enhancing the overall skeletal mass and bone quality of a patient. For patients suffering from osteoporotic fractures which show an impaired ability to heal with prolonged healing times [22], or for those with orthopaedic conditions which eventuate in the creation of significantly-sized bone voids, there are a number of orthobiologic adjuvants available for faster and more effective healing of bone tissue.

The slow albeit steady shift towards the clinical uptake of orthobiologics-based therapies and the increase in orthobiologics research in recent years stems from the clinical need for catalysts of healing in skeletal injuries or defects. Serious skeletal injuries, such as those that have progressed into cases requiring surgical intervention, usually also impede the range of motion of the associated body area. When lower limbs, lower extremities or lumbar/sacral spine is involved, this could go further to result in a non-ambulant patient. Thus, the antecedence of the surgeon becomes the speedy restoration of such defects. The Diamond Concept in orthopaedics states that a tissue repair material must be supplemented with growth factors and cells and be ensured sufficient stability in order to provide the intended support for critically-large defects [22]. As such, for effective healing, an orthobiologics approach must incorporate the following three ingredients:

- *Matrix*: A material which is to accommodate the cells of the healing process must be conducive to their migration, attachment, proliferation and growth by means of both chemically and structurally appropriate surfaces for successful cell-material interactions, as well as macro- and microstructures suitable for vascularisation. Traditionally, autografts (bone from the patient) or allografts (bone from another patient) have been used as matrix materials, however, the former is limited by issues

such as availability and donor site morbidity, whilst the latter option may present risks of incompatibility and disease transfer. These tissue types may be decellularised to present as cell-less scaffolds for bone regeneration [23]. They may also be combined with cells [24], ceramics [25], polymers [26] or any other materials inductive or conducive to bone growth. Alternatively, biodegradable artificial matrix materials can be fabricated to exhibit the features of natural tissues, including both the organic and inorganic phases. The advantage to their biodegradability is that it eliminates the need for a second surgical site.

- *Growth factors*: Growth factors may be stimulators or inhibitors of bone formation or resorption, respectively. They are usually proteins that manipulate bone cells, controlling their differentiation processes and actions by affecting surface receptors and initiating a cascade of chemical pathways. Their ability to chemo-attract stem or other cells to areas of need depends on the degree of vascularisation available to the area. Although available throughout the body in low concentrations, bone tissue engineering matrices are usually doped with much higher concentrations of growth factors to improve tissue healing in challenging areas. One common factor that bone repair materials are commonly embedded with is bone morphogenetic proteins.

- *Stem cells*: Cells of pluripotent or multipotent status can differentiate into specialised cell types responsible for bone turnover activities. For example, osteoblasts are derived from the mesenchymal stem cell (MSC), osteoclasts stem from the hematopoietic stem cell lineage. Stem cell recruitment and differentiation is directed by the presence of chemotactic factors secreted by local cells in defect areas.

1.2.2.1. Matrix Materials

A matrix or primary vessel of an orthobiologic biomaterial must have structural features and properties that mimic native bone structure, constituents (including blood supply, cells and extracellular matrix) to orchestrate the remodelling of bone in compromised bone tissue [2, 11]. This requirement applies to all bone tissue engineering scaffolds; however, criteria may vary for injectable biomaterials. Bone void filler materials, for example, have the consistency of paste and are delivered to bone defect sites with a syringe or similar apparatus. The relatively rigid mechanical

structures provided by tissue engineering scaffolds accommodate bone regenerative cells by means of providing a highly interconnected network through which new bone formation and angiogenesis can occur. Properties such as pore size, porosity and mechanical strength are usual measures of material appropriateness for bone tissue engineering scaffolds. For injectable bone grafts, however, properties such as viscosity, injectability, cohesion, thermodynamics, degradation, washout resistance and cellular interaction are of primary concern. The injectable bone graft is essentially a bone void filler material that may also act as carriers of critical bone regenerative agents to initiate or support new bone formation before the material itself is degraded and resorbed by the body. To achieve this, its primary 'matrix' i.e. carrier/liquid phase must be tailored to avoid premature degradation. This is achieved with additives or materials that promote cohesiveness and anti-washout effects, without hampering the viscosity and injectability of the material.

As previously discussed, natural bone tissues of autogenic, allogeneic or xenogeneic origin can be decellularised or demineralised and reprocessed into bone tissue engineering scaffolds supplemented with additives to enhance bone regeneration. However, due to some critical drawbacks of these tissue types, also previously discussed, synthetic materials have been generated much research interest. Much of bone tissue engineering research efforts have been directed towards the development of materials capable of mimicking the structure and surface kinetics of bone. These materials would thus be able to facilitate the migration, attachment and proliferation of mesenchymal stem cells which later differentiate into osteoprogenitor cells. Non-biological structures of this capacity are considered 'osteoconductive'. The range of material options for these tissue engineering scaffolds is vast. These synthetic scaffolds are generally produced from polymers, ceramics and their blends. Metals have been dismissed as suitable materials for interfacing with areas of bone that requires the formation of new bone tissue, for several reasons. They are non-biodegradable, introduce stress shielding problems [27], require surface conditioning to overcome poor material-tissue interactions [28] and thus often require surgical reintervention [29]. Polymers in particular are opted as scaffold materials as due to the versatility of their possible architectures, composition, degradation rates and manufacturing techniques [30].

Some polymer types that are frequently utilised in these applications are poly(ϵ -caprolactone), poly(propylene fumarate), poly(phosphazene), poly (anhydride) and poly(α -hydroxy acids) [31]. Of these, poly(α -hydroxy acids) are the most popular as they are highly versatile thermoplastics which are made from glycolic acid and lactic acid monomers, which themselves have an extensive history of FDA approval in bone tissue engineering [32, 33]. Also, the degradation rates of polymers can be matched to the rate of tissue formation and the non-cytotoxic degradation products of polymeric 3D tissue engineering constructs in medical and tissue engineering applications can be removed through natural metabolic pathways. Literature is abundant with research of polymer-ceramic materials. Natural polymer (chitin, chitosan, collagen etc.) composites with ceramics [34] or combined with proteins, polysaccharides, minerals, growth factors or cells etc. [35] have been extensively reviewed. The same applies to synthetic polymers [36, 37]. Also outside the scope of this thesis yet important for a general understanding of bone tissue engineering approaches, is the myriad of scaffold fabrication techniques and technologies which range from traditional methods such as solvent casting and particulate leaching [38], to more recently 3D printing [39].

1.2.2.2. Growth Factors

Synthetic bone grafts may attempt to coordinate bone regeneration through physical or structural characteristics, however, they lack biological cues for signalling the migration, attachment, growth and proliferation of osteoprogenitors, which autogenic, allogenic or xenogeneic grafts may inherently possess. Although microarchitectural features or surface chemistry can be tailored to support material-cell interactions to some degree, true tissue formation is best achieved with the presence of bioactive factors. Synthetic bone grafts are therefore usually supplemented with drugs or agents that are pro-osteogenesis. The remodelling pathways are manipulated with the use of specific modulators. These modulators may be either anabolic (formation stimulators) or anti-catabolic (resorption inhibitors). A popular approach is to utilise the naturally-occurring factors within the body such as transforming growth factor (TGF- β), insulin-like growth factor (IGF I and II), platelet-derived growth factor (PDGF), fibroblast growth factor (FGF) and various types of bone morphogenetic proteins (BMPs) [40]. Other additives such as

bioglass [41] are also commonly used as a means of increasing the bioactivity of bone graft substitutes.

One of the most clinically-covered bone growth stimulants used in orthopaedic treatment is bone morphogenetic protein (BMP). BMPs are a part of the TGF-Beta superfamily and have been clinically proven to have strong chondro- and osteo-inductive effects [42-44]. A study on the treatment of peri-implant defects in a dog model with a combination of growth factors (bone morphogenetic protein-2 (BMP-2), transforming growth factor-beta (TGF-beta), platelet-derived growth factor (PDGF), basic fibroblast growth factor (bFGF)) and bone cement found a significant increase in the amount of bone formed as well as material-bone surface contact [45]. The use of BMPs in humans, however, is limited to indications – BMP-7/OP-1 is indicated for non-unions and some cases of spinal fusion, whereas BMP-2 is indicated for open tibial fracture surgeries, as explained by Janicki *et al.* [46]. Furthermore, BMPs bind better to calcium phosphates than polymers as BMPs are water-soluble and polymers are hydrophobic, although some techniques such as solution dipping or oxygen plasma treatment of polymers yield promising results [47]. It is also worthy to note that BMP-release behaviour of materials may show variation between *in vitro* and *in vivo* tests [48]. Therefore, release profiles for BMPs are difficult to predict as they are affected not only by material type (adsorption capacity) but also the experimental environment.

Bisphosphonates are chemically-stable derivatives of inorganic pyrophosphate have been shown to suppress bone resorption by preventing calcification by binding to hydroxyapatite crystals and also inhibiting their breakdown [49, 50]. Bisphosphonates display a very high affinity for calcium ions in the mineral phase of bone and their use in osteoporotic patients have shown a reduction in the risk of secondary fractures [51]. An injectable bone graft composed of alendronate (bisphosphonate) and calcium phosphate was tried in proximal medial tibia defects in a rabbit model, however, no remarkable difference with respect to improving the bone healing process compared to calcium phosphate-only groups was evident [52]. Many studies suggest, however, that the positive effects of bisphosphonates are activated when there is low bone turnover i.e. in unhealthy bone models [53].

Platelet-rich plasma (PRP) is widely known to be a source of concentrated growth factors, cytokines, proteins, and ions [54]. There are studies which have shown that PRP facilitates cellular migration, adhesion, proliferation and *in vivo* tissue

regeneration through the release of growth factors and cytokines from its α -granules [55, 56]. Other studies confirm the osteogenic effects of PRP in PRP-embedded biomaterials. Examples include the report of Rai *et al.* who used a polycaprolactone-tricalcium phosphate scaffold containing PRP and saw that both vascularisation during bone regeneration and bone volume fraction showed an increase [57]. Concurring results obtained by Bi *et al.* show that injectable TCP/chitosan materials carrying PRP promotes new bone formation [58]. A recent study on platelet-rich plasma (PRP) - enriched brushite bone cement revealed a marked improvement in surface reactivity, and a better early-stage tissue response and bony ingrowths [59]. Another recent study presents a novel injectable tissue-engineered bone composed of PRP and human-adipose-derived stromal cells which was able to form bone structure in heterotopic sites of nude mice [60]. Previously demonstrated abilities to obtain sustained release of growth factors from PRP-carrying biomaterials presents opportunities for prolonged treatments of large bone defects that take longer to heal [61]. There is some converse data, however, regarding the ability of PRP to induce MSCs differentiation into osteoblasts as a failure rate of 38.5% was reported for PRP-supplemented long bone non-union treatments, as opposed to only 6.2% observed for BMP-treated cases [62]. Nonetheless, the overriding positive outcomes associated with PRP use continues to engage research and commercial interest in PRP-based therapies.

BMPs, bisphosphonates and PRP are only some examples of the exhaustive list of additive factors that could be used to improve the bioactivity of a bone tissue engineering material. From cathepsin K inhibitors [63] to synthetic small peptides (P-15) [64], there exists many unique scaffold-factor composites for bone tissue regeneration purposes.

1.2.2.3. Cells

Bone tissue engineering scaffolds usually have the dual function of both providing a physical support structure for newly formed bone tissue, as well as serving as a vehicle for drug and cell delivery. Drug delivery via scaffold materials has a long and successful history of clinical application. Bone formation stimulants can be embedded into or onto the fabric of the construct during manufacturing processes. The delivery of cells is a more complicated endeavour as ensuring the viability of a

sufficient number of cells to the defect site has many technical difficulties during application. The problems are amplified for dynamic carriers such as putties or pastes which cannot retain a static or rigid structure – a key requirement for sustaining cellular attachment and growth. Cell delivery via injectable bone pastes has created a host of new issues that scientists are currently seeking to overcome. Traditionally, cells are cultured with matrix materials *ex vivo* and the biological construct is then implanted at tissue repair sites with the intention that cell growth, proliferation and tissue regenerative activities will be sustained by the local environment. Stem cells in particular have shown great potential in regenerative orthopaedic medicine. In the presence of media additives such as dexamethasone, β -glycerophosphate and ascorbic acid, MSCs can be stimulated to produce extracellular matrix and upregulate genes involved in *in vivo* osteogenesis [65, 66]. Delivering MSCs, influencing their specialisation into osteogenic cells in orthotopic or ectopic environments, and ensuring that they also maintain adherence to the scaffold material, is still a challenge today for tissue engineers. The use of MSCs with autografts for the accelerated repair of non-union defects was previously demonstrated clinically, and it was found that an amount of less than 1000 progenitor cells/cm³ was not sufficient for obtaining union in patients [67] but this could be achieved through centrifugation prior to injection of cells [68]. In one study, MSCs cultured *ex vivo* on a hydroxyapatite scaffold was implanted into large defects (4-7 cm) and was shown to induce healing of the defects 10-16 months quicker compared to conventional grafting [69]. The success of including osteoprogenitors in synthetic bone grafts depend heavily on the cell source, cell isolation method, *ex vivo* culture conditions, implantation site, cell numbers and differentiation capacity of the cell line, as comprehensively reviewed by Janicki *et al.* [46].

Scientists have also successfully developed a stem-cell carrying bone cement. Zhao *et al.* propose an injectable composite bone cement for the delivery of human umbilical cord mesenchymal stem cells (hUCMSCs) for the minimally-invasive treatment of load-bearing defects [70]. The calcium phosphate cement combined with hydrogel microbeads encapsulating hUCMSCs was injectable with minimal pressure, displayed mechanical strength similar to cancellous bone, maintained cell viability after injection, and cells showed osteo-differentiation, yielding high alkaline phosphatase, osteocalcin, collagen Type I, and osterix gene expressions in cell culture.

The delivery of a cell population to a defect area in the bid to kick-start the tissue regeneration process is a highly successful approach, when it works. To meet essential requirements stated in the Diamond Concept for bone tissue engineering, the option to synthetically regulate the activity of bone cells can be used as an alternate route to integrating the role of cells into the bone regeneration objective.

1.2.3. Injectable Bone Substitutes (IBS)

An injectable bone substitute is essentially a synthetic bone graft which has a solid bioactive material dispersed throughout a liquid carrier phase. The injectable gel or putty-like formulation is injected into a bone void where it will fill the space and augment local tissue repair. Bone graft substitutes in injectable form offer several advantages over the commonly encountered pre-fabricated granules or blocks. These advantages include the ability to easily mould the material so that it contours complex-shaped defects, the reduction of associated tissue scarring and postoperative pain, and the elimination of complications of revision surgery [71].

Though there are several ways in which injectable bone graft substitutes have previously been categorised in literature, for the purposes of this research, IBSs will be divided and discussed as setting (cements) and non-setting (putties) bone graft materials. Further classification is also possible based on the composition of the IBS, where an IBS may be categorised as either organic-based (partial or complete), or completely synthetic. The former relates mostly to treated allogenic or xenogeneic tissues that are usually combined with other natural or synthetic ingredients to assume a paste-like injectable form. Demineralised bone, for example, is often mixed with resorbable carriers or plasticizers (such as chitosan or hydroxypropyl methylcellulose) and presented as injectable pastes. Synthetic IBSs are comprised synthetically-derived biocompatible and biodegradable matter.

Currently there is an extensive market range of bone cements and putties available. Some of these commercially-available products have histories that span at least a few decades. Over recent years research regarding strategies to optimise the properties (such as injectability, setting time (for cements), cohesion and *in vivo* performance) of bone grafts substitutes has intensified. There is also ongoing effort to enhance other important factors such as delivery methods, storage requirements, sterilization methods and prolonged shelf-life. The material developed in this study

is an injectable, non-setting, off-the-shelf synthetic IBS intended for the repair of bony defects in non-load bearing areas. Most commercially-available synthetic bone graft substitutes incorporate some form of bioceramic (granules or powder) into a hydrogel carrier, with or without the addition of other bioactive or stabilizing agents. The aim of infusing ceramic particles in a viscous matrix is an attempt to mimic the combined mineral and inorganic phases of bone. The IBS developed in this study is a composite of β -TCP particles (of various sizes), bioactive glass particles and a polyethylene glycol-glycerol carrier.

1.2.3.1 TYPES OF INJECTABLE BONE SUBSTITUTES

1.2.3.1.1. Setting Injectable Bone Substitutes

Bone cements are ceramic-based viscous liquids that undergo chemical reactions to harden or set *in situ* via exothermic or isothermal reactions. These materials solidify to form bone-supporting structures. As such, they are used to provide mechanical support during the bone forming process. Furthermore, hardening pastes are usually injected into fracture spaces or around orthopaedic implants to augment hardware fixation into weak bone. Clinically-used injectable bone cements include, in order of popularity, calcium phosphate cements (CPCs), calcium sulphate cements (CSCs) and poly(methyl methacrylate) (PMMA) cements.

1.2.3.1.1.1. CSCs

The first calcium sulphate-based bone grafts were based on dihydrate calcium sulphate ('Plaster of Paris'). Plaster of Paris has a long history of clinical use. Calcium sulphate can be produced by chemical synthesis or by a gypsum calcinating process, can be gamma-sterilised, is biocompatible and bioactive, is completely resorbed through a process of dissolution, but lacks macro porosity which is considered essential for bone ingrowth [72]. There are reports of calcium sulphate-based materials achieving osseous repair in patients treated for bone cysts or benign tumours, even when demineralised bone matrix is not provided as a supplementary material [73, 74]. However, with a compressive strength of only 20-30 MPa [75] (compared to 20-60 MPa for CPCs [76]) compounded with the fact that it loses strength soon after implantation due to its rapid rate of resorption through

dissolution, calcium sulphate–based bone cements have become the least favoured clinical choice of setting IBSs.

1.2.3.1.1.2. PMMA

Originally stemming from applications in the ophthalmological and dental fields, PMMA has also been utilized in orthopaedics as a fixation material for implants and in the repair of fractures. It also has also been successfully applied as an antibiotic-loaded joint spacer in revision surgeries of chronically-infected joint prostheses [77]. This non-resorbable acrylic injectable bone cement has, however, certain drawbacks. These include its inability to actively bond with surrounding bone [78], its exothermic setting reaction which potentiates tissue necrosis [79], and its dissimilarity to surrounding bone which has been shown to lead to further vertebral fractures [80].

1.2.3.1.1.3 CPCs

First appearing on the market in porous block or granular forms, the discovery of calcium phosphate-based bone cements (CPCs) in the 1980s was a major leap in orthopaedic medicine. CPCs have an extensive history of use in dentistry, orthopaedics and reconstructive surgery due to their high interactivity and compatibility with bone [81]. Apatite (precipitated hydroxyapatite) and brushite (dicalcium phosphate dehydrate, DCPD) form the two primary classes of CPCs currently used. These cements are used alone, in conjunction with orthopaedic implants to provide a fixation interface between the hardware and bone, or in areas that must withstand compressive forces (compressive strengths up to 80 MPa). Some apatite-based commercial products include Norian SRS[®] (Synthes Inc.), Norian Drillable[®] (Synthes Inc.), BoneSource[®] (Stryker Inc.), HydroSet[®] (Stryker Inc.), Calcibon[®] (Biomet Inc.), alpha-BSM[®] (ETEX Corp.), Callos[®] (Skeletal Kinetics LLC), and known brushite-based commercially-available cements include ChronOs inject[®] (Synthes Inc.) [82].

Scientists have found that slurries of tetracalcium phosphate (TTCP) and dicalcium phosphate dihydrate (or dicalcium phosphate anhydrous (DCPA)) react to form HA whilst becoming a hardened mass [83]. Other research [84, 85] has revealed that implanted CPCs are gradually replaced by new bone without loss in volume, which has driven FDA approval for their commercial use in humans. The carrier or liquid

phase of bone cement undergoes a chemical reaction causing the injected material to harden either at room temperature or *in situ*. Depending on the chemical composition, both the carrier and embedded additives may be completely resorbed by the body over time. Whilst CSCs dissolve much faster than CPCs through non-cellular routes, CPCs are remodelled/degraded mainly through cell-mediated processes.

Injectable CPCs are self-setting and are made by combining one or two solid compounds of calcium phosphate salts with water or aqueous solution. The CPC pastes form when reactive calcium phosphate ceramic particles are mixed in aqueous solutions at concentrations greater than 1.5 g/mL [86]. Furthermore, unlike CSCs, CPCs set at physiological pH with minimal exotherm. For most CPCs, crystallisation (hardening) occurs within a few minutes of the two phases contacting each other, and the material normally 'sets' completely around 24 hours later. Chow [87] explains the setting of CPCs as a two-step process. In the first step hardening occurs through dissolution/precipitation reactions between the calcium compounds. The driving force for these reactions is based on the relative solubilities of the reactants and products. The solubility of calcium phosphates can be manipulated by changing the pH concentration of the aqueous environment. It is now known that there are at least 10 different calcium compounds, some which are in fact products of other cement systems, and used as ingredients for enhanced CPCs.

Based on chemical composition and structure, CPCs can be further classified - apatite cements include tetracalcium or α -tricalcium phosphate and brushite cements include a mix of β -tricalcium phosphate and monocalcium phosphate monohydrate. Brushite cements have great utility in certain applications due to their fast degradation rate and osteoclast-mediated resorption [88] which allows for bony ingrowths [89, 90], however, some findings suggest that this rapid resorption might in fact lead to lower quality bone formation [91]. Most commercial CPCs are products of a reaction between calcium compounds and carboxylic acids (e.g. glycolic, citric, tartaric, etc.) [92-94] and are chosen for their favourable properties e.g. fast setting time, cohesiveness etc. Most reported final products are apatitic, although the molar Ca/P ratio can be tuned to obtain DCPD or DCPA. HA is the most stable compound, maintaining its stability over a wide range of pH (4.4 and above). Other non-HA calcium compounds can also be used as starting cement materials to create cements in which water is used as the carrier phase, and HA

and its related apatitic phases (e.g. Ca-deficient HA, carbonated HA etc.) are formed as end products. These reactions are commonly supported by accelerators such as sodium phosphate solutions that speed up the hardening of the cement. In reverse, for $\text{pH} < 4$ conditions, DCPD and DCPA is formed as they are the least soluble calcium compounds in this pH range. General findings indicate that DCPD-forming cements are mechanically weaker than HA-forming cements. Amorphous calcium phosphates also exist, and though known to be successful in initiating bone formation [95], manufacturing difficulties have limited their application (Biobon[®] cement is the only commercially-available CPC containing amorphous calcium phosphate [96]).

The brittleness of CPCs is a cause for concern as disintegrated cement particles may leak into surrounding tissues and lead to problems such as nerve pain or venous and pulmonary embolisms [97]. This is one concern contributing to the ongoing efforts towards improving the mechanical, biological and degradation properties of CPCs. The most common approach to achieving this is to combine two or more types of calcium phosphates or to develop hybrids with polymers. Calcium phosphate compounds can be reacted with polymeric solutions to obtain a mouldable, self-hardening biomaterial [98]. In the 1980s some of the first injectable and hardening bone paste developed included biphasic cements [99], sodium alginate β -TCP cements [100] and gelatine and β -TCP mixtures [101]. The reaction occurs between the carboxyl group of the polymer and the alkaline calcium phosphate. Many studies based on aqueous solutions of chitosan mixed with calcium phosphate compounds demonstrate that after an initial hardening stage of the cement formed, calcium phosphate compounds continue to react amongst themselves, resulting in HA as the major final product [102, 103], as well as yielding a higher flexural strength [103, 104].

Although pre-fabricated blocks or granules are readily-available products for the surgeon to use, injectable forms of CPCs offer the important advantage mouldability to or conformation to defect shape. However, there are still many aspects of CPCs that need improvement if their use is to be streamlined for the operating theatre. In addition to their brittleness, setting bone pastes, are also limited by the curing times, polymerisation exotherms and post-polymerisation strengths [105]. Injectable CPCs have also been linked to many health complications, known as Bone Cement

Implantation Syndrome (BCIS), in patients who have received bone cement implants [106], which has also raised some concerns regarding their clinical uptake. Setting pastes should be injected very early in the setting phase, while only nucleation is taking place, so as to avoid injection of partially reacted cement which has been shown to lead to poor structure and mechanical strength in the final product [86]. The ideal cement should undergo rapid curing *after* injection. For PMMA bone cements, the degree of curing is also known to effect the degree of systemic absorption of the cement [106]. Method of improving cement curing time has been extensively studied as this is a limiting factor to most surgeries. This is addition to the cement preparation time, which is usually done manually in a mixing bowl during surgery. One study found that offering cements in a syringe applicator as opposed to manual mixing in a bowl saved significant time in the operating theatre, which the researchers extrapolated as nearly \$71,000,000 national and \$110,000 individual surgeon annual cost savings [107]. Another study brings to focus the effects of storage temperature and equilibration time on bone cement polymerisation in the operating theatre – an aspect formerly unregulated by bone cement manufacturers and surgeons [108].

The interest in injectable *foams*, which are essentially macro-porotic ($>10\ \mu\text{m}$) bone cements, has risen in recent years as the importance of cell infiltration for biomaterials is continuously reiterated in orthopaedic research. The term injectable foams is applied in literature [109] to calcium phosphate cements, biphasic hydrogels, hydrophobic polymeric scaffolds, and gas-foamed polymer scaffolds. For setting bone pastes, tissue-material interaction can be promoted through the incorporation of micro and macro-pores for tissue ingrowth as the characteristic slow resorption rate of cements could impede bone healing. First-generation CPCs have small pore sizes ($0.1 - 10\ \mu\text{m}$) and low porosity which has been associated with slow bone remodelling and poor bone ingrowth and ultimately cement failure [89, 110]. Porous cements experience a significant decrease in mechanical strength. To counteract this shortcoming, bioresorbable polymers can be incorporated into the paste which, after the material is set, can be degraded to create vacuoles that surrounding tissues can penetrate [104]. Sugawara *et al.* report the use of a sugar (mannitol) particles embedded in a CPC which later formed macro-pores *in situ* for tissue ingrowth [111].

1.2.3.1.2. Non-Setting Bone Pastes

1.2.3.2. Injectable Bone Grafts - Composition

1.2.3.2.1. Carrier Materials

Injectable bone pastes are typically multi-phase materials. The 'active' phase is generally an osteoconductive and/or osteoinductive material, such as a bioceramic and/or drug. The secondary phase is the carrier phase within which the former ingredients are homogeneously dispersed. To date, a number of carrier materials have been proposed and tested. Although there are some clear advantages or disadvantages that could be associated with different types of carriers, the choice or success of a carrier is also interdependent on the type of material/s it is actually carrying. The weight, size, morphology, dissolution kinetics, reactivity, charge and on the type of carrier that can be used in the IBS. As these carriers are non-setting viscous liquids, they are not impaired by issues such as curing rates or polymerisation by-products. They are, however, defined by properties such as degree of viscoelasticity or anti-washout resistance. Although these factors are assessed for the IBS as a whole, solid and liquid phase combined, the independent effects of each phase can be deduced, and materials selected accordingly.

Popular carriers for IBSs as cited in literature include hydroxypropyl methylcellulose (HPMC) – based polymers [112], alginate gels [113], poly(aldehyde guluronate) gels [114], hyaluronan gels [115], poly(propylene fumarate) (PPF)-based injectables [116] and composites such as PEG – PLGA [117]. The number of combinations of liquid polymers mixed to form injectable gels for drug or cell delivery in tissue engineering applications is extensive. For the purposes of this research thesis we will discuss the two main components of the liquid phase of the IBS studied here.

1.2.3.2.1.1. Glycerol

Glycerol is a naturally-occurring, strongly hydrophilic, polybasic alcohol, that has a diverse range of applications in medicine, from assisting water retention in severe cases of vomiting or diarrhea, reducing brain pressure in cases such as encephalitis, or as weight loss supplements. Glycerol may also be referred to with different names, including the commonly used glycerine. Since 1949, when the cryo-protective properties of glycerol was first discovered, glycerol has been used as a tissue-preserving medium [118]. Glycerol is also soluble in water, as hydrogen

bonding of water molecules to the hydroxyl groups in glycerol occurs. Furthermore, glycerol is an organic, non-toxic material which further supports its suitability as a carrier material in IBSs. Glycerol is commonly used in IBSs as the or part of the carrier phase as it is an additive that is known to improve the viscosity of the IBS, decreases interactions between particles to assist homogenous mixing of phases, and prevents separation of the liquid and solid phases [119].

Glycerol has been used previously as a carrier material in both setting and non-setting IBSs. In setting pastes, such as the calcium phosphate cement-glycerol pastes studied by Rajzer *et al.* [120], the hardening of pastes occur due to glycerol-water exchange, where following dissolution reactions precipitated crystals become entangled and thus cause hardening of the cement. By embedding the constituents of the CPC into glycerol, it has been possible to develop CPCs that are injectable and which self-set *in situ* when they come into contact with physiological fluids (due to the dissolution of glycerol) [121]. One study found that of the various carriers (glycerol, polyethylene glycol and polypropylene glycol) tested as the carrier phase of pre-mixed calcium phosphate cements based on α - tricalcium phosphate and calcium dihydrogen phosphate monohydrate, those that were composed of glycerol had higher compressive strength and were more cohesive [122]. Whilst glycerol may improve the injectability and setting time of injectable bone cements, they have been shown to also cause a decrease in material properties [123].

There are examples in literature, as well, of non-setting IBSs in which glycerol has been used in the liquid phase. Glycerol alone, does not appear to have any influence on the repair of bone defects when applied as a sole material [124], however, it has been shown to positively influence the consistency and handling of a non-setting IBS.

In a chitosan/hydroxypropyl methylcellulose/glycerol composite IBS, glycerol was included as it would promote, at specific concentrations, the formation of hydrophobic regions in the HPMC-based carrier phase of the IBS, thereby lowering also its phase transition temperature so that gelation of the IBS could be achieved at body temperature [125]. One commercially-available product, Grafton™ (Osteotech, Eatontown, NJ, USA), uses glycerol as the carrier matrix for its insoluble collagen-proteins mix obtained from demineralised human bone. Another DBM-based non-setting IBS which uses glycerol as a carrier is Viagraf (Smith and Nephew). The reason for including glycerol in injectable bone substitutes is that it

has a hygroscopic nature acting as a humectant (i.e. it holds moisture) and therefore allows preparations to remain 'wet' over longer storage times [126].

1.2.3.2.1.2. Poly (ethylene glycol) (PEG)

PEG, commonly also known as poly (ethylene oxide) (PEO) (they share the same chemical formula and CAS number), is a polyether composed of glycerol monomers, is another preferred polymer for medical applications. 'PEG' is generally used when the polymer is less than 50,000 Da, whilst 'PEO' is used for higher molecular weights. The interest in PEG in both controlled delivery and tissue engineering applications has grown rapidly in recent years. One reason for the popularity of PEG in biomaterials research is its ability to be manufactured into water, oxygen and nutrients permeable materials, making them ideal for use in tissue engineering applications [127]. PEG is soluble in water. This is due to the hydrogen bonds formed between water molecules and the electron-rich oxygen atoms in PEG chains. In fact, the hydrophilic nature of PEG makes them excellent carriers for water-free CPCs, allowing them to be stored for long periods of time without degradation or reaction [128].

PEG based hydrogels in bone tissue engineering are widely popular, for several reasons – they are highly hydrophilic, bioinert and have outstanding biocompatibility. Furthermore, their chains are terminated by hydroxyl groups which can be converted to more reactive groups, allowing the chains to undergo polymerisation and form networks or polymerise with other species and form functionalised materials. PEG is also miscible in in other forms of PEG. PEG lends itself to tuning methods which are used to either further functionalise the chains themselves or create cross-links between chains as a means of varying rheological performance of the hydrogel networks. For example, cell adhesion and BMP entrapment and delivery was achieved with pendant oligopeptide ligands and matrix metalloproteinase, respectively, in a PEG hydrogel for the repair of bone defects [129]. In another example of hybrid PEG networks, the successful repair of rat tibial defects using PEG-fibrinogen hydrogels cross-linked through photo polymerisation, was demonstrated by Peled *et al.* [130]. Literature is filled with studies that support the notion that modified-PEG composites are highly successful in delivering cells to defect sites for tissue regeneration [131-133].

In hybrid injectable scaffolds involving PEG, it has been shown that varying both the ratio and molecular weight of PEG will vary the mechanical properties of material [134]. Combining PEG with other materials such as poly (propylene fumarate) [135] or polycarbonates [136]. Furthermore, varying the density of cross-linking between PEG chains, amongst other factors, is a tool for controlling the degree of compression and nutrient flow to proliferating chondrocytes encapsulated in PEG hydrogels [137]. The degradation property of PEG is also usually altered by infusing other more degradable polymers into PEG systems to increase their degradation rates. This was achieved by Kaihara *et al.* who successfully synthesised a cyclic acetal-modified PEG hydrogel [138], in which the incorporation of terminal cyclic acetals was found to be an effective way of tuning the degradation profile without causing the release of acidic by-products upon degradation of the material [131]. PEG-alone hydrogels have previously been found to be pro-inflammatory when not combined with attenuating additives, are degraded by stimulated macrophages, and are also some susceptible to oxidative degradation as well [139].

1.2.3.2.2. Bioceramics

Biocompatible ceramics as bone graft substitutes have over a 100-year history of use, however their popularity grew exponentially after the 1970s. The term 'bioceramic' is used in literature to cover glasses, glass-ceramics and ceramics that are used as orthopaedic implant materials. Most medically-used bioceramics are of the calcium phosphates family. Calcium phosphate ceramics (CPCs) are used as alternatives to autologous bone grafts to fill tumour defects, tibial plateau fractures, spinal fusion, scoliosis surgery etc. [140]. Calcium phosphate-based ceramics make up for most of the bone graft substitutes in the market as they have a uniquely strong material-tissue bond and do not form fibrous interfaces as do bio-inert materials. CP ceramics differ in their composition, which is also a reflection of the source of origin and preparation method. They can be manufactured into many different forms including dense or porous (macro-porous / micro-porous) particles or blocks. A range of fabrication techniques have been previously explored for the preparation of CP ceramics and some include hydrolysis, hydrothermal synthesis, hydrothermal exchange (coral-derived ceramics), solid process from bovine bone (ceramised xenograft), sol-gel processes, spray pyrolysis from natural coralline, and wet

chemical methods [72]. Conventional CP ceramics are prepared from highly purified pre-powders in 4 broad stages: 1° Powders are calcined (<900 °C), 2° Powders are compacted and sintered (1100 – 1300 °C), 3° Cooling (at controlled rates). During the cooling stage, re-crystallisation and grain growth of the original powder is observed. The final material is an aggregate of crystals, with redefined chemical, physical and biological properties.

The calcium to phosphate (Ca/P) ratio of the starting material determines the physical and chemical qualities of the final CP ceramic synthesised. Generally, low Ca/P ratios mean faster degradation, and this translates as a rapid loss of strength in a physiological setting. Slow degradation, however, as seen for HA, prevents the replacement of the ceramic material with newly formed native bone and is generally characterised with less bone formation. Moreover, slowly degrading CP ceramics may give rise to remnants that may later trigger inflammation. It has been found that the mechanism of degradation for a calcium phosphate based materials is also directly related to the method of synthesis. Lu et al. explain that whilst sintered bioceramics show good crystallinity and are degraded by a process dependent on interstitial fluids, bone cements synthesised via physiochemical crystallisation are degraded by a cell-driven dissolution process [141]. Different calcium phosphate ceramics are often combined as a strategy for controlling the degradation rates. Some popular calcium phosphates and their Ca/P ratios are presented in the table below:

Table 1. Ca/P Ratios for Popular Calcium Phosphates

Ca/P	Name	Formula	Acronym
2.0	Tetracalcium phosphate	$\text{Ca}_4\text{O}(\text{PO}_4)_2$	TTCP
1.67	Hydroxyapatite	$\text{Ca}_{10}(\text{PO}_4)_6(\text{OH})_2$	HAP
1.67-1.50	Calcium-deficient HAP	$\text{Ca}_{10-x}(\text{HPO}_4)_x(\text{PO}_4)_{6-x}(\text{OH})_{2-x}$	CDHAP
1.50	Apatitic tricalcium phosphate	$\text{Ca}_9(\text{HPO}_4)(\text{PO}_4)_5(\text{OH})$	ATP
1.50	Tricalcium phosphate (α, β, γ)	$\text{Ca}_3(\text{PO}_4)_2$	TCP
1.33	Octacalcium phosphate	$\text{Ca}_8\text{H}_2(\text{PO}_4)_6 \cdot 5\text{H}_2\text{O}$	OCP
1.0	Dicalcium phosphate dihydrate	$\text{CaHPO}_4 \cdot 2\text{H}_2\text{O}$	DCPD
1.0	Dicalcium phosphate anhydrous	CaHPO_4	DCPA
1.0	Calcium pyrophosphate (α, β, γ)	$\text{Ca}_2\text{P}_2\text{O}_7$	CPP
1.0	Calcium pyrophosphate dihydrate	$\text{Ca}_2\text{P}_2\text{O}_7 \cdot 2\text{H}_2\text{O}$	CPPD
0.7	Heptacalcium phosphate	$\text{Ca}_7(\text{P}_5\text{O}_{16})_2$	HCP
0.67	Tetracalcium dihydrogen phosphate	$\text{Ca}_4\text{H}_2\text{P}_6\text{O}_{20}$	TDHP
0.5	Monocalcium phosphate monohydrate	$\text{Ca}(\text{H}_2\text{PO}_4)_2 \cdot \text{H}_2\text{O}$	MCPM
0.5	Calcium metaphosphate (α, β, γ)	$\text{Ca}(\text{PO}_3)_2$	CMP

There are four main groups of calcium phosphate ceramics used in medicine. Calcium tetrphosphate, hydroxyapatite (or hydroxylapatite) (HA), tricalcium phosphate and dicalcium phosphate, of which hydroxyapatite and β -TCP are the most widely used. HA is much less resorbable than β -TCP [142-144].

Hydroxyapatite (HA) belongs to the calcium phosphate ceramics group and can be either coral-based or chemically-derived ($\text{Ca}_{10}(\text{PO}_4)_6(\text{OH})_2$). Hydroxyapatite is the primary inorganic component of bone. Ceramics such HA can be produced from natural sources such as the *Porites* and *Goniopora* coralline species through a hydrothermal exchange reaction that can convert the calcium carbonate coral skeleton to CP. Synthetic HA is obtained from the precipitation of calcium nitrate and ammonium dihydrogen phosphate. Clinically, HA presents many benefits including good mechanical properties, radio opacity and ability to be re-sterilised. The first successful use of HA as bone substitute dates back to 1951 [145]. In commercial HA-based products, it is important that each product is uniform in the Ca-P ratio, particle and pore sizes for reproducible results. HA ceramics are slow-degrading ceramics with clinical reports confirming no radiologically obvious degradation of HA blocks/granules observed up to 5 years post-implantation [146]. HA and β -TCP are often combined to form biphasic calcium phosphate (BCP) to optimise their advantages [147]. They are mixed in variable ratios to tailor degradation rate, mechanical strength and bioactivity to specific applications [148]. There is also evidence to suggest that HA, or HA alone, may not be the best biologically-interactive material in tissue regeneration applications. One group compared the *in vivo* performance of HA and β -TCP porous ceramics of approximately the same mean pore size (100-300 μm), mean porosity (50%) and mean interconnection size (30-100 μm), and the results indicated that new bone growth and calcification rate inside β -TCP ceramics significantly correlated with increasing density of interconnectedness, whereas this rate did not differ in HA scaffolds [149]. HA-TCP hybrids possess an excellent bone incorporation capacity [150].

Tricalcium phosphate (TCP) exists at room temperature in two crystal forms, namely, α -TCP and β -TCP. α -TCP, is considerably more soluble than β -TCP. Both α - and β -TCP can be subjected to an amorphisation process the products of which, when combined with water form cements with very different properties [151].

Octacalcium phosphate (OCP) is the only non-sintered granular calcium phosphate (prepared by precipitation methods) that has shown promise as a bone graft substitute. In one study fine filaments and granular materials in newly formed bone surrounded OCP aggregates only 7 days post-implantation in mice [152], and in another study synthetic OCP was able to initiate new bone formation in critical-sized defects both on the implanted OCP away from the defect margin and also from the margin of the defect to the implanted OCP [153]. OCP has been shown the ability to serve as a core for initiating bone formation, causing both osteoinduction and osteoconduction in rat skull defects [153].

There are many parameters that influence the biodegradability, mechanical strength, cell adhesiveness and bone-ingrowth capacity (bioactivity) of a calcium phosphate ceramic. These include its crystallinity and crystal size, particle size and distribution, surface roughness, porosity and pore interconnectedness [143, 144, 154]. Chang *et al.* demonstrated that different pore geometries in HA cylindrical blocks each produced different histological changes depending on pore geometry [155].

The porosity of the final material can be tweaked through the addition (followed by elimination) of porogens (such as naphthalene) in the sintering step. Traditional sintering, as prescribed, gives rise to pores $<100\ \mu\text{m}$. The sintering process can also be completed in other ways such as microwave processing. Many sintering techniques exist for bioceramics such as two-step sintering, liquid phase sintering, hot pressing, hot isostatic pressing, ultrahigh pressure, microwave and spark plasma sintering, as extensively reviewed by Champion [156]. Microwave sintering holds great appeal for calcium phosphate ceramics manufacturers due to the significantly reduced processing times possible with this method. More importantly, authors report that smaller grain size, higher compressive strengths and overall better architecture within calcium phosphate ceramics can be obtained with this method, in addition to significantly reduced processing times which holds commercial appeal [156-158]. The biocompatibility of ceramics prepared with microwave sintering also appear to be unaffected [159, 160].

The bioactivity of bioceramics is the degree to which the synthetic material can communicate with and conduct local proteins and cells toward new bone production. The mechanism of interaction is initiated by the recruitment of Ca^{2+} and PO_4^{2-} ions from surrounding bone tissue as well as releasing them from the ceramic itself. This

ion deposition on the surface of the implanted ceramic forms a biological apatite layer. The apatite crystals bond and work with the local proteins (e.g. collagen) and factors (e.g. growth factors) present in the extracellular matrix to form a biological interface with the host tissue. Meanwhile, osteoblasts, other cells of the osteogenic lineage and angiogenic migrate into the material, attach, differentiate and proliferate, depositing newly formed bony matter. Running simultaneous to these events is the disintegration of the bioceramic through catabolic cellular mechanisms. Cellular breakdown of the material by giant cells and macrophages is mediated through the chemotactic agents present in the apatite HA layer formed. Direct contact between material and tissue is important otherwise the implant material experiences the interposition of a fibrous layer that blocks bone tissue infiltration. The degradation rates of bioceramics must harmonise with the rate of bone formation and any degradation products must not cause any cytotoxicity to the cells at work within and around the implanted material.

CP ceramics, particularly porous CP ceramics, suffer from poor mechanical strength under shear and tension, with limited capacity for compressional loads as well. They are thus usually not indicated for constrained or load-bearing areas. CP ceramics may therefore be offered in combination with other biocompatible synthetics that can aid the overall mechanical performance of the implant. Hybrids with polysaccharides such as chitosan have produced encouraging results. A biodegradable scaffold composed of β -TCP, chitosan and gelatin developed by Yin *et al.* displayed improved compressive strengths and potential use for non-load-bearing applications [161]. The 2006 work by Ding, however, found that a CaP/chitosan ratio of 5% by mass to volume in the composite achieved the significantly highest bending strength with any further CaP ceramic addition yielding poorer outcomes [162]. The study highlights the notion of optimal ceramic-polymer ratios. The mechanical properties of a CP ceramic are also highly dependent on the manufacturing process used during production. Laasri *et al.* present the influence of powder manufacturing and sintering temperature on densification, microstructure and mechanical properties of β -TCP [163]. They explain that properties such as hardness and flexion toughness decrease with higher sintering temperatures, even though higher densities are obtained. Properties such as hardness, fracture toughness and Young's modulus, however, increase in direct proportion to sintering temperatures, up until 1160 °C. Thermal-activated grain growth, the presence of

micro-cracks and pores were thought to relax residual stresses in the material. This study is a prime example of the sensitivities of bioceramic mechanical properties to manufacturing parameters.

1.2.3.2.1. Bioactive Glass

Bioactive glass (BG), has become an increasingly popular bioceramic for both the clinic and scientific research. The interest in bioactive glass was first stimulated by Larry Hench in 1969 when he was able to demonstrate its superior ability to chemically bond with and stimulate bone regeneration. This first bioactive glass material, referred to as Bioglass[®] (trademarked by the University of Florida), Hench's Bioglass[®] or 45S5, was composed of 46.1 mol.% SiO₂, 24.4 mol.% Na₂O, 26.9 mol.% CaO and 2.6 mol.% P₂O₅. Bioactive glasses have not received the same wide commercial uptake as calcium phosphates such as tricalcium phosphate or synthetic hydroxyapatite due to some of the manufacturing limitations experienced initially with Bioglass[®] 45S5. Today, several fabrication techniques have been developed to process melt- and sol-gel- derived bioactive glass into porous or solid particles, blocks or scaffolds for bone tissue engineering applications. The potential uses of bioactive glasses have increased by combining them with polymeric materials, producing a material that is no longer incapable of cyclic loading due to its brittleness, but rather more aligned to the mechanical characteristics of native bone.

The extremely strong bonding of Bioglass[®] 45S5 to bone is thought to be facilitated through the exposure of hydroxycarbonate apatite (HCA) (formed after initial dissolution) which interacts with collagen fibrils in the tissue matrix and prompts new bone formation [164, 165]. Calcium phosphate nucleation on Si-OH groups precedes HCA nucleation on glass surfaces, and the degree of HCA nucleation depends on silica content (essentially the connectivity of the network) and the presence of other glass-modifying ions [166]. The bone forming ability of bioactive glass occurs through the adsorption of proteins to the HCA layer, which conducts cell attachment and differentiation and finally 'osteoproduction' [167]. Furthermore, its osteoinductive properties have been attributed to the release of dissolution products such as soluble silica and calcium ions which go on to stimulate osteogenic cells to produce more bone matrix [168]. Also, cation release during dissolution increases local pH which in effect gives bioactive glass its antimicrobial quality [169].

The effect may even be enhanced by introducing silver ions into the glass structure [170]. Strontium-doping of BG has also been shown to inhibit osteoclast activity whilst promoting osteoblast metabolism [171]. Bioglass[®] 45S5-coated PLGA scaffolds doped with vascular endothelial growth factor also demonstrated better mitogenic stimulation of endothelial cells compared to uncoated samples, signifying the contributions of bioactive glass towards angiogenesis in bone repair [172]. For these reasons, bioactive glass is deemed 'bioactive' as it imparts many benefits to the bone repair process.

There are several classes of bioactive glass: silica-based, phosphate-based and borate-based. Each composition of bioactive glass has its own advantages and thus suitability for specific applications, although there is, to date, no bioactive glass that has performed better than the original Bioglass[®] 45S5 composition, bar the difficulty in creating fibres, scaffolds or coatings. Its application falls into 4 main categories: monolithic medical devices, particulates for bone regeneration, hypersensitivity treatment in oral care and coating for implants. Bioglass[®] 45S5 has been available commercially in the forms of Middle Ear Prosthesis (MEP[®]) [173], Endosseous Ridge Maintenance Implant (ERMI[®]) [174], and orbital implants [175]. The history of Bioglass[®] 45S5 in bone regenerative medicine began in 1993 as PerioGlass[®] (NovaBone Products LLC, Alachua, FL) and has a successful clinical history in periodontal defects, or for fixation of dental implants [176-179]. Novabone[®] (NovaBone Products LLC, Alachua, FL) followed the success of PerioGlass[®], as a synthetic bone graft material for non-load bearing orthopaedic defects (e.g. as a bone substitute in spinal fusion surgery) [180]. There are several other bioactive glass-based products currently available including Biogran[®] (BIOMET 3i, Palm Beach Gardens, FL) (45S5 composition, but with a narrower (300 – 360 µm) particle size) and BonAlive[®] (BonAlive Biomaterials, Turku, Finland) (S53P4 composition). In oral care, NovaMin[®] (NovaMin Technology, FL; now owned by GlaxoSmithKline, UK), a very fine Bioglass 45S5 particulate has been used to combat teeth hypersensitivity as it adheres to dentine, forming a HCA layer that blocks tubules within dentine connected nerve endings [181-183]. As a method of preventing fibre encapsulation of metal implant surfaces and improving the tissue-implant interface bioactive glass is, in principle, an ideal coating material. However, not only is bioactive glass biodegradable leaving it to long-term instability of implants, they are also unable to undergo sintering which is key for a good coating. The crystallisation

temperature has been reported to be 650 °C for Bioglass® 45S5 [184], and current research efforts are geared towards developing composites that can overcome the low-temperature crystallisation problem [185]. Jones presents an extensive review of bioactive glass-polymer composite materials developed for tissue engineering and repair applications [166]. Furthermore, BG does not readily match the thermal expansion coefficient of most commonly used biomedical metals which means separation between the two materials occurs during manufacturing [186].

There are two main methods of producing bioactive glass. The first is the highly versatile sol-gel route involving the mixing of compositional precursors which coalesce to form a gel, silica network which is then dried and heated to remove the water and alcohol produced during condensation, leaving behind an interconnected porous glass. Pore sizes typically range between 1 - 30 nm. These nanoporous glasses (whilst using only a few components), can be further processed to obtain nanoparticles, powders or monoliths. With higher surface area to volume ratios, they have higher dissolution rates than melt-quenched glasses. The melt-quenching technique involves the melting together oxides at high temperatures followed by quenching and is generally preferred when crack-free monolithic structures are required.

Numerous *in vivo* studies confirm the biocompatibility, degradation profiles, osteogenic behaviour and non-cytotoxicity of bioactive glasses. The degradation rate of bioactive glasses depends on graft morphology, size, particulate size and implantation site. In one study [187], bioactive glass of narrow size range (300 - 355 µm) showed a superior bone formation capacity. Histological analyses revealed the formation of protective pouches within the particles, within which islands of newly formed bone were present. The pouches form as a side effect of the corrosive reactions of the bioactive glass. Oonishi *et al.* have shown that Bioglass® 45S5 particles (300 - 360 µm) are capable of completely restoring load-bearing defect sites within 2 weeks [188]. On the other hand, Hollinger *et al.* demonstrated that particles (90 - 710 µm) of Bioglass® 45S5 were able to facilitate union in only one of six critical-sized defects created in rabbit radius [189].

The degradation mechanisms of bioactive glasses are believed to initially be solution-mediated dissolution, followed by osteoclast intervention [190]. Compositions of 45S5, 52S, and 55S implanted in the distal femoral epiphysis of rabbits were found in one study to degrade in either in Si-rich remnants or in CaP-

shells [191]. Osteoclast-mediated degradation was also observed. The authors further concluded that the composition of the substrate influences the types of multinuclear giant cells which arrive at the degradation site. *In vivo* models have been used to prove the safe excretion of Si through urine with no observable damage to important organs [192, 193].

Bioactive glasses are hard, non-porous materials consisting of silicon with a mixture of sodium, calcium, phosphate or borate—silicon is the network forming atom. In silicate glasses the sodium and calcium disrupt the network by forming non-bridging oxygen bonds. Phosphate is only present in orthophosphate environments, is rapidly dissolved in aqueous environments and negates the roles of sodium and calcium when present [194]. The solubility/resorbability of bioactive glasses can be altered by varying the ratio of sodium oxide, calcium oxide and silicon dioxide.

1.2.4. Design Considerations for Injectable Bone Grafts

Factors such as pore size, porosity and interconnectivity play a paramount role in the *in vivo* performance of bioceramics used in regenerative orthopaedics. Pores allow space for biological and cellular events to proceed toward bone formation. A pore size of at least 100 μm is optimal for bone growth [195] and pore sizes greater than at least 200 μm have been shown to facilitate the development of mature osteon [196]. Porosity, is the degree of distribution of pores throughout a biomaterial. High porosity presents the challenge of reduced mechanical strength, and for brittle bioceramics, this becomes a limiting factor. Equally important to porosity, however, is interconnectivity between pores. Interconnectivity is related to the vacuous pathways between pores and is essential for supporting vascular supply to the in-growing bone. Lu *et al.* [149] propose the concept of interconnection density as a quantitative approach to measuring the quantity of links between the pores of porous materials. Working with HA and β -TCP ceramics, they were able to determine that although 20 μm interconnection size allows cell infiltration and chondroid tissue formation, this size should be at least 50 μm to ensure new bone ingrowth inside pores.

1.2.4.1. Rheological Properties

Rheological properties such as injectability, cohesion and viscosity are of critical importance for an injectable bone graft substitute. The ingredients of a synthetic bone paste must satisfy the requirements of all three properties to ensure that a stable, injectable and clinically-effective biomaterial is obtained. Solids dispersed in a carrier phase have the tendency to phase separate. The challenge is to determine the ratio of solid to liquid particles, such that most biological and mechanical effectiveness of the synthetic graft is maximised, whilst the viscosity is low and stable enough to allow ease of injection without phase separation. The graft itself is expected to not disintegrate or wash away once within the physiological environment of the body and thus cohesion vs velocity becomes another interplaying issue. All bone paste materials are thus designed to be of:

1. viscosity that requires only a reasonable amount of pressure for injection
2. chemical cohesiveness sufficient to prevent phase separation (for multi-phase pastes) during application
3. anti-washout quality which is generally achieved via additives that promote viscosity or cohesiveness.

To date, there is no universally accepted single definition of injectability. The concept of injectability varies between various studies, however, some common approaches state that injectability is:

- related to the force required to be applied to the syringe for material to be ejected (independent to the fact that force is a function of syringe size) [197]
- related to a specific cannula size (typically <0.1 mm for minimally-invasive surgeries) below which the paste cannot be fully injected anymore [198]
- related to the ability of the paste to remain homogenous under pressure of injection i.e. no phase separation (which results in filter-pressing (discussed later)) occurs [199]
- related to the recorded mass of the extruded paste compared to the original mass of the total paste in the syringe prior to extrusion [70, 200]

Baroud *et al.* [86] explain the underlying pressure mechanism of injectability as a two-step process: a) the pressure required to overcome the yield stress of the paste and trigger paste flow and b) the pressure required to maintain the flow of the paste. The former is a parameter that has not been widely explored in literature and the latter is a direct reflectance of paste viscosity.

This is particularly true for biphasic pastes composed of a hydrogel and fine ceramic particles where upon ejection from a syringe, the flow of the liquid phase (hydrogel) surpasses the flow of the solid phase (ceramic particles) leaving the solid phase to remain within the barrel of the syringe whilst the liquid phase is ejected. Previous studies have found that such phase separation results in a thick, wet powder rather than paste forming at the plunger, preventing its motion (also known as filter-pressing) [201-203]. As the solid-liquid phase separation phenomenon follows the principles of high-low pressure gradients (from the plunger to the canula tip, respectively), the effects observed are dynamic i.e. more wet powder forms as the plunger is pushed and the liquid phase is ejected. Consequently, valuable synthetic graft material is lost - a highly problematic situation during surgery.

Several studies have contributed to understanding the key parameters that impact filter-pressing. In a study performed by Bohner and Baroud [201], it was found that reducing the size of the particles of the solid phase in calcium phosphate ceramics significantly counters filter-pressing. Others have shown that the use of rounder particles or additives also have a positive impact on injectability [204]. Bohner and Baroud have demonstrated that the LSR and plastic limit may be interchangeably manipulated to control the viscosity of pastes. The plastic limit is described as the minimum amount of liquid required to form a paste. The authors describe that a larger difference between the LSR and plastic limit leads to greater viscosity. To achieve this, the LSR could be kept high [201, 205], whilst the plastic limit could be reduced with additives to the liquid phase such as citrate ions or polyacrylic acid [151, 201, 206, 207]. Ionic modifiers alter the zeta potential of the suspension leading to an increase in the electrostatic repulsion forces between the solid particles [208].

The concept of viscosity for non-setting bone pastes or bone cements is in technical terms a discussion of viscosity as a function of shear stress as these materials are non-Newtonian fluids [86]. The viscosity of calcium phosphate pastes was first studied by Bujake [209] who investigated a dicalcium phosphate dihydrate,

glycerine, and water - based suspension. The particle size of the solids dispersed in the liquid phase of the paste has been found to be inversely proportional to the viscosity of the paste, observations made also by other authors [210-212]. Rao and Kannan [213] observed a yield stress of 5 Pa, and a shear-thinning followed by shear-thickening behaviour in hydroxyapatite suspensions, which is a finding supported by other studies that confirm that shear thickening occurs at high particle loading in calcium carbonate [214] , silica-based [211] and calcite [215] suspensions.

There are several methods of modifying the viscosity of bone pastes. The first method is to alter the LSR of the paste. The second option is to vary the particle size distribution of the solid phase which is possible by varying the milling times of the ceramic particles. Gbureck *et al.* [207] reaffirmed the notion that viscosity could be enhanced through a greater particle size distribution of solid particles. The final technique is changing the ingredients of the synthetic graft material through the addition of viscosity modifiers. Several studies have also demonstrated that polymeric additives such as polysaccharides can increase the viscosity and thus injectability of bone cements [128] . These additives play a double role in promoting both higher cohesiveness with lower paste viscosity.

The comprehensive study performed by Baroud *et al.* investigated the effect of all three abovementioned factors on aqueous β -TCP suspensions and found a strong positive correlation between yield stress and viscosity, the addition of xanthan increased yield stress and viscosity, the addition of sodium polyacrylate reduced yield stress and viscosity, extended milling of β -TCP particles resulted in higher yield stress, increasing the LSR caused lower yield stress and lower viscosity [86]. The results of this study are a valuable insight into the rheological behaviour of non-setting pastes and considerations for commercial products. For example,

The viscosity of bone filler materials is largely related to and important to the cohesiveness of the material. Cohesion, also referred to as 'non-decay', is the ability of the material to keep its geometrical integrity in aqueous solutions. Cohesion is one of the primary properties of non-setting synthetic bone pastes that must be tailored to the intended degradation profile for the material. Although a degradation profile generally addresses the amount of material degraded over a given period, for multi-component systems a simultaneous degradation of all phases is critical. The burst release or rapid elution of milliparticles or microparticles from synthetic

suspensions could potentiate negative *in vivo* reactions if released in copious amounts too quickly [216, 217], or otherwise, diminish the expected long-lasting effect of the biomaterial.

Cohesiveness of injectable bone graft materials can essentially be improved by factors enhancing the attractive forces between the particles of the material such as van der Waals forces, and decreasing electrostatic forces (repulsive). Bohner *et al.* showed that this was possible through decreasing mean particle size and LSR, and increasing the ionic strength of the mixing solution [218].

Polymeric substances or hydrogels capable of creating consistent viscosity and cohesion in injectable bone grafts have received much research interest over the past decades. The addition of soluble polymers to the liquid phase assists in preventing the penetration of surrounding fluids and thus the disintegration of the paste. Various gelling agents such as hydroxypropyl methylcellulose (HPMC), carboxyl methylcellulose (CMC), collagen and hyaluronan are known to significantly improve washout resistance and handling properties of injectable bone substitutes [52, 219-221]. CMC is particularly useful for calcium phosphate-based injectable bone grafts as this versatile polysaccharide is not only biocompatible and biodegradable but cathodic in nature and promotes calcium phosphate mineralisation through the interaction of its carboxyl group with calcium ions [222, 223]. It also has reported benefits such as improved handling and support of bone formation in calvarial defect models when used as a binder in calcium sulphate pastes simultaneously carrying de-mineralised bone matrix [224]. Similarly, hyaluronic acid, one of the most widely distributed glycosaminoglycans in animal tissues, is proven to increase viscosity and therefore the handling properties of calcium phosphate grafts due to its high affinity for calcium phosphate [225]. Many more agents are available for the purposes of enhancing viscosity and cohesiveness of pastes such as sodium alginate [226] and gelatin [227] and the suitability of the additive depends on the final application of the product, its reactivity with other constituents, and for commercial applications, any regulatory regulations or standards.

1.2.4.2. Handling and Delivery

The commercial success of an IBS is heavily dependent on two major factors – handling properties and delivery. Handling refers to the ability to install the product

without any loss of its chemical or physical properties whilst doing so. For IBSs, this also includes the degree to which the product can be manually moulded or manipulated to conform it to the shape of a defect site. The cohesive and adhesive properties play a particularly important role in the maintenance of material consistency during handling. The method of delivery is also of paramount importance to the design, function and marketability of an IBS. The clinician is always interested in a relatively simple delivery apparatus that is easy to prepare and/or use during implantation. Injectability and viscosity impacts on how well the material is expelled from the delivery device into the treated area and thus how much effort is required by the surgeon. Furthermore, high radio-opacity is highly favourable for optimal control during injection and post-operative examination to ensure degradation is occurring at the expected rate and that the material has not migrated. Aside from its chemical, biological and physical performance superiority, these key requirements also have an immense impact on the handling and delivery, and largely the popularity of an IBS.

Commercially-available IBSs are available in either pre-mixed forms ('ready-to-use') or are those which require a preparatory step during surgery. It is worthwhile considering the respective advantages and disadvantages of each form and the scenarios in which they may be deemed the necessary option. Whilst the time saved, ease-of-use and the elimination of the risk human error during mixing are some of the assets of pre-mixed IBSs, the 'pre-defined' nature of the products could be seen as a restrictive feature for some cases. Products that are prepared in the operating theatre have the added option of combining other therapeutic agents such as drugs or platelet-rich plasma to the base constituents of the paste, to enhance healing. Products that require mixing on-site, have the flexibility of including other therapeutic products such as drugs or platelet-rich plasma as desired or required. This may be particularly useful in more significant defects that require a boost in healing mechanisms. Offering this sort of versatility may thus be in the interest of both the producer as well as the surgeon. Fixed compositions that are unable to hybridise with other factors retain their popularity in more straightforward treatments where its inherent capabilities are sufficient for successful bone repair.

The commercial forms of IBSs are essentially influenced by the chemical nature of the product i.e. whether it is a setting or non-setting paste/composition. Non-setting pastes are generally offered as single-use pre-mixed delivered via open-bore

syringes. Prepared, packed, sealed and sterilised during the manufacturing process, the surgeon receives the end-product made ready for injection. Pre-mixed IBSs may contain allogenic (demineralised bone matrix, animal-sourced collagen) and/or non-allogenic (calcium phosphate ceramics) content. There are a large variety of ingredients that have been used in non-allogenic, synthetic pre-mixed formulations. The solid phases of currently marketed pre-mixed putties vary from hydroxyapatite to bioactive glass, whilst carriers range from water to synthetic binders such as hydroxypropyl methyl cellulose. Such pastes do not pose a time constraint for application as is the case for cements that experience hardening reactions. There are two current methods for developing a pre-mixed calcium phosphate cement. The first is through the use of non-aqueous carrier materials that prevent hardening of the mixture until it is exposed to physiological fluids. Aberg *et al.* [121] have developed a pre-mixed CPC containing glycerol as a carrier, reporting excellent post-implantation bone growth in rabbit femur defect models. Xu *et al.* [228] also report a number of potential premixed CPC formulations consisting of CPC powder, non-aqueous liquid (PEG 400), gelling agent (hydroxypropyl methylcellulose) and hardening accelerator (tartaric acid, malic acid, malonic acid, citric acid, and glycolic acid) that have good setting, strength and osteoblast viability properties and which harden upon contact with physiological fluids. The second method for obtaining a premixed CPC, as first described by Grover *et al.* [229], is a freeze down approach. The group disclose brushite cement formulations which are frozen and stored at -80 °C or less immediately after mixing the solid and liquid components. The researchers report there was no loss of functional performance compared to the control (unfrozen formulations) and in fact that for brushite cement formed from the combination of β -tricalcium phosphate with 2 M orthophosphoric acid solution, freezing increased compression strength (from 4 to 20 MPa) and reduced setting rate. Such cements do, however, still have drawbacks such the inability to effectively control the *in vivo* hardening reaction.

Another delivery option that allows the clinician to dispense the manual mixing stage for setting CPCs have been previously proposed [230, 231] where the reactive phases of CPCs are combined inside a static mixer during injection. This removes the issue regarding time constraints, and the syringe can be discarded if any problems during the reaction occur. However, cannula blockage is a possibility for more viscous pastes and the method has been previously described for only

brushite CPCs (less common than apatite CPCs) [230] and CPCs that contain non-aqueous carriers [231]. CPCs provided as pre-mixed products remains a problem for the synthetic bone graft industry. Mixing CPC components during surgery could negatively impact the performance of setting IBSs if the operator uses inappropriate liquid-to-solid ratios or does not prepare a homogenous mixture.

As mentioned previously, the radiopacity of a biomaterial adds tremendously to its utility both during delivery and for post-operative clinical observation [232]. An increase in radiopacity values over time of implanted bone graft materials can provide information to a clinician as to whether healing is occurring and thus whether a bone substitute material is osteoconductive or not, as demonstrated by Bucchi *et al.* [233]. It has therefore become a growing interest of material scientists to enhance the radiographic properties of synthetic bone grafts with contrast-enhancing materials such as iron oxide nanoparticles [234].

Table 2 given below is adapted from Bohner [199] and provides an overview of some commercial IBSs that are offered in ‘pre-mixed’ or ‘to-be-mixed’ forms.

Table 2. List of commercially-available ‘pre-mixed’, ‘to-be-mixed’ and other injectable bone graft substitutes (adapted from Bohner [199] with permission

Producer	Product name	Composition	Form
ApaTech (UK)	Actifuse™	HA, polymer and aqueous solution ¹	Pre-mixed
	Actifuse™ Shape Actifuse™ ABX	Silicon-substituted calcium phosphate and polymer	Pre-mixed
Baxter (US)	TricOs T TricOs	BCP (60% HA, 40% β -TCP) granules and Tissucol (fibrin glue) ¹	To be mixed
Berkeley Advanced Biomaterials	Bi-Ostetic Putty	Non-disclosed ¹	Not disclosed
BioForm (US)	“Calcium hydroxylapatite implant”	HA powder embedded in a mixture of glycerine, water, and CMC ¹	Pre-mixed
Biomatlante (FR)	MBCP Gel®	BCP granules (60% HA, 40% β -TCP; 0.08-0.2mm) and 2% HPMC (Boix <i>et al.</i> , 2006; Gauthier <i>et al.</i> , 2005)	Pre-mixed

	Hydr'O's	BCP granules (60% HA, 40% β -TCP; micro and nanoparticles) and saline solution (Biomatlante, private communication)	Pre-mixed
Degradable solutions (CH)	easy graft™	β -TCP or BCP granules (0.45-1.00mm) coated with 10 μ m PLGA, N-methyl-2-pyrrolidone (K. Ruffieux, private communication)	To be mixed
Dentsply (US)	Pepgen P-15® flow	Hydroxyapatite (0.25-0.42mm), P-15 peptide and aqueous sodium hyaluronate solution (product brochure)	To be mixed
DePuy Spine (US)	Healos® Fx	HA (20-30%) and collagen ¹	To be mixed
Fluidinova (P)	nanoXIM TCP	β -TCP (5 or 15%) and water (company website)	Pre-mixed
	nanoXIM HA	HA (5, 15, 30, or 40%) and water (company website)	Pre-mixed
Integra LifeSciences (US)	Mozaik Osteoconductive Scaffold	β -TCP (80%) and type 1 collagen (20%)	To be mixed
Mathys Ltd (CH)	Ceros® Putty / cycLOS® Putty	β -TCP granules (0.125-0.71mm; 94%) and recombinant sodium hyaluronate powder (6%)	To be mixed
Medtronic (US)	Mastergraft®	BCP (85% HA, 15% β -TCP) and bovine collagen ¹	To be mixed
NovaBone (US)	NovaBone® Putty	Bioglass and synthetic binder ¹	Pre-mixed
Orthovita (US)	Vitoss Flow	Contains at least bioactive glass and saline solution (or blood marrow aspirate, or blood) ¹	To be mixed
	Vitoss Pack	Contains at least bioactive glass and saline solution (or blood marrow aspirate, or blood) ¹	To be mixed

Osartis / AAP (GER)	Ostim®	Nanocrystalline HA (35%) and water (65%) (Laschke et al., 2007)	Pre-mixed
Smith & Nephew (US)	JAX CS	CSD granules and an aqueous solution (http://global.smithnephew.com/us/JAX_CS_OVERVIEW_7221.htm)	To be mixed
	JAX TCP	β-TCP granules and an aqueous solution of 1.75% CMC and 10% glycerol (Clarke <i>et al.</i> , 2007)	To be mixed
Stryker (US)	Calstrux™	β-TCP granules and CMC ¹	To be mixed
Teknimed (FR)	Nanogel	Nanocrystalline HA (100-200nm) (30%) and water (70%) (S. Goncalves, private communication)	Pre-mixed
Therics (US)	Therigraft™ Putty	β-TCP granules and polymer ¹	Pre-mixed
Zimmer (US)	Collagraft	BCP granules (65% HA, 35% β-TCP; 0.5-1.0 mm), bovine collagen, and bone marrow aspirate (Bucholz, 2002)	To be mixed
BMT Calsis (Turkey)	Suprabone™ Putty	β-TCP (0.075-0.2 mm), Hydroxypropyl methylcellulose	To be mixed

¹FDA website (<http://www.fda.gov/search.html>) – Classification product code: MQV

1.2.4.3. Sterilisation Methods

All biomaterials intended for clinical use are classified as medical devices. Medical devices are required by law to conform to the standards and requirements set out by local jurisdictions. Medical devices that are to be commercially distributed in the EU are affixed with the "Conformité Européene" or "European Conformity" mark (CE), whilst those manufactured or distributed in the US require FDA-approval. According to the degree of risk a medical device poses to the patient, and according to the duration and degree of contact time and areas, respectively, a medical device will fall into a specific 'class'. Almost all medical devices, particularly implants, are required to either be aseptically prepared or to be terminally sterilised, to eliminate any potential biological risk to the patient. The type of sterilisation that a medical

device such as an IBS is to be subjected to depends on both the requirements of the medical device class to which it belongs, as well as the nature of the device itself i.e. materials, durability, function. Aseptic preparation in controlled environments, alone, is usually insufficient for high risk medical devices (implants). Terminal sterilisation methods are considered as much more thorough and harsh compared to aseptic techniques. There are a variety of terminal sterilisation techniques available to medical device manufacturers however, again, choice is dictated by the nature of the material/s involved. Whilst most metal and ceramic medical devices are readily sterilised with conventional methods, polymeric components may undergo physiochemical changes during sterilisation which could potentially affect their clinical performance. Historically, steam sterilisation or autoclaves have been used in clinical setting to sterilise devices, tool and equipment that are heat-resistant. More recent methods fall into two main categories: chemical-based methods (vaporised hydrogen peroxide (VHP, H_2O_2) and ethylene oxide (EtO) and radiation-based methods (gamma and E-beam). There are numerous studies which reveal the effects of these terminal sterilisation techniques for specific biomedical polymers. Depending on polymer type, material architecture and testing conditions the results of these sterilisation processes vary, as discussed below.

Ethylene oxide (EtO) sterilisation is applicable to a wide range of materials used in medical devices or pharmaceutical packaging. EtO gas acts by infiltrating products and packaging to inactivate and kill cells due to its alkylating effects on sulfhydryl, amino, carboxyl and hydroxyl groups within the cell [235]. Products are exposed to this extremely explosive gas mixture in controlled facilities and undergo a three-stage process of preconditioning, sterilisation and degassing. Degassing is critical as all traces of toxic and carcinogenic EtO gas residues must be removed effectively from the product and packaging. The producer may opt for EtO sterilisation when the polymer in question is unable to withstand the high temperatures of steam sterilisation. EtO gas was used in the sterilisation of PLGA fiber membranes, and results indicated a loss in fiber orientation and morphology, in comparison to no notable changes in morphological, thermal or mechanical properties when samples were treated with gamma radiation or UV light [236]. This finding was confirmed by another study in which PLGA scaffolds were shown to significantly shrink in volume (60%) with this sterilisation technique. EtO was shown to significantly decrease cell proliferation rate and gamma radiation caused an increase in degradation rate [237].

However, Bliley *et al.* report that polycaprolactone nerve conduits exhibited no effect of room temperature EtO sterilisation on the bioactivity of glial cell line-derived neurotrophic factor in Schwannoma cell migration studies [238]. In fact, they found that EtO sterilisation attenuates the unfavoured burst release of this factor from the synthetic nerve guides. Nevertheless, EtO treatment raises concerns for any residuals that may be left on both the manufacturing environment and the product itself.

VHP sterilisation is a lower-temperature alternative to EtO and offers faster processing times and simpler setups. Products are placed inside a chamber which fills with vaporised H₂O₂ (and low temperature gas plasma) which contacts and sterilises the material and is later vacuumed from the chamber and converted to water and oxygen. H₂O₂ is a known antimicrobial and has been used in the treatment of many polymeric materials that are heat-sensitive (temperatures in the chamber do not exceed 50 °C). However, it too has previously been found to cause detriment to polymeric structures including those of polyurethane, polyethylene and poly(vinylchloride) [239, 240]. This is largely due to the oxidising effects of VHP which lead to an increase of free radicals on polymeric surfaces, which in turn effects its mechanical properties, microarchitecture and bioactivity.

Gamma sterilisation is much faster than chemical sterilisation techniques and is also suitable for heat-sensitive materials. It involves the transportation of products around a strong radiation source such as cobalt-60 for a defined period. However, the high energy radiation causes ionisation and excitation in polymer molecules, the formation of free radicals due to the radiolysis of water molecules (which pose harm to living cells). The high energy species produced with this method leads to dissociation, abstraction and addition reactions which often eventuate as physical or chemical cross-linking or chain scission in the polymer chains. The resulting material is one with altered chemical and mechanical properties including changes to molecular weight, colour, odour, stiffness, chemical resistance and melting temperature. The dose applied to common polymers range from 4-105 kGy and depends on the type of polymer. For medical devices, the most commonly used validated dose is 25 kGy. It is known that almost all thermosets, most thermoplastics most elastomers of undergoing at least one gamma radiation treatment at doses <50 kGy without significant damage. Polymers that are higher in molecular weight,

aromatic, amorphous, low-density, have small side groups and have low oxygen permeability are particularly resistant to the effects of radiation.

Treatment with electron beam radiation has a similar operating principle to gamma radiation treatment in that products are transported on a conveyor past a window where machine-generated accelerated electrons contacts the material, causes free radical formation and thereby kills and micro-organisms present. E-beam radiation is, however, known to cause molecular weight degradation and crosslinking in polymers. The degradative effects of E-beam sterilisation, though, is more likely in thinner polymeric materials due to its limited penetration capacity. Although, depending on the dose rate and total dose applied, E-beam radiation is sometimes viewed as less damaging than gamma radiation, studies have shown that it is in fact in some cases more detrimental to certain material properties. Nuutinen *et al.* [241] show that on comparison of the effects of E-beam and gamma sterilisation on self-reinforced poly(lactic acid) fibres, E-beam exposure caused a much greater decrease in ultimate tensile strength although the intrinsic viscosity and degradation rate of the polymers were similarly affected (directly proportional to dose) by both techniques.

The table below taken from the paper by Dai *et al.* [242] provides a concise summary of the relative advantages and disadvantages of sterilisation techniques for biodegradable polymers used in tissue engineering applications.

Table 3. Advantages and disadvantages of sterilisation techniques [242]

Method	Method	Advantages	Disadvantages
Heat	Heat treatment	Simple, fast, effective, high penetration ability, no toxic residues	High temperature, affect the structural properties of biodegradable polymers
	Irradiation	Gamma	High penetration ability, low temperature, effective, easy to control, no residue
E-beam		Low temperature, easy to control, no residue, fast	Induce structural properties changes, electron accelerator needed, low penetration ability
UV		Fast, low temperature, low cost, no toxic residues	Not effective, induce structural and biochemical properties changes of biodegradable polymers under long exposure duration
Plasma	Plasma	Low temperature, improved cell interaction, increasing wettability on surface of biodegradable polymers, fast	May cause changes in chemical and mechanical properties of polymers, leave reactive species

Chemical treatment	EtO	Effective, low temperature	Induce structural property change, leave toxic residue, flammable, explosive, carcinogenic
	Peracetic acid	Low temperature, effective	Structural and biochemical properties change, residual acidic environment
	Ethanol	Low temperature, low cost, no complex equipment, no toxic residue, fast	Not effective, structural and biochemical property change of scaffolds
	Iodine	Low temperature, no structural property change, fast	Affect biochemical property
Novel Techniques	sc-CO ₂	No toxic residue, no biochemical property change	May affect porosity and morphology of scaffolds
	Antibiotics	Convenient, simple	Harmful residue, not effective
	Freeze-drying	Low temperature, no structure property change, no toxic residue	Not effective, may affect the biochemical properties of scaffold

1.2.4.3.1. Sterilisation of PEG

As a widely used polymer in biomedical applications, there has been great research interest in the approaches to sterilising PEG. PEG polymers are known to undergo random cross-linking between or cleavage of polymer chains when subjected to ionising radiation such as E-beam or gamma radiation. The absorbed ionising radiation creates free radicals which facilitate the formation of random chains and networks of PEG polymers. This, in effect, alters the chemical and mechanical properties of the material. Many authors have provided interesting outcomes of testing various sterilisation methods on various PEG-based polymeric structures. Kanjickal *et al.* have studied the effects of popular sterilisation techniques (EtO, H₂O₂ and gamma radiation) on PEG hydrogels intended as both a drug delivery and tissue engineering material [235]. Their results showed that the drug release profiles of the material depended on the drug used, but more importantly, varied according to sterilisation technique. EtO did not have any effect on the roughness parameter of the material, however, statistically significant differences were observed for H₂O₂ and gamma irradiated samples. Although all treatments were found to cause radical pieces in sterilised samples, H₂O₂ and gamma-sterilised samples showed much higher concentrations than EtO treated samples.

Issues regarding oxidation caused by gamma radiation has also been described by Calvet *et al.* who researched the effects of sterilisation on star-shaped PEG coated polymer surfaces [243]. Furthermore, a study exploring the effects of sterilisation techniques on different polymeric coatings reported PEG coatings (on silicon) less

than 5% change in thickness for PEG coatings sterilised via autoclave or EtO, whilst hydrogen peroxide caused at least 30% decrease in thickness for all coatings [244]. The uses of PEG as carriers in synthetic bone grafts has been previously reported [245]. These reports confirm that the radiation sterilisation of PEG may also cause cleavage of polymer chains leading to a decrease in molecular weight and melting temperature of the product. The overall effect observed in these reports is that the material assumes a softer and more mouldable consistency. In these cases, the softening of the material due to radiation-induced changes to the PEG-phase is considered a positive outcome, as viscosity, injectability and handling and delivery become more apt for the operator of the product.

1.2.4.3.2. Sterilisation of Bioactive Glass

Tablawy *et al.* [246] have investigated the effects that gamma radiation (25 kGy and 50 kGy) has on the antimicrobial activity of 45S5 bioactive glass intended as a biofilm eradicator on artificial discs. They calculated an optical energy gap of 4.387 eV for bioactive glass treated at 25 kGy, compared to untreated materials, with a more prominent band at 230 nm and a new absorbance band at 500 nm post-sterilisation, indicating a shift in phase of the material due to radiation exposure. Also, there was slight increase in the 900–1200 cm^{-1} region of FT-IR spectroscopy measurements, again signifying alterations to the chemical structure of treated bioactive glass. The microbiological studies indicate that gamma-treated bioactive glass leads to a significant increase in ion concentrations (particularly Si) in culture medium and overall, treated bioactive glass is more effective at attenuating the formation of biofilm by microbial species.

Bioactive glass is also used in its nanoparticle forms as drug delivery vehicles. Research into the effects of gamma sterilisation on the bioactivity, drug-loading and drug-releasing capacity of nano-bioactive glass show that not only are these capacities not hindered in gamma irradiated samples, but for 25 kGy doses, drug release kinetics were improved although this dose was the least successful (compared to 0 and 50 kGy doses) at adsorbing the studied drug (vancomycin) [247]. The authors explain this as the result of an increase in Si-OH groups and non-bridging oxygen species on the already negatively charged glass surface at 25 kGy, impeding binding of the negatively charged vancomycin. The reverse effect was seen for 50 kGy treated bioactive glass. Intensity of XRD peaks, however, increased

with increasing radiation doses, with radiation enhancing the formation of an apatite layer on the glass particles. This study therefore highlights that the change in behaviour of bioactive glass may not necessarily be directly proportional to increases in radiation dose.

Another group looked at the effect of gamma irradiation (as well as strontium substitution) on the bioactivity, cytotoxicity and antimicrobial properties of 45S5 bioactive glass [248]. Their findings concluded that at irradiated bioactive glass was more prone to dissolution in simulated body fluid and this was accelerated for sample also containing strontium substitution (used as a means of promoting antibacterial properties). The researchers attribute this effect to the non-bridging oxygen species formed by the radiation process. They also concluded that up to a 25 kGy radiation of bioglass did not affect the proliferation of fibroblasts.

1.2.4.3.3. Sterilisation of β -TCP

β -TCP is a ceramic that has an extensive history of clinical use. It has superior biocompatibility and processability for orthopaedic applications due to its inherent chemical and mechanical qualities. Gamma irradiation is the known and preferred method of sterilisation for β -TCP and there are numerous studies supporting this notion. Turker *et al.* [249] subjected dental graft materials (β -TCP, bioactive glass and equine bone tissue) to gamma irradiation and found that β -TCP was the most gamma-stable material showing the least chemical and physical changes. The group also compared the effects of EtO and gamma on β -TCP by looking at resorption times of the dental graft in New Zealand rabbits over 12 weeks. Resorption and bone formation were faster for the gamma-irradiated grafts than EtO-sterilised grafts. Sarikaya *et al.* investigated the effects of gamma irradiation (25 kGy) on collagen/ β -TCP-based synthetic bone grafts prepared via dehydrothermal processing. SEM imaging revealed appropriate bonding between ceramic and collagen phases, FT-IR spectroscopy indicated no significant changes to the ceramic phase though an increase in cross-link density of collagen fibers were observed and electron spin resonance did not detect any free radicals formed in the grafts, post-sterilisation [250].

1.3. Materials and Method

1.3.1. Material Constituents

β -TCP powder was provided by BMT Calsis Health Technologies Co. (Ankara, Turkey). For the purposes of this study, the β -TCP powder provided was filtered with a manual sieve to separate the material into a finer 'powder' form and a coarser 'particle' form. The terms 'powder' and 'particle' used hereon in are ascribed the aforementioned definitions. Poly(ethylene glycol) (MW 400, MW 1500 and MW 2000) was purchased from Sigma Aldrich (Germany) and used as is. Glycerol was purchased from Sigma Aldrich (Germany) and used as is. Bioactive glass (45S5) was purchased from Mo-Sci Corporation, Mo-Sci Healthcare, LLC and Mo-Sci Specialty Products LLC (U.S.A) and used as is.

1.3.2. Material Preparation

The injectable bone substitute was prepared by first mixing all of wet constituents (poly (ethylene glycol) (MW400) and glycerol in a beaker at room temperature. The beaker containing this mixture was then placed in a water bath set to 60°C and, with the use of a mechanical stirrer (at 200 rpm for 5 minutes), the high molecular weight polyethylene glycol (MW 1500 and MW 2000) was added to the mixture. Once the higher MW polyethylene flakes visibly dissolved in the mixture, the β -TCP powder and particles and bioactive glass powder was added to the mixture. Stirring continued until a visibly homogenous paste was obtained. The paste was cooled at 4 °C before transfer to syringes. Previously EtO treated polypropylene syringes (3 cc, 7.6 mm inner barrel diameter), fitted with lubricated silicone plungers, were manually filled with prepared putty compositions. A total of 5 g of putty was packed into each syringe. The filled syringes were then capped and stored in ambient conditions until further use. The gamma sterilisation of the IBS samples were performed under Co-60-based gamma irradiation. One group of samples were irradiated at a gamma dose of 10 kGy and the other at 25 kGy. The following IBS compositions were prepared with this method:

Table 4. Synthesised IBS Compositions

Group	Carrier: Solid (CP+BG)*	Glycerol : PEG	PEG**
Carrier 1 (B11)	50:50	35:65	HHMW

Carrier 2 (B12)	50:50	35:65	LHMW
Carrier 3 (B21)	50:50	45:55	HHMW
Carrier 4 (B22)	50:50	45:55	LHMW
Carrier 5 (B31)	50:50	55:45	HHMW
Carrier 6 (B32)	50:50	55:45	LHMW
Carrier 7 (A31)	40:60	55:45	HHMW

* The amount of calcium phosphate (CP) and Bioglass (BG) forming the solid phase of the IBS is not equal.

**PEG content is separated and referred to as Higher High Molecular Weight (HHMW) content and Lower High Molecular Weight (LHMW) content.

All formulations given in Table 4 were prepared as gamma-sterilised and non-sterile counterparts in each group. The prepared IBS compositions were subjected to various morphological, chemical, rheological and *in vitro* analyses.

1.3.3. Testing Protocols

1.3.3.1. Scanning Electron Microscopy (SEM)

Scanning electron microscopy is used to obtain high-resolution microscopic images that can provide qualitative (e.g. phase identification, crystalline structure) or quantitative (e.g. Energy-Dispersive X-ray Spectroscopy (EDS)) data regarding the composition of a material. A QUANTA 400F Field Emission scanning electron microscope (1.2 nm resolution) was used to obtain images of samples at 50x, 250x, 1000x and 5000x magnification. The samples that were used were placed in an incubator at 37 °C and low vacuum to remove as much moisture from the sample as possible, as a necessary step for SEM imaging preparation. The samples were coated with gold-palladium conductive metal and subjected to vacuum in the preparatory step for SEM.

1.3.3.2. Micro-Computerised Tomography (μ -CT)

To observe macroscopically the phase distribution of composite materials, micro-computerised tomography may be used. μ -CT scanners provide high-resolution 3D images of a material without damaging the specimen. It is a widely-popular tool for calculating bone density and other parameters in the field of bone research. μ -CT data were acquired with a SkyScan 1173 μ -CT unit (Bruker, Kontich, Belgium,

output 100 kV, electric current 100 μ A, voxel 8 μ m, 0.5 mm-thick aluminum filter, 360° rotation, rotation step 0.4, scanning time 43 min).

1.3.3.3. Fourier Transform Infrared (FT-IR) Spectroscopy

FTIR analysis in the ATR mode probes the surface properties of materials rather than their bulk properties, with a penetration depth in the range of microns. This technique is particularly useful for studying polymer surfaces, especially for soft polymers. Chemical analysis of the composite material was carried out with an Attenuated Total Reflectance - Fourier transform infrared spectrophotometer (ATR-FTIR) (Perkin Elmer 400, UK) over the range between 4000 - 500 cm^{-1} at 4 cm^{-1} resolution averaging 16 scans.

1.3.3.4. Thermogravimetric Analysis (TGA)

TGA is a thermal analysis technique in which the weight loss of a material over time, in a controlled atmosphere, at various temperature. It is a particularly popular method for studying the decomposition and thermal stability of polymeric materials. TGA analysis of prepared IBS compositions, were performed with a thermogravimetric analyser (SDT 650, TA Instruments) running from 25 - 950 $^{\circ}\text{C}$ at heating rate of 10 $^{\circ}\text{C}$ / minute in ambient (air) conditions.

1.3.3.5. Washout-Resistance Study

The resistance of prepared IBS compositions against washout or disintegration in an aqueous environment was tested to reflect potential degradation behaviour of the materials under physiological conditions. The wells of 12 well plates were completely lined, to form a pouch, with gauze (1 mm pore size) material of the same size for each well. 3 mL of ultrapure water Type 1 (Direct-Q and Direct-Q 3 UV) was added to each well. 0.5 g of each IBS composition previously prepared (n=3) and weighed was gently placed into each well. The plates were placed into a thermoshaker incubator (Thermoshake, Gerhardt, Laboshake, Germany) at 37 $^{\circ}\text{C}$ and 20 rpm agitation. The samples were removed, contained inside the gauze pads, at 1 h, 6 h, 12 h and 24 h time points, and weighed. The total time taken to weigh all samples was kept to 15 minutes, at each time point. To minimise the effects of water absorption by the gauze material, each pouch was dabbed gently on

absorbent paper 3 times before weighing. The amount of material washout was calculated according to the following formula:

$$\text{Washout (\%)} = \frac{\text{Original Mass} - \text{Final Mass}}{\text{Original Mass}} \times 100 \quad \text{Equation 1}$$

All experimental results were expressed as the mean \pm standard deviation (SD) for $n > 3$. The difference between the groups was determined using repeated measures analysis of variance (ANOVA) with a Bonferroni post-hoc test, and $p < 0.01$ (due to violation of homogeneity) were considered to be statistically significant. A paired t-test was also used to compare differences between IBS groups.

1.3.3.6. Cohesion Study

To determine the amount and release profile of calcium ions released from the IBS composites in aqueous environments, 0.5 g of each composition ($n=3$), was added to 25 mL falcon tubes containing 25 mL of ultrapure water Type 1 (Direct-Q and Direct-Q 3 UV). Each sample was added to the falcon tubes by placing the material at the surface of the water and allowing the material to sink to the bottom. The tubes containing the samples were placed in a thermoshaker incubator (Thermoshake, Gerhardt, Laboshake, Germany) at 37 °C and 20 rpm agitation. At each pre-determined time point samples were removed from the incubator and 2 mL of supernatant was collected with a pipette from each falcon. To reduce the time and costs associated with the planned cohesion analysis, the supernatants collected from each sample group at a single time point were pooled to form a total of 6 mL aliquot. The total sample collection time was kept to 15 minutes at each time point. The collected samples were then analysed via Inductively-Coupled Plasma Optical Emission Spectrometry (ICP-OES) (Perkin Elmer Optima 4300DV) to measure the amount of calcium species eluted over time from the samples incubated and agitated in ultrapure water.

1.3.3.7. Injectability Study

Injectability of an IBS can be performed with various methods, all of which involve observations of how much of the material is extrude from a syringe or spread across a surface, when subjected to a predetermined load. Injectability of the prepared IBSs

was analysed using a universal testing machine (Zwick/Roell Z250), with three repeats tested per group. Each syringe containing an IBS composition was placed in a custom apparatus under the load cell of the machine. The syringe barrel was then loaded with a 100 N load and compressed at a crosshead speed of 1 mm / min, in ambient conditions. Data in the form of plunger displacement (mm) vs applied force (N) was collected from the experiment. The maximum applied force was taken as the maximum injection force required during the injection/application of the IBS. All experimental results were expressed as the mean \pm standard deviation (SD) for $n > 3$. Statistical evaluation of the results was performed using a two-way analysis of variance (ANOVA) with a Bonferroni post-hoc test, and $p < 0.05$ was considered statistically significant. The analysis of variances revealed a violation of homogeneity as determined by a significance of $p < 0.05$ in the Levine's test of equality of variances.

1.3.3.8. Viscosity Study

To evaluate the rheological properties of the synthesised IBS compositions, a rheometer (TA Instruments ARES Rheometer) was used in a parallel plate-plate configuration, operating in a frequency sweep mode in constant ambient conditions. Data obtained from the device and analyses included modulus of storage modulus (G'), loss modulus (G''), complex viscosity (η^*) and $\tan \delta$ (dampening factor). Both gamma-sterilised and unsterilized samples were tested from all groups so as to observe the effects of ionising gamma-radiation on the viscosity of the synthetic bone graft material.

1.3.3.9. *In Vitro* Study

Cytotoxicity tests were performed according to ISO 10993-5: Biological evaluation of medical devices standard. Within this scope, a L929 mouse fibroblast cell line (NCTC clone 929, ATCC, USA) recommended by the relevant standard was used in this study and the sample preparation was performed according to 'ISO 10993-12: Sample preparation and reference materials'. As the ISO 10993 standard recommends for composites, where possible, materials should be accepted to test as a single material rather than its individual components. For this purpose, the materials proposed in this study was accepted as a composite material regarding to its contents. When the constituents of the resulting material were evaluated for

cytotoxicity test, it has been found that both glycerol and PEG are hygroscopic and hydrophilic polymers in the light of the previous literature studies. The definition of hydrocolloids also encompasses hydrophilic polymers that are able to form gels. Hence, relevant part of the standard for hydrocolloids has been taken into consideration. The standard recommends first performing a water absorption test to see the amount of water that 2 g of the material absorbs. The standard states that the amount of extraction medium to be used will then be 20 mL greater than this absorbed amount. The IBS developed here was found to absorb water at a rate of 2 mL per 2 g of IBS. Therefore, an extraction ratio of approximately 2 g per 22 mL (i.e. 0.09 g of sample per 1 mL of culture medium) was calculated.

Briefly, 90 mg of gamma sterilized test materials were dispersed in 22 mL DMEM High Glucose (Capricorn, Germany) medium and incubated at 37 °C in 95% humidity in a carbon dioxide incubator for 24 hours. In some groups, incubation period was prolonged to 48 and 72 hours to assess the effect of incubation period on cytotoxicity. In parallel to this, the cells were expanded by using Dulbecco's Modified Eagle's Medium - high glucose (DMEM-High Glucose) supplemented with fetal bovine serum (FBS) (10% v/v), antibiotic-antimycotic (AA) (1% v/v) and L-glutamine (1% v/v). All materials used within the analysis were purchased from Capricorn, Germany. The study was carried out in a 24-well culture plate that contains 2.5×10^4 cells in each well.

The filtered extraction medium was supplemented with the serum, antibiotic and L-glutamine at the abovementioned ratios and allowed to react with the cells in the 24 well culture plates and the cells were further cultured for 24 hours. At the end of the incubation period, the culture media on the cells was discarded and 600 μ L of serum free, antibiotic-free medium containing 60 μ L MTT (5 mg/ mL) were added and subjected to 4 hours of incubation. At the end of the incubation period, 200 μ L DMSO was added to the wells in which the medium was removed from each well to dissolve the formed formazan crystals. Subsequently, 200 μ L samples were taken from each well and read in a 96-well culture dishes at 570 nm (BioTek, USA). The viability of the control cells was accepted as 100% and the viability of test groups was computed as a percentage of the control group. Two-way analysis of variance (ANOVA) using GraphPad Prism 6 Software was performed to make multiple comparisons. P values below 0.05 were accepted as significant.

2. Results and Discussion

2.1. Morphological Analyses - SEM

SEM images of selected sample of sterile (+) and unsterile (-) samples of 50:50 (A) and 40:60 (B) IBS compositions (B31+, B31-, A31+, A31-; respectively) were evaluated to obtain information about phase distribution of the various constituents of the composite material, as well as observe the morphological features of each composition. In Figure 3 below, an even distribution of the particles infused into the carrier phase can be seen, indicating that the method of material preparation is appropriate for obtaining a homogenous material. A more dry and granular appearance of samples containing a greater amount of carrier (B31+ and B31-), compared to samples with a lower carrier content, is apparent. At closer inspection at larger magnifications, such as 250x or 1000x, this feature becomes more apparent. Clusters of larger β -TCP particles are more clearly identifiable in groups containing a greater carrier phase. Vacuoles in the sample are present in images of all groups, at smaller magnifications (50x). Considering material composition of the B31 samples, a smaller amount of ceramic and bioglass particles have a larger volume of carrier to move around and form clusters in. When subjected to vacuum in the preparatory steps for SEM analysis, this large carrier content may have been removed, exposing clumps of particles left behind to form a more vacuous structure. A higher amount of ceramic and bioglass particles in less carrier volume, as in samples A31, would have led to a more tightly packed distribution of these particles. Upon subjection to vacuuming, the little carrier present is removed to reveal an almost monolithic solid of tightly packed particles. Particles of varying size distributed throughout the material is seen in all groups, at high magnifications. Higher magnifications (1000x and 5000x) bring to focus the presence of particles less than 20 μm in size that have been deposited onto the surfaces of much larger-sized particles such as those particles of 100 μm size seen in sample B31+ at 1000x magnification. There is clearly a degree of agglomeration of particles. Particle shapes range from globular to flakes, with clearer outlines of these shapes significantly easier to observe in samples B31+ and B31- compared to A31+ and A31-. There is no visibly comparable difference between sterile and unsterile

samples of the same group, yielding no evidence of any effects of exposure to gamma irradiation

The carrier phase of the injectable bone paste consists of polyethylene glycol and glycerol. Polyethylene glycol has been studied extensively in hydrogel systems as they are biocompatible, are capable of encapsulating and transporting both cells [251] and molecules [252]. They are, however, unable to promote mineralisation of newly formed tissue at implant sites, and thus are usually combined with materials or factors which do, such as calcium phosphate or calcium phosphosilicate particles.

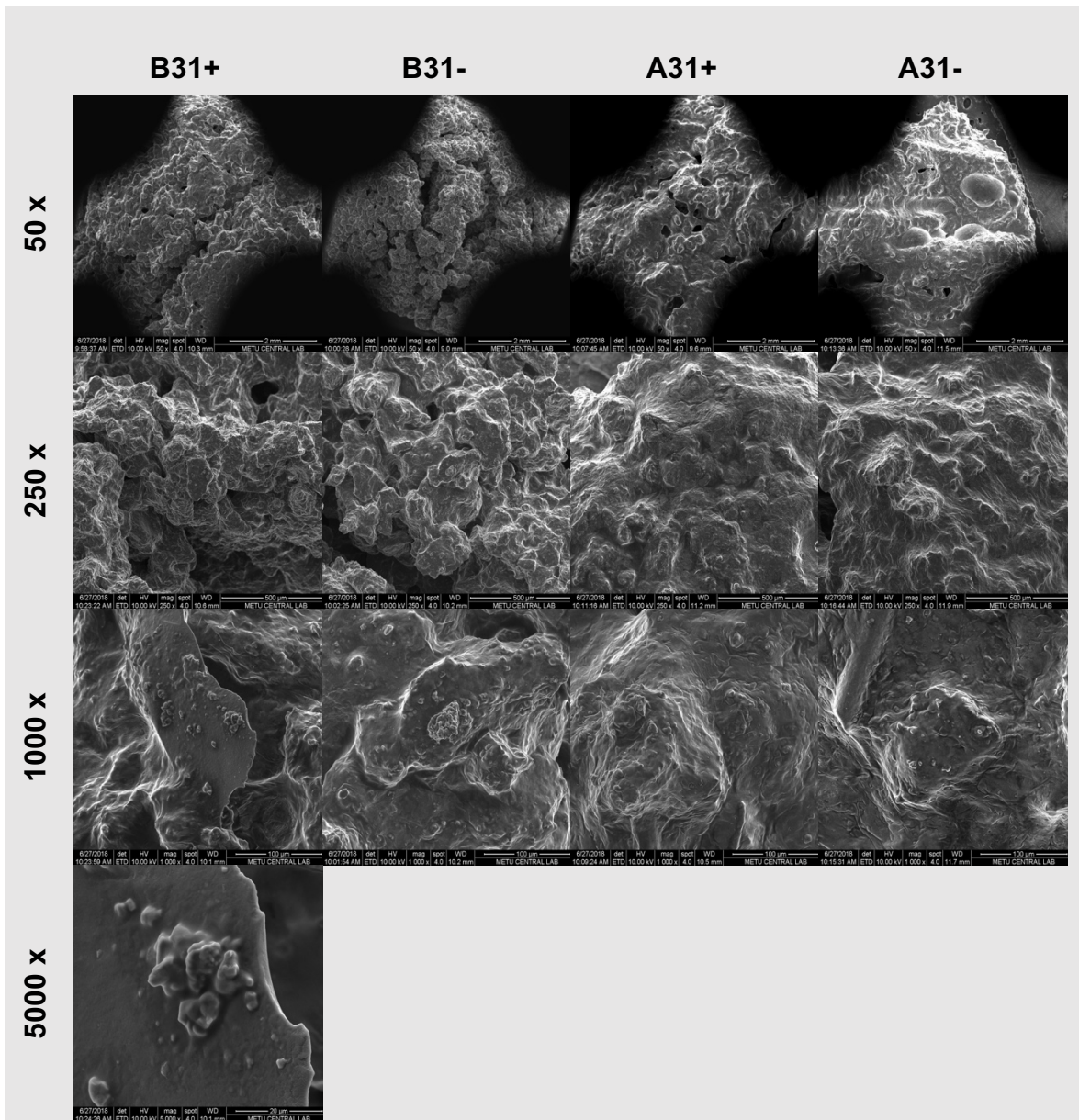


Figure 3. SEM images of IBS compositions B31 sterile, B31 unsterile, A31 sterile and A31 unsterile (groups left to right), at 50x, 250x, 1000x and 5000x magnification (top to bottom)

2.2. Morphological Analyses - μ -CT

The 3D images of samples A31+, A31- , B31+ and B31- obtained from the μ -CT scanner are given below in Figure 4. Firstly, features that may arise from the amount and placement of the material onto the scanner platform, will be ignored to compare samples on features that are not dependent on such physical and human factors. With inspection of the surface characteristics of the materials in the images below, a uniform material composition is seen in all samples. The visible surfaces of the 'B' groups, however, have a more speckled (white) appearance. The whiter, more radio-opaque spots seen in the specimens are attributed to the ceramic particles in the material. 'B' groups have, however, less ceramic content. Although there is no evidence of agglomeration of calcium phosphate or bioglass particles in the carrier matrix as seen in the μ -CT images for the representative samples, the impact of inhomogeneous distribution of particles, if any, will be revealed in rheological analyses. Morphological or compositional inhomogeneity has previously been shown to hinder the mechanical and rheological performances of ceramic-polymer systems [253, 254]. There was no visible difference between sterile and unsterile samples of either group.

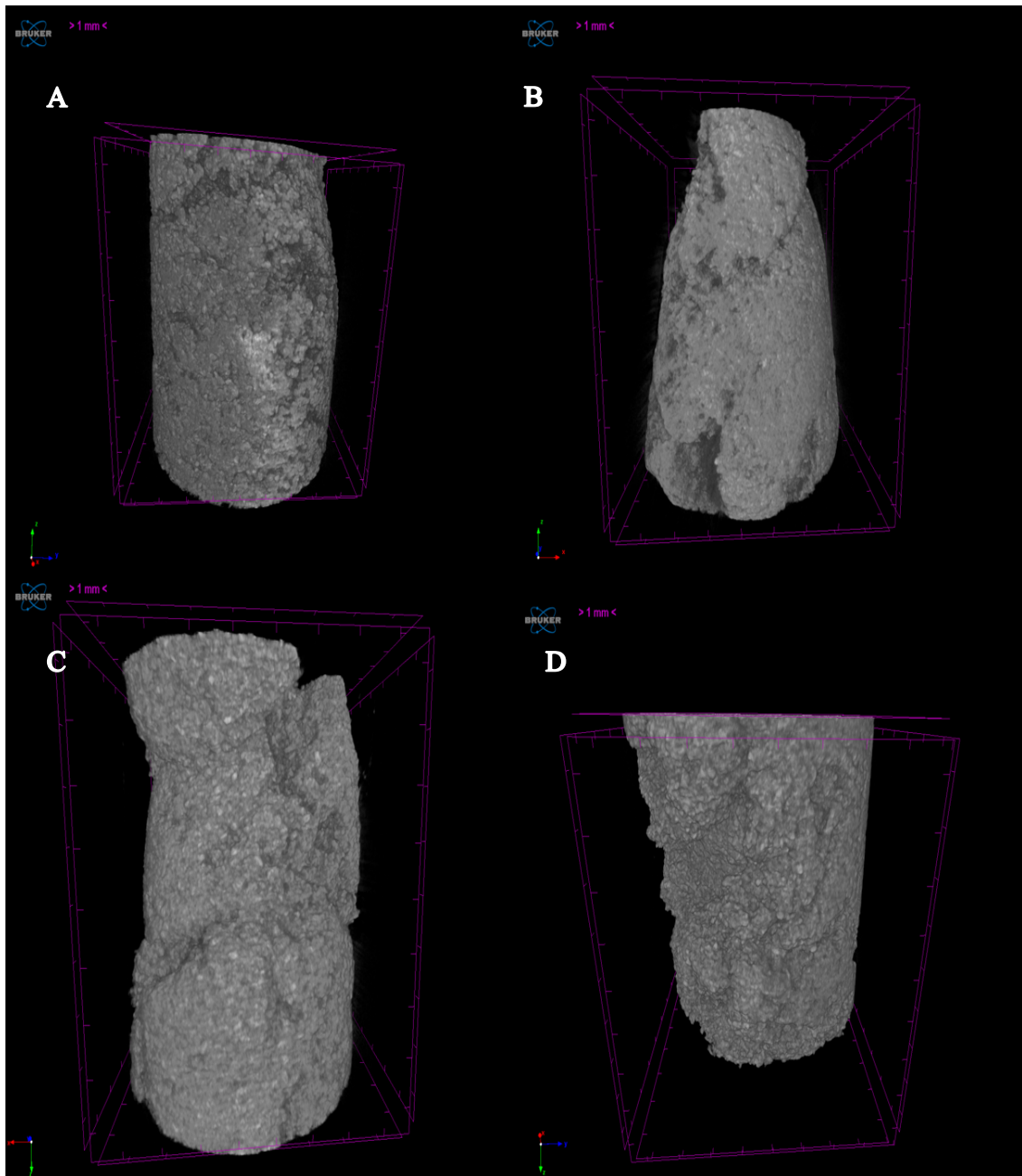


Figure 4. Micro -CT scans of sterile A31 (A), unsterile A31 (B), sterile B31 (C) and unsterile B31 (D)

2.3. Chemical Analyses - FT-IR Analysis

ATR-FTIR analysis was used to identify the key chemical groups present in the IBS and whether gamma irradiation had any effect on their chemical composition. Chemical groups were identified based on their characteristic absorbance peaks at specific wavelengths, as given in literature. ATR-FTIR spectra of samples B31+ and B31-, selected as representative samples, are given in Figure 5. The ATR-FTIR

spectra of all other chemical constituents of the IBS have been provided in the appendix and used as reference information. In the FT-IR spectrogram of the IBS absorbance peaks seen at 1023 cm^{-1} and 1107 cm^{-1} were attributed to the Si-O stretching in the 45S5 bioglass additives within the composites. The typical peak between $400 - 500\text{ cm}^{-1}$ (usually around 460 cm^{-1}) due to Si-O bending in 45S5 bioglass was present in the spectrogram of bioglass (487 cm^{-1}), however, it was not found in the spectrogram for the IBS. The scan range was, however, only between $4000 - 500\text{ cm}^{-1}$, therefore a second peak due to Si-O bending in bioglass may be absent in the IBS spectrogram if it occurred at a wavelength between $400 - 487\text{ cm}^{-1}$.

The characteristic FT-IR spectra for PEG has been cited in literature [255]. PEG has two characteristic strong absorbance peaks which indicate the presence of saturated carbons $(\text{CH}_2\text{CH}_2)_n$. The first is typically seen at around 2886 cm^{-1} due to the stretching of alkanes, and this peak has appeared at 2886 cm^{-1} , 2882 cm^{-1} , 2882 cm^{-1} , 2884 cm^{-1} and 2883 cm^{-1} in PEG400, PEG1500, PEG2000, unsterile putty and sterile IBS spectrograms, respectively. The second strong absorbance peak appears at about 3400 cm^{-1} and is due to the stretching of the hydroxyl group. This peak appears at 3446 cm^{-1} , 3414 cm^{-1} , 3424 cm^{-1} for PEG400, PEG1500, PEG2000, respectively. This peak appears to have shifted to about 3326 cm^{-1} for both sterile and unsterile IBS samples. There are also many other characteristic peaks for PEG, such as those that may be seen at around 885 cm^{-1} , 944 cm^{-1} , 1096 cm^{-1} , 1287 cm^{-1} , 1296 cm^{-1} , 1349 cm^{-1} which can also be identified in the sterile and unsterile IBS spectrograms. The C-H scissor bending between $1450 - 1292\text{ cm}^{-1}$ is evident in all of the various PEG types with absorbance peaks seen at 1324 cm^{-1} , 1340 cm^{-1} , 1341 cm^{-1} , 1349 cm^{-1} , 1359 cm^{-1} , 1414 cm^{-1} , 1413 cm^{-1} . The C-O-C stretching of PEG usually seen between $1100-1060\text{ cm}^{-1}$ is seen in the spectra for all of the PEG types (1095 cm^{-1} for PEG 400, 1060 cm^{-1} , 1099 cm^{-1} for PEG 1500 and 1059 cm^{-1} , 1096 cm^{-1} for PEG 2000, and 1107 cm^{-1} for all PEG types). Similarly, in the IBS composition spectra, peaks appear at approximately 1100 cm^{-1} and 1060 cm^{-1} . The effects of C-O stretching of alcohol at 1250 cm^{-1} is present in the spectrograms of both the IBS samples and each PEG type.

The key absorption bands for β -TCP include 947 cm^{-1} , 974 cm^{-1} and 1120 cm^{-1} . The spectrogram for β -TCP and both sterile and non-sterile IBS samples exhibit

these characteristic peaks. Bands at 603 cm^{-1} , 565 cm^{-1} , 1094 cm^{-1} , 1032 cm^{-1} are usually characteristic of PO_4^{3-} within β -TCP sintered at $1100\text{ }^\circ\text{C}$, and all four peaks appear in the β -TCP and IBS samples' spectrograms. For β -TCP ceramics, bands at 725 cm^{-1} indicate the presence of $\text{P}_2\text{O}_7^{4-}$ (characteristic to calcium pyrophosphate phase). A peak at this wavelength is more pronounced in the IBS samples' spectrograms than in the β -TCP spectrogram used for reference.

Glycerol FT-IR spectrograms display a broad range of peaks between $600 - 3000\text{ cm}^{-1}$ caused by stretching of O-H bonds with either inter or intra-molecular hydrogen bonds [256]. Other key peaks include that related to the intense CO stretching at 1735 cm^{-1} in OH groups. In our FT-IR results for glycerol, we see peaks at 3292 cm^{-1} , 2932 cm^{-1} , 2879 cm^{-1} and 1030 cm^{-1} , amongst others. We have identified the peak at 1030 cm^{-1} in the IBS FT-IR spectrogram as well.

Sanjeeva Rao *et al.* [255] have reported that in their FT-IR analysis of pure and gamma-irradiated PEG samples they observed a change in intensity of 1720 cm^{-1} and 1680 cm^{-1} absorption bands, and that the intensity of the peaks showed a gradual increase with increasing radiation dose. There were no significant differences observed between the FT-IR spectra of the synthesised unsterile and sterile IBS (subjected to 25 kGy radiation). The key absorbance bands remained almost identical for both samples, which indicate that the dose of gamma irradiation selected for sterilising the IBS does not cause any observable changes to the chemical composition of the synthetic bone graft material.

FT-IR results indicate that the resulting composition of bioglass, β -TCP, PEG and glycerol retains the chemical properties of the individual constituents before and after exposure to gamma sterilisation. Furthermore, a pronounced peak in the IBS spectrograms at approximately 3400 cm^{-1} indicates some chemical activity in the O-H region of PEG, signifying the possible formation of a network between the PEG chains in the IBS formulation.

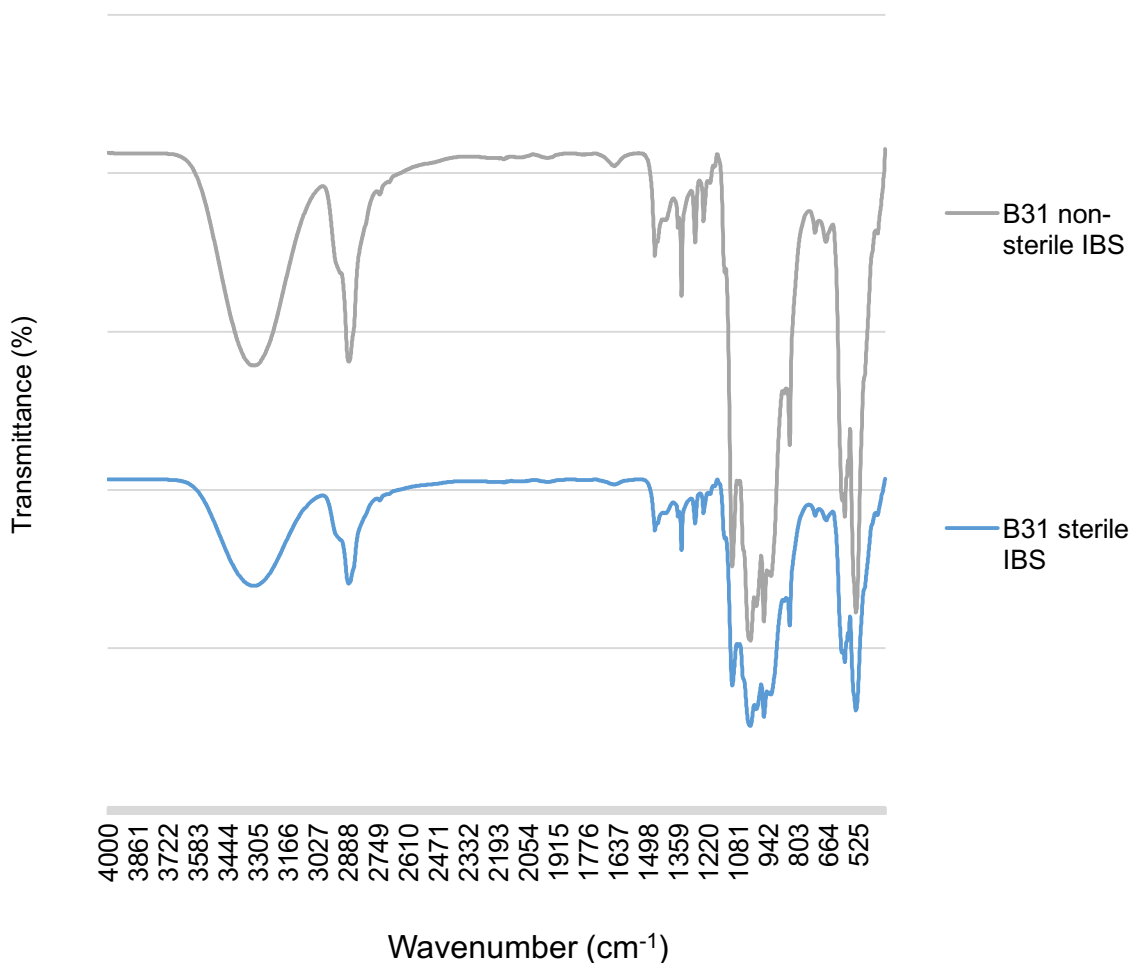


Figure 5. FT-IR spectra of sterile and non-sterile IBS

2.4. Thermal Analyses - Thermogravimetric Analysis

The TGA thermograms obtained for each representative IBS samples are given the figures below (Figure 6, Figure 7, Figure 8 and Figure 9). The TGA results for the various IBS compositions prepared show that between groups A31 and B31 the thermograms display the same general trend. The overall weight loss (%) seen in the thermograms below, for samples sterile A31, unsterile A31, sterile B31 and unsterile B31 are 40.880 %, 40.937 %, 49.724 % and 49.988 % respectively. This translates to a final residue of the material of approximately 60 % and 50 % for group 'A' and 'B' samples, respectively. As there is a greater amount of polymeric carrier in group B samples, a higher degree of weight loss is expected in these samples. Group A samples were included in this study to confirm the carrier-based increase in thermal decomposition phenomenon occurred. The proportional decrease in

weight loss with a greater carrier phase shows that the material preparation method used has successfully produced homogenous phase distribution in the prepared samples. Group B31 samples were chosen as representative samples to showcase the thermal decomposition of the lowest HMW PEG and highest glycerol-containing sample group of all the formulations prepared, for reasons discussed below.

The TGA thermograms reveal that thermal decomposition of B31 samples begin long after the physiologically and clinically relevant temperature of 37 °C. In all four samples the initial decomposition temperature (IDT) is approximately the same i.e. 150 °C, which is usually attributed to the removal of solvents or moisture from the sample. Although the IDT represents the initial point of decomposition of a material, it provides only a partial analysis of the thermal stability of a material. Whilst the profile for weight loss with increasing temperature may appear similar amongst different samples, the change in the molecular weight of the sample constituents with increasing temperatures, particularly those exposed to gamma radiation, may be different. The thermograms show that there is almost no difference between gamma-sterilised and unsterilised samples in either group A or group B samples, which means that the choice of terminal sterilisation via gamma irradiation at 25 kGy does not affect the thermal decomposition properties of the IBSs developed.

Smaller molecular weight yet more volatile compounds causing reduced thermal stability may be formed in some materials when exposed to higher temperatures, but the weight of the overall samples may remain the same. In literature, the reported IDT for PEG 400 is 226 °C [257] and approximately 350 °C for PEG 1500 and PEG 2000. Furthermore, when the effect of glycerol on the performance of a rice straw-starch based polymer was investigated, a higher glycerol content was shown to decrease the degradation temperature of the composite [258]. A higher IDT would therefore be expected in formulations of IBS with less glycerol content.

Group 'A' samples do not have a D1/2 (half-life temperature) present on their TGA thermograms as there is only an overall 40 % decrease in material weight throughout the tests. All samples tested experience a rapid and dramatic weight loss less than 250 °C. Group 'A' and 'B' samples, irrespective of gamma exposure, reach their maximum weight loss at this temperature. Therefore, a more rapid decomposition profile in group 'A' samples, whereas a relatively slower rate of maximum material decomposition, at higher temperatures, is seen for group 'B'

samples. The area under the derivative curve provides a qualitative analysis of how much of the component responsible for a decrease in weight of the total sample has decomposed. The area under the derivative curve is greater for group 'B' samples. This result correlates with the fact that the weight loss of the total material is attributed primarily to the decomposition of the polymeric i.e. carrier phase of the IBS, and as this phase is larger in group 'B' samples, a larger area under the derivative curve of group 'B' thermograms is expected.

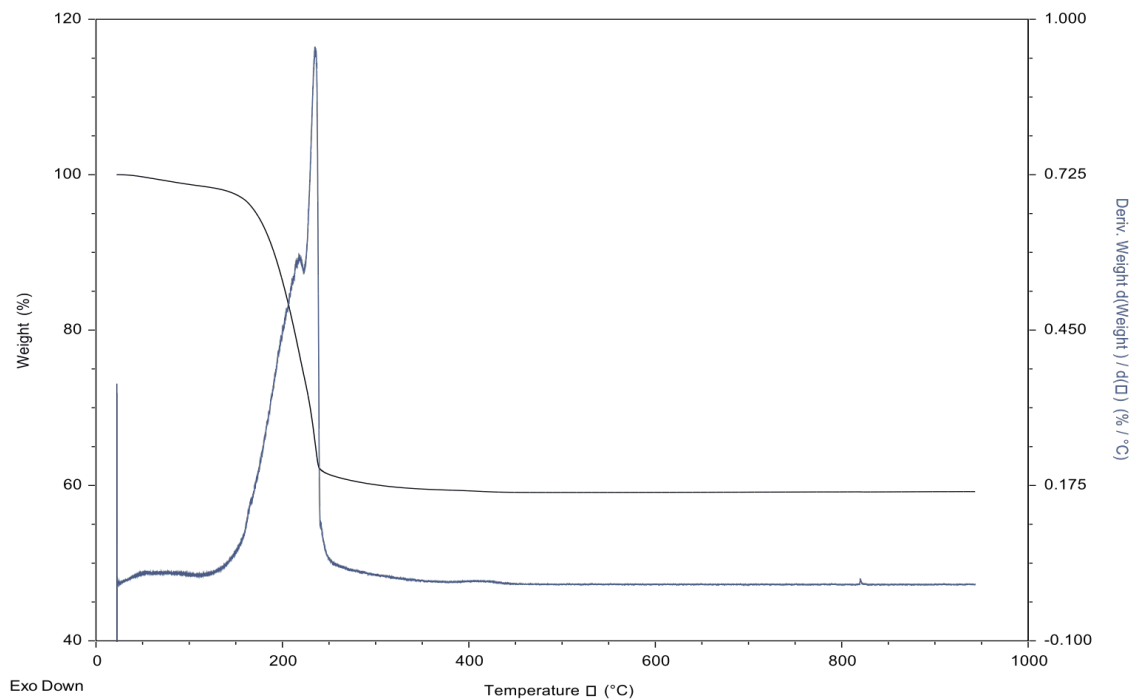


Figure 6. TGA thermogram of Sterile A31 IBS Composition

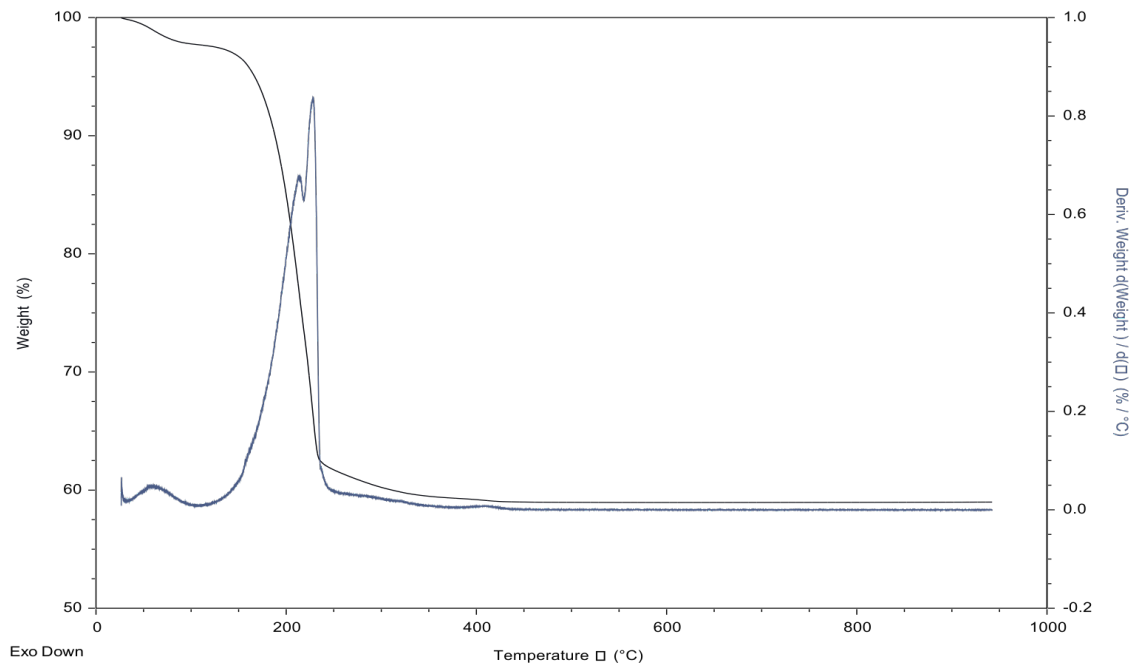


Figure 7. TGA thermogram of non-sterile A31 IBS Composition

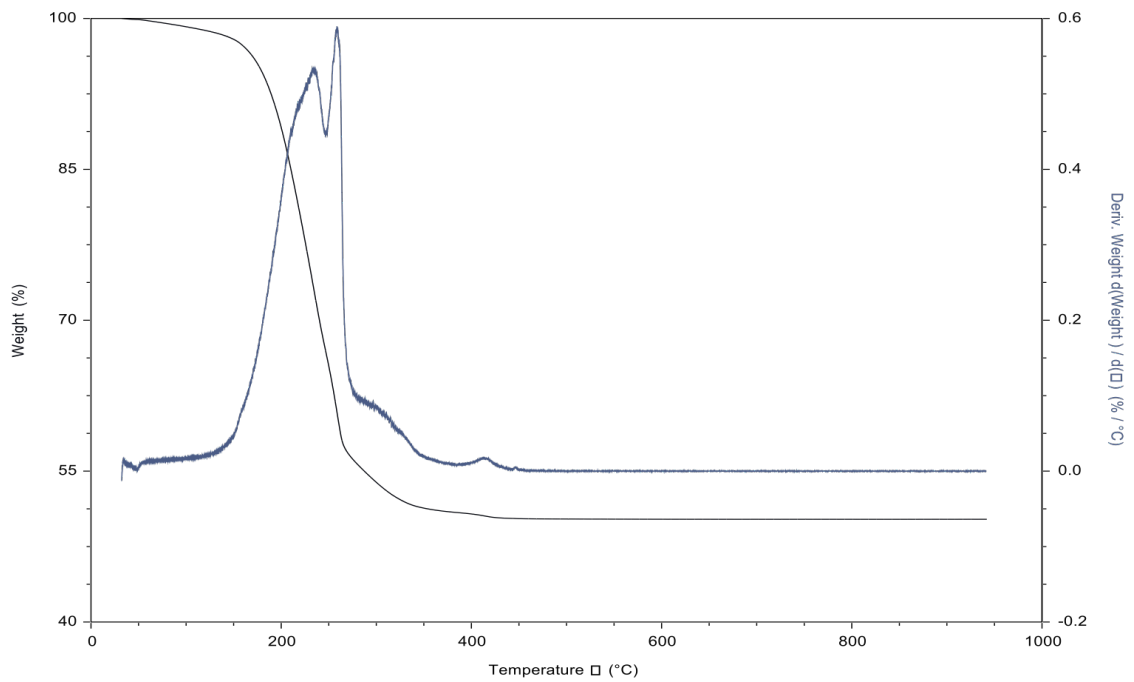


Figure 8. TGA thermogram of sterile B31 IBS Composition.

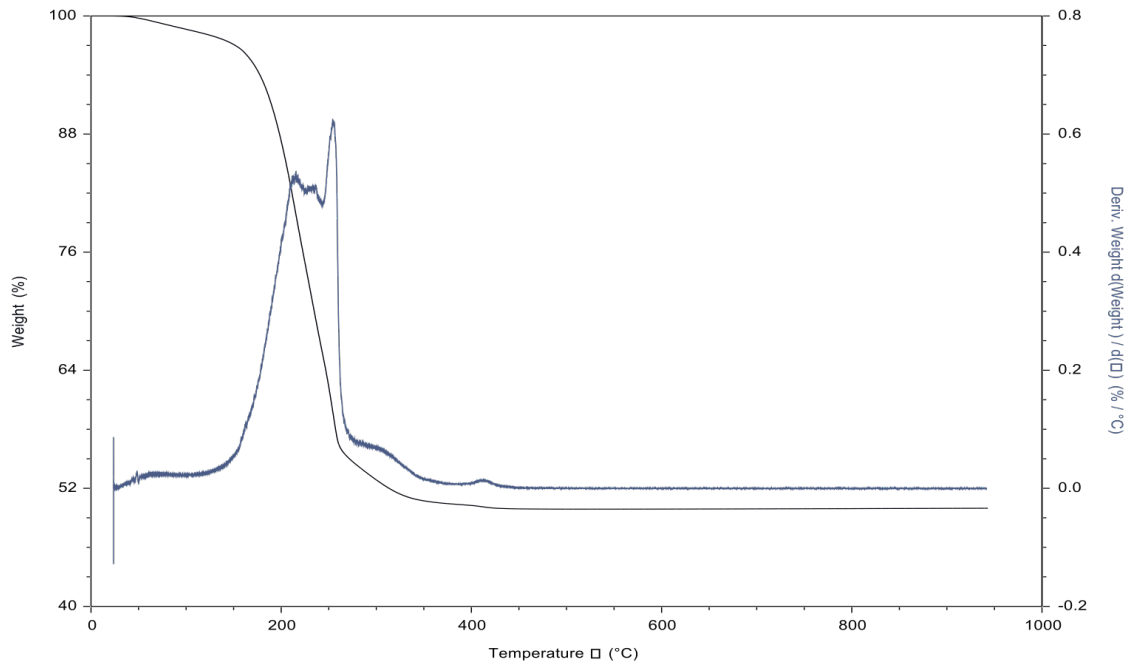


Figure 9. TGA thermogram of non-sterile B31 IBS Composition

2.5. Washout Study

A washout experiment was performed to gain insight into the disintegration behaviour of prepared sterilised and non-sterile IBSs when they are exposed to aqueous environments. The effect of carrier composition and gamma irradiation on the IBS degradation was investigated. The quantification of disintegration of CP-based bone substitutes in solution have previously been based on mass change in the sample [259, 260]. Different researchers have employed different weight measurement apparatuses for this purpose, with the design of the study being dictated mainly by the type of IBS being tested. In one study [226], the change in weight of a hydroxyapatite/collagen injectable bone paste before and after soaking the material in Dulbecco's phosphate buffered saline for 72 hours was recorded. In another study, a bone cement was placed in a custom metal mould containing a 6 mm diameter hole at its base, and the mould was suspended in 10 mL of milli-Q water for 4 hours, after which the supernatant was removed and the sediment was freeze dried and weighed [261]. The weight of the sediment was compared to the original weight of the cement to give a material washout value (percentage).

For the IBS developed in this research, a custom anti-washout test method was designed, inspired by a combination of examples from literature. Firstly, ultrapure water was used as the disintegration medium to negate the potential disintegrative

effects of acidic or other reactive species that may be present in traditional cell culture media. Also, incubation conditions involved the use of an incubator set at 37°C and a shaking platform agitating the samples at a speed of 20 rpm, in order to simulate, as much as possible, the physiological conditions the IBS will encounter. Furthermore, gauze material was used to form inserts for submerging the IBS samples into the ultrapure water. Gauze was utilised due to both ease of its preparation as well as its accessibility, as we desired to work simultaneously with triplicates for all 12 IBS groups.

The image in Figure 10 shows the IBS samples inside the gauze that was then placed into the wells of a 24-well plate containing 2 mL of ultrapure water per well. The image of the samples was taken after 1 hour of incubation. From gross observation, there was visible disintegration of the samples at this time point. In fact, all samples had started to visibly disintegrate at 15 minutes post-incubation (data not provided). Based on this observation, a 24-hour period of testing was deemed sufficient, as the material exhibited relatively rapid disintegration in the given conditions.



Figure 10. Image of sterile IBS samples in ultrapure water after 1 hour of incubation. B11(1), B11(2), B11(3), B12(1), B12(2), B12(3), B22(1), B22(2), B22(3), B21(1), B21(2) and B21(3) (from left to right)

At 24 hours of incubation all the samples had disintegrated almost completely. Figure 11 is a representative image showing the trace amounts of IBS remaining on the gauze at 24 hours post-incubation.

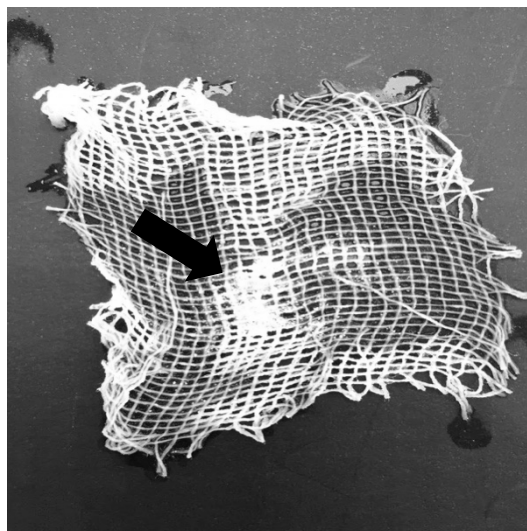


Figure 11. Representative sample showing the amount of IBS remaining on gauze pad after 24 hours of incubation

Plotting the recorded weight of the samples at each time point tested, the time-dependent weight loss of unsterile (Figure 12) and sterile (Figure 13) IBSs becomes apparent. Measurements of weight were recorded at 1, 6, 12 and 24-hour time points. Comparing Figure 12 and 13, there appears to be a gain of disorder to the washout profiles for some IBS samples such as B11 and B31 after gamma-sterilisation, with the curves of the graphs fluctuating in these samples. This alludes to a structural change at the molecular level that may have occurred in some sterilised samples. Statistical analyses of the weight loss of samples with time and under the effect of gamma-irradiation was conducted using a repeated measures ANOVA test revealed that as expected time did have a significant ($p < 0.001$) impact on sample weight. There was, however, no statistical significance in the average weight loss amongst all of the various (sterile non-sterile) IBS groups ($p > 0.001$). Thus, carrier composition and gamma-sterilisation of these compositions do not have a significant impact on the final washout of the IBSs, even though very slight time-dependent fluctuations in anti-washout resistance of the IBS samples is seen from Figure 12 and Figure 13.

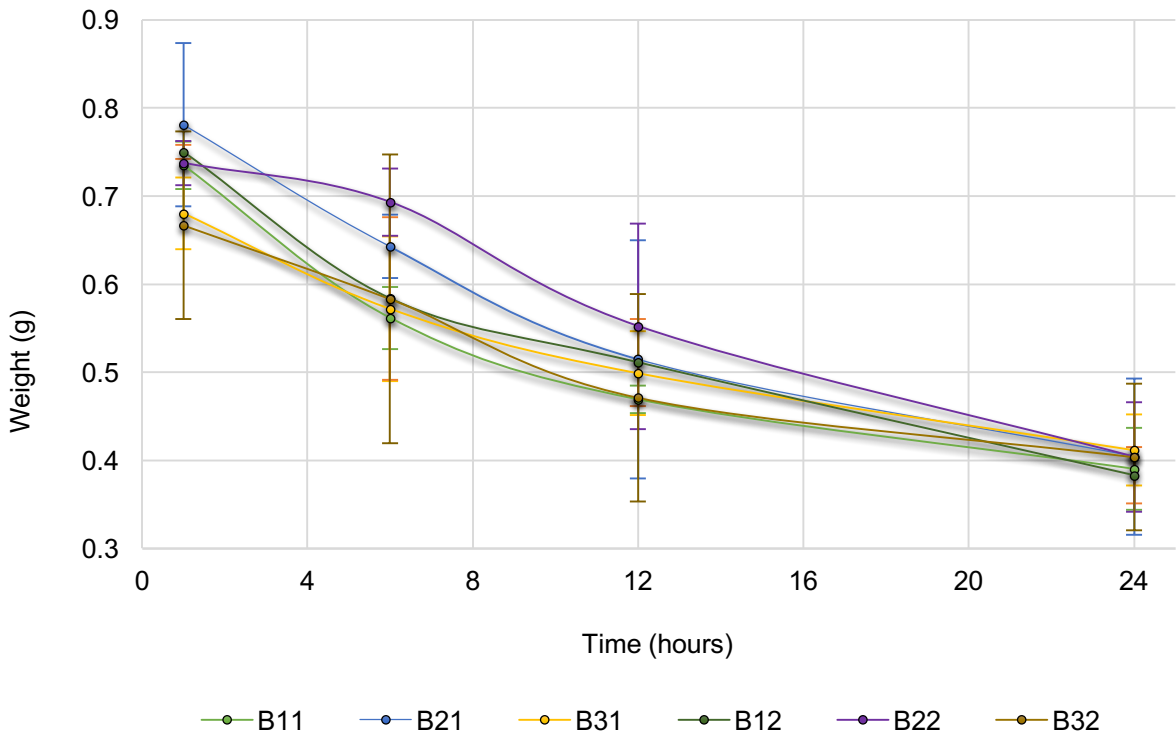


Figure 12. Disintegration profile of sterile samples over time. Error bars represent to standard deviation from the mean for each IBS group

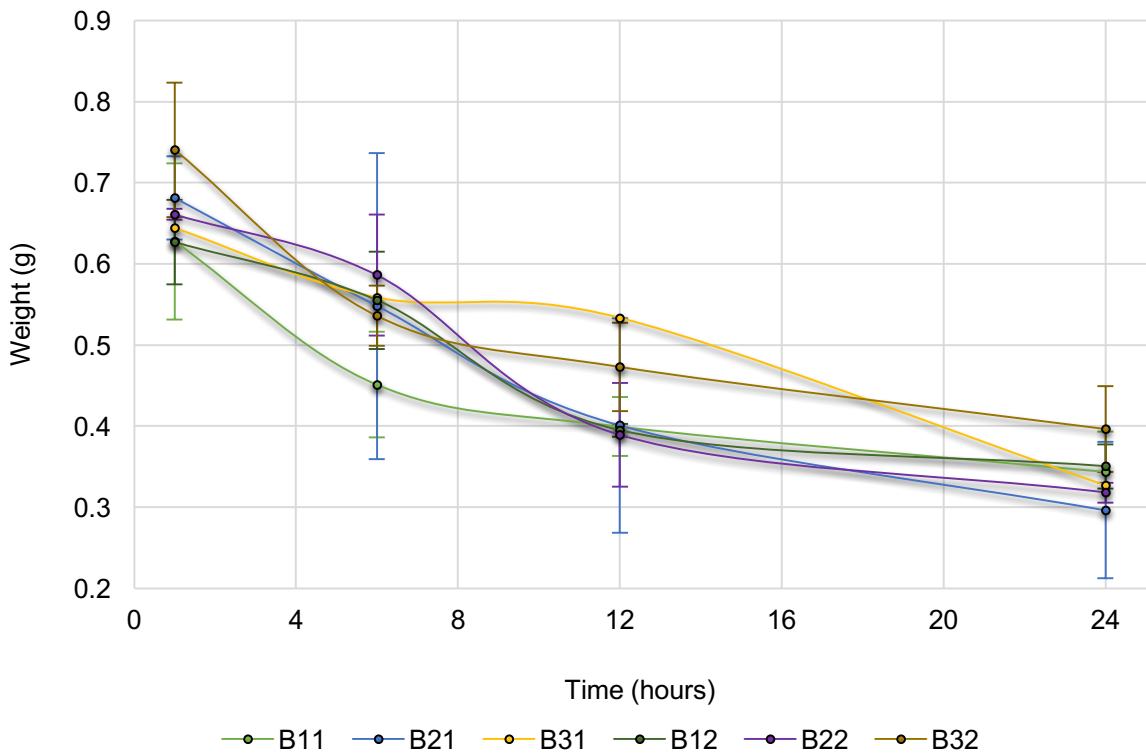


Figure 12. Disintegration profile of unsterile samples over time. Error bars represent to standard deviation from the mean for each IBS group

Figure 14 is a graphical comparison of the weight loss observed, as a percentage loss of original mass (at 1 hour), in various IBS samples. Initial weight was taken as the average weight of the sample (3 replicates) at 1 hour and final weight was taken as the average weight of the sample (3 replicates) at 24 hours. In this graph, sterile and non-sterile IBS samples are compared to see the effects of gamma-irradiation on the overall washout-resistance of the biomaterial. Compositional effects can also be compared across the different IBS groups.

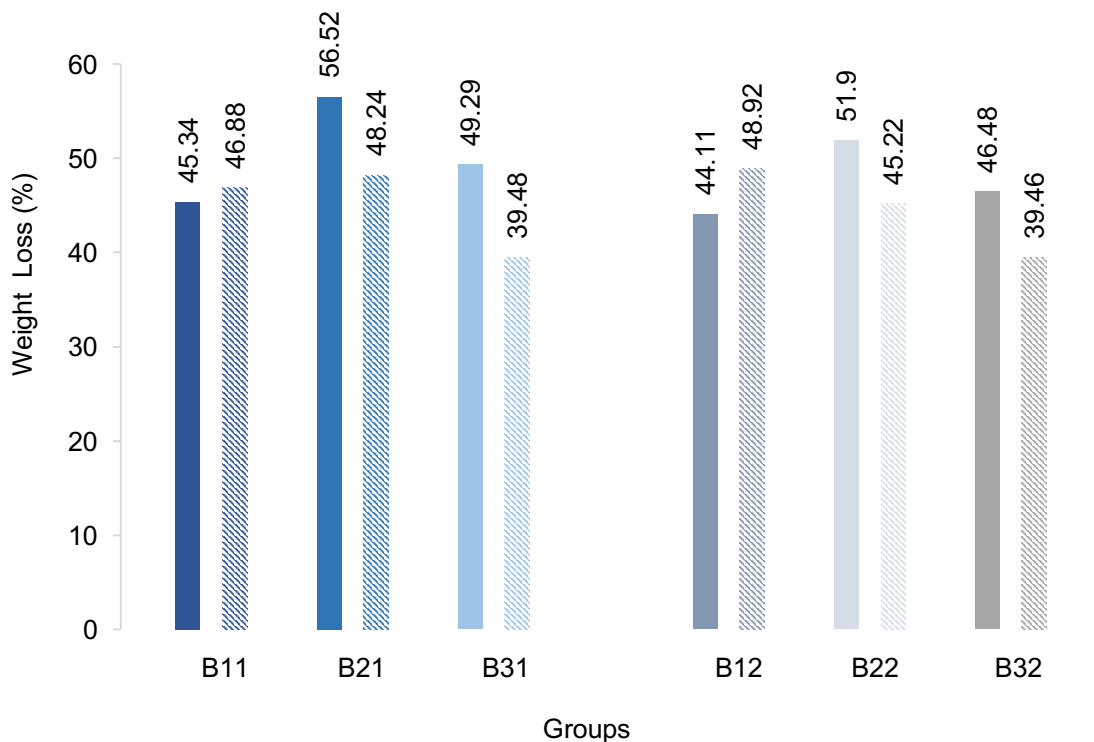


Figure 13. Comparison of material loss in various IBS compositions in aqueous environment. Solid columns represent sterile IBS samples and striped columns represent non-sterile IBS samples

Firstly, B11 and B12 contain the highest amount of PEG content amongst the various IBS groups and thus the effects of gamma, if any, would be expected to be amplified in these groups. These results in addition to those obtained from the injectability and viscosity studies, reveal that Group B11 and B12 samples behave differently to other sample groups. In fact, the data shows that gamma-irradiated B11 and B12 samples have a higher anti-washout capacity. This may be due to

irradiation-related chain cross-linking in PEG chains, of which there are is a HHMW amount of in B11 and B12. This is concurrent with the higher injection force and complex viscosity observed for B11 and B12 in the injectability study, respectively. Interestingly, amongst all sterilised IBS samples (sterile and non-sterile included) the most amount of material lost or 'washed-out' is seen in groups B21 and B22. Examining group B21 and B22 alone does not lead to any meaningful comparisons or deductions, however, in looking at the washout amounts in groups B31 and B32, a plausible explanation concerning the role of glycerol can be made.

Increasing glycerol content in the IBS carrier was expected, due to its significantly lower molecular weight than PEG, to increase the amount of material dissolution in water. Similar to PEG, glycerol is a highly hydrophilic substance and is highly miscible in water. It also has three hydroxyl groups that are responsible for its hygroscopic nature. It would be assumed that the low molecular weight of glycerol allows it to interpose between larger molecules, such as HHMW PEG chains, increasing the free volume between the chains and reducing the cohesive tension between them. As known in industry, due to its low molecular weight, glycerol is used as a plasticiser to reduce the physical properties of materials. Thus, an increasing glycerol content should lead to a greater amount of material wash-out (glycerol is most likely 'washed-out' itself) from the original form. However, an increasing glycerol content in the carrier of the prepared IBS compositions from 45 parts to 55 parts of the carrier (B21 and B22 vs B31 and B32) appears to have a positive impact on the washout resistance of the pastes. The presence of more HHMW PEG, does improve the washout capacity as sterilised B31 samples have lost more material than sterilised B32 samples. Therefore, it can be assumed that there are overriding effects of increased glycerol content on washout resistance when a threshold amount of glycerol is present in the carrier. The amount of PEG in the carrier or subjection to gamma irradiation can therefore be rejected as the only key factors contributing to variance in the washout resistance of the IBS.

Farahnaky *et al.* [262] provide concurring results by showing that whilst glycerol increases the solubility of wheat starch edible films when it forms more than 30% of the material, below this amount, it decreases the water vapour permeability of the films. Statistically (paired t-test) comparing the recorded weights for sterile B21 with B31 and B22 with B23 samples at 24 hours post-incubation, no statistical significance was found ($p < 0.05$). Nor was there a significant difference in the final

weight of sterile B11 to B31. The study, if repeated with a larger sample size and sample weight, may produce statistically significant results that may concur with literature assessing the role of glycerol in IBSs.

Studies given in literature involving a washout resistance analysis of IBSs are mostly based on investigating the washout behaviour of setting bone cements. Thus, the use of more intensive incubation and sample agitation conditions (for example, Liu *et al.* test their wollastonite/calcium phosphate composite cement in a shaker at 37 °C and shaken at the speed of 120 rpm [200]), as well as larger sample containers with larger pore sizes is cited in related literature. The method and materials used for washout analysis in this research project have been adapted to the nature of the material tested. However, the use of a metal wire mesh of smaller pore size (pore size of gauze pad was 1 mm) made from a non-reacting metal, as opposed to sterile gauze material, could potentially have a great impact on the accuracy of the weight measurements collected in the experiment, eliminating human error during handling and weighing of the samples. A similar method for non-setting IBSs has previously been demonstrated by Sato *et al.* [226].

Important points to note regarding this study is that a larger amount of starting material, as would be used in a clinical application, could produce disintegration profiles that are significantly different amongst various IBS compositions. Therefore, this study should be repeated with samples of greater size, preferably in amounts that would be typically applied in a clinical scenario. For consideration, the study can be enhanced with attempts to improve washout-resistance of the IBS with the addition of hardening agents such as sodium alginate [226]. Also, a qualitative analysis component to the washout study could be added in future derivative research, by following the example of Liu *et al.* [200] and observing the disintegration of the material in petri dishes (or similar), as opposed to the well plates that were used here.

From the overall results of this study, we are also able to deduce that the IBSs disintegrate up to 50 % of their original mass at around 8 hours of exposure to incubation conditions in a shaker. This rate of bulk material degradation may produce a burst release of IBS components when placed *in vivo*. It is important for biomaterials to degrade at rates appropriate to their intended applications and bone formation rates. The clinical expectation is that the material remains in the defect

zone for a sufficient amount of time to ensure that the cells and other agents of bone repair have sufficient access and exposure to the content of the bone paste, to reap the benefits of the augmentation material. However, *in vitro* models are not always appropriate as a basis on which *in vivo* performance can be predicted, as discussed in the Biocompatibility Study section of this thesis. Rapid degradation or burst release behaviour of biomaterials in *in vitro* experiments, may not necessarily translate to toxicity *in vivo*, where there are many other mechanisms at play. IBSs are implanted within a confined space in bony tissue where material surface interactions are maximised, thus the traceability of the microscopic degradation products of the IBS would be more difficult. In the body, where cellular degradation is to occur, and degradation products are dispersed through the perfusion of blood and lymphatic fluids, the degradation of the IBS will depend on a much more complex interaction of factors that are essentially impossible to re-create *in vitro*. Thus, the limitations and implications of an *in vitro* washout resistance study should be duly noted.

Weights recorded at 1 hour are actually greater than the 0.5 g of actual IBS placed into each well. The recorded weight at all time points also includes the weight of the hydrophilic gauze which contain the IBS samples, and thus initial recorded weights are greater than 0.5 g. Measurements of all sample weights at all time points were taken with the addition of the gauze. In other studies, the dry weight of IBSs is recorded prior to immersion in liquid, and this is compared to the final *wet* weight of the sample after a period of soaking in solution. However, the degree of degradation and types of materials used in cited studies differ greatly from the IBS developed here. The IBS developed in our study is one that dissolves relatively fast in water which makes the IBS sensitive to handling after soaking in solution for a short period of time. Also, unlike other examples in literature, there are no washout products or remaining structures of the IBS post-soaking that are lyophilised or physically handled to obtain weight-based measurements of. Furthermore, the amounts of IBS used for this experiment are relatively smaller than those encountered in literature as the sheer number of samples included in the study was larger than those previously reported. This meant that not only was the order of weight change in each sample was small, but the experiment was also sensitive to manual handling.

2.6. Cohesion Study

The cohesion of a material can be defined as the degree to which the constituents of the material remain intact at the molecular and larger level, even under exposure to detrimental environmental conditions. Similarly, to washout resistance, it is also linked to the concept of material disintegration. A material that is highly cohesive is also expected to have a high resistance to 'washing out' under irrigation. The cohesiveness of an IBS can be tested by examining the removal/release of chemical constituents/s after placing the IBS in media or solution. Both washout resistance and cohesiveness are tested in aqueous environments to simulate physiological conditions as closely as possible.

PEG and glycerol were chosen as the carrier materials of the IBS developed and researched in this study, not only due to their known biocompatibility, but also because of their high solubility in water. Furthermore, it forms an injectable, mouldable and degradable IBS when mixed with calcium phosphates and bioglass. The cohesion capacity of the IBS developed here was tested by not only the elution of its most fundamental chemical constituents, but also the rate at which its elution occurred. To this end, we observed the amount of Ca^{2+} ions released from the ceramic component of the IBS following the degradation of its carrier, which is the only quantitative method of cohesion measurement as recommended by Bohner *et al.* [263].

Ca^{2+} ion release from group B11 samples over a period of 48 hours was observed. B11 was chosen as a representative group. The calcium release of B11 samples was evaluated over a greater number of time points compared to all other composition groups that were samples at 1 and 48 hours. Based on preliminary analysis of injectability, handling and washout-resistance, B11 exhibits the most favourable properties and was thus chosen as a representative sample of the ideal IBS. Furthermore, including 10 samples (10 time points) per IBS group in the ICP-OES analysis was not practically or economically feasible for the purposes of this research. Sample aliquots were taken at closer time points initially, to investigate if a burst-release effect would be seen. Also, to investigate the effects of gamma sterilisation on bioceramic disintegration both sterile and non-sterile B11 samples were analysed. The calcium release profile for sterile and unsterile B11 samples is given in Figure 15 below.

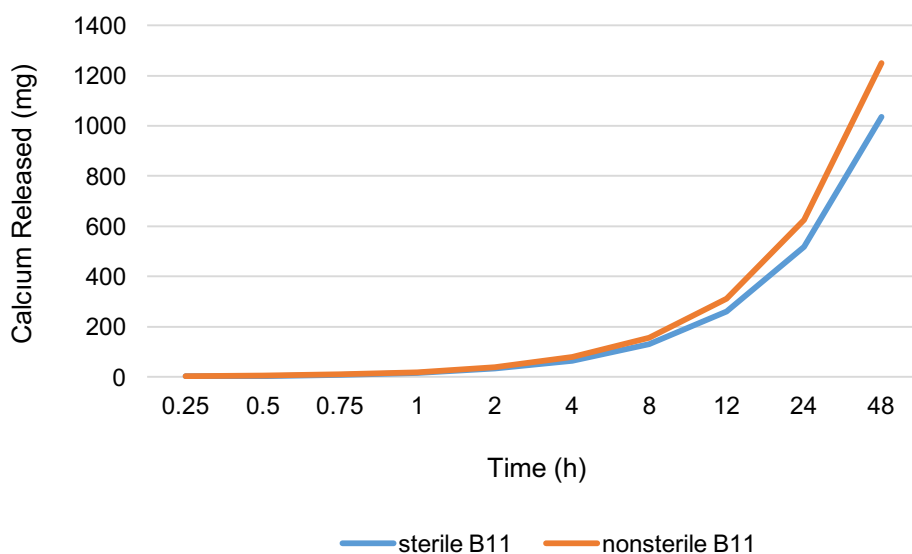


Figure 14. Calcium ion release from sterile and unsterile B11 samples over 48 hours

From Figure 15 it can be seen that both the sterilised and non-sterile IBS appears to release similar amounts of calcium over time, post-submersion. The general calcium release profile for both types of samples is similar throughout the experimental period. At 8 h, however, sterile B11 releases less calcium than non-sterile B11, and this trend follows through until the end of the testing period. We speculate that gamma irradiation is potentially stabilising for the ceramic particles and/or carrier of the IBS. The results from ICP-OES analysis of aliquots taken from sterilised samples at 1 h and 48 h is given in Figure 16. From this information we can speculate as to whether the calcium release capacity of the initial samples increase, decrease or remain largely the same as at the beginning of the study. At an overview, B11 samples have released the least calcium into the dissolution media at both 1 h and 48 h post-incubation. B12 has released a much larger amount of calcium at both time points compared to B11. This may signify the greater capacity of IBSs with more HMW PEG content at protecting ceramic particles against exposure to water.

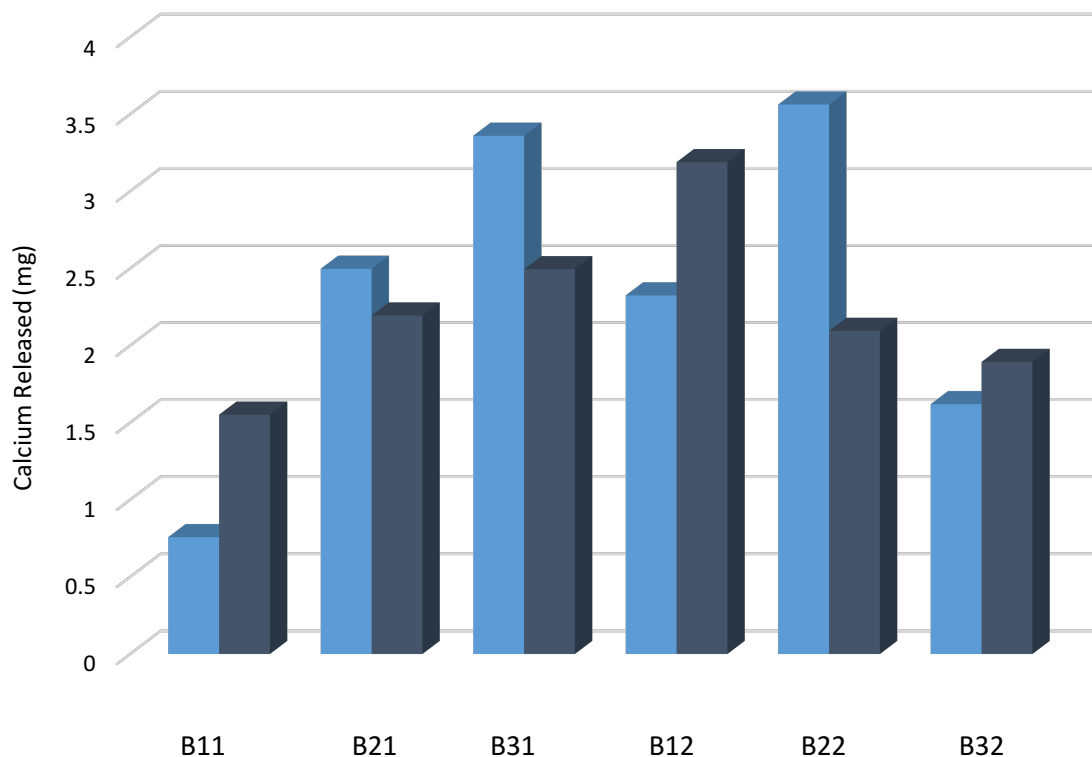


Figure 15. Amount of calcium release from sterile IBS samples. Light blue columns represent calcium release from sample at 1 hour, dark grey columns represent calcium release from sample at 24 hours

At 48 h, B12 is found to have released the most amount of calcium, and B11 the least. Between HMW samples (B11, B21 and B31) there is an apparent incremental increase in the amount of calcium released at 1 and 48 hours with increasing glycerol content (B31>B21>B11). This trend is reversed in the low HMW groups (B12>B22> B32) for the 48 hour measurements. According to the 1 hour measurements for B12, B22 and B32 do not appear to follow a composition-based trend for calcium release. Interestingly, when lower HMW PEG is used the effects of glycerol as an anti-washout (see Washout Study) or positive cohesion agent become apparent. According to these results, sample B32 is the overall second-most cohesive IBS formulation, at both 1 and 24 h post-incubation. More importantly, we deduce that calcium release does not decrease to a great extent for any of the samples. This provides some argument for the necessity of long-term incubation of samples in *in vitro* testing, to allow for the reduction in ion release in bioceramic-based biomaterials (see *In Vitro* Study).

As the correction-factor method [264] was used to calculate the concentration of calcium within the solution, the volume of which decreased with each sample collected, we can negate any concerns of calcium loss due to sampling. Furthermore, as samples were collected manually (pipetting) at each time point, care was taken to ensure that the pipette was inserted to approximately 5 mm from the surface of the solution each time. Also, great care was taken when handling the samples to ensure the falcon tubes were not agitated enough to cause the sediment IBS to rise in the solution and leading to measurement inaccuracies.

In literature, the methods of testing cohesion or anti-washout properties of IBSs are used interchangeably. Bohner *et al.* [218] provides a comprehensive review of the theoretical and experimental approaches to testing the cohesion of calcium phosphate pastes. One interesting custom apparatus for testing cohesion is presented in the work of Ishikawa *et al.* [204]. With the custom-apparatus a continuous and quantitative method of measuring the weight change of the sample (a 6 g β -TCP powder – 2.6 mL 0.6% xanthan solution mixture over time is made possible. A sample-containing casing is submerged in distilled water and connected to a weight placed on a scale. As the IBS leaches from the casing and sediments to the bottom of the test fluid the weight of the casing registered on the scale changes, indicating the amount of material that has disintegrated. This method however, and as agreed by Bohner *et al.* [218], is not appropriate for flowing pastes but rather cements.

Bohner *et al.* [218] have performed a comprehensive study on the cohesiveness of calcium phosphate based injectable bone substitutes. They have reported two methods of improving paste cohesion. The first is to decrease the average particle size of the particle phase, and the other is to, in some cases, add xanthan. Previously, xanthan has been added to glycerol-based foam, film, aerogel and xerogel [265], as a cross-linking agent to improve gel cohesion, and xanthan-based thickeners have also been demonstrated to have high compatibility with PEG [266, 267]. An interesting finding of Bohner *et al.* [218], was that the addition of HA powder to β -TCP powder-xanthan pastes, significantly improved paste cohesion, whereas the addition β -TCP particle to the same paste led to a continuous disintegration of the paste, reducing its cohesion capacity. Where β -TCP was used as the sole constituent of the particle phase in the carrier (xanthan or deionised water), a rapid

weight loss in the paste was observed, whereas the presence of HA or other additives such as citrate ions showed a more continuous degradation profile. In another study, hydroxyapatite-based bone cements were infused with bisphosphonates as a means of sequestering calcium ions in the cement matrix and preventing it from leaching into the solution (milli-Q water) in which the cohesion of the cements were tested [220]. Bisphosphonates have a very strong affinity for calcium ions and its addition to the IBS was found to dramatically improve the cohesion of the matrix.

One study found that the addition of HMW PEG to a PLGA-PEG based *in situ* gel-forming peptide delivery system, resulted in a decreased amount of drug release [268]. The authors suggest that the reason for this could be the effect of PEG as a cross-linking agent or the formation of PEG complexes formed with HMW PEG chains that are effective in trapping drugs. These findings are echoed in the results of cohesion and anti-washout, which parallel the results of injectability and viscosity, as introducing a greater amount of HMW PEG seems to add cohesiveness and anti-washout resistance to the IBS, as well increase its viscosity and injection force.

2.7. Injectability Study

Although the concept of 'injectability' as it is applied to IBSs has long been a topic of discussion for scientists, for the purposes of this research we analysed the maximum compressive force that would be required to keep the plunger of the syringe moving through the barrel until all of the IBS was expelled. The experimental setup used during the injectability test performed with a mechanical testing machine is given in Figure 17:

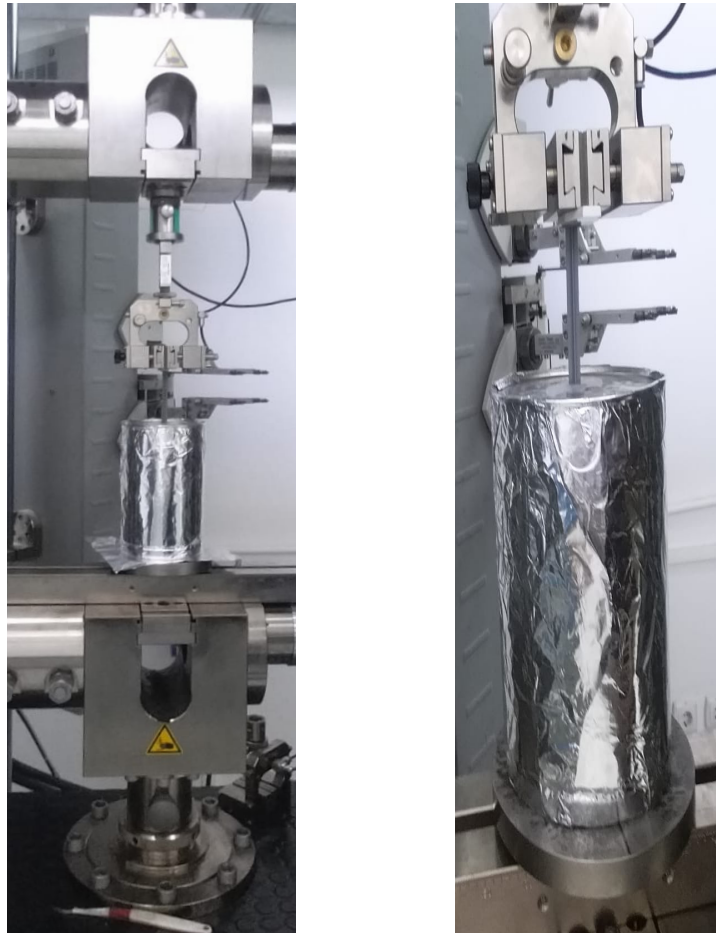


Figure 16. Experimental setup for mechanical testing machine and syringe apparatus during injectability tests

To compare the samples, the peak injection force that had to be applied during the compression of the syringe was used. As the syringes were filled with the IBS (5 g/syringe) via manual methods, air entrapment in syringes led to the self-ejection of material in some syringes upon removal of the syringe cap. This ultimately affected the original starting position of the plunger, which was set at 70 mm for all samples in the software of the mechanical testing machine. As this would affect the validity of injectability interpretations based on plunger displacement, the maximum peak force obtained during material ejection from the plunger was used to make comparisons between samples. The force vs plunger displacement curve obtained for sample sterile B11 (first of three repeats) is given below as a representative

graph of those obtained for each sample. For this sample, for example, the peak force at 73 N was reached at approximately 2.2 mm of plunger travel distance.

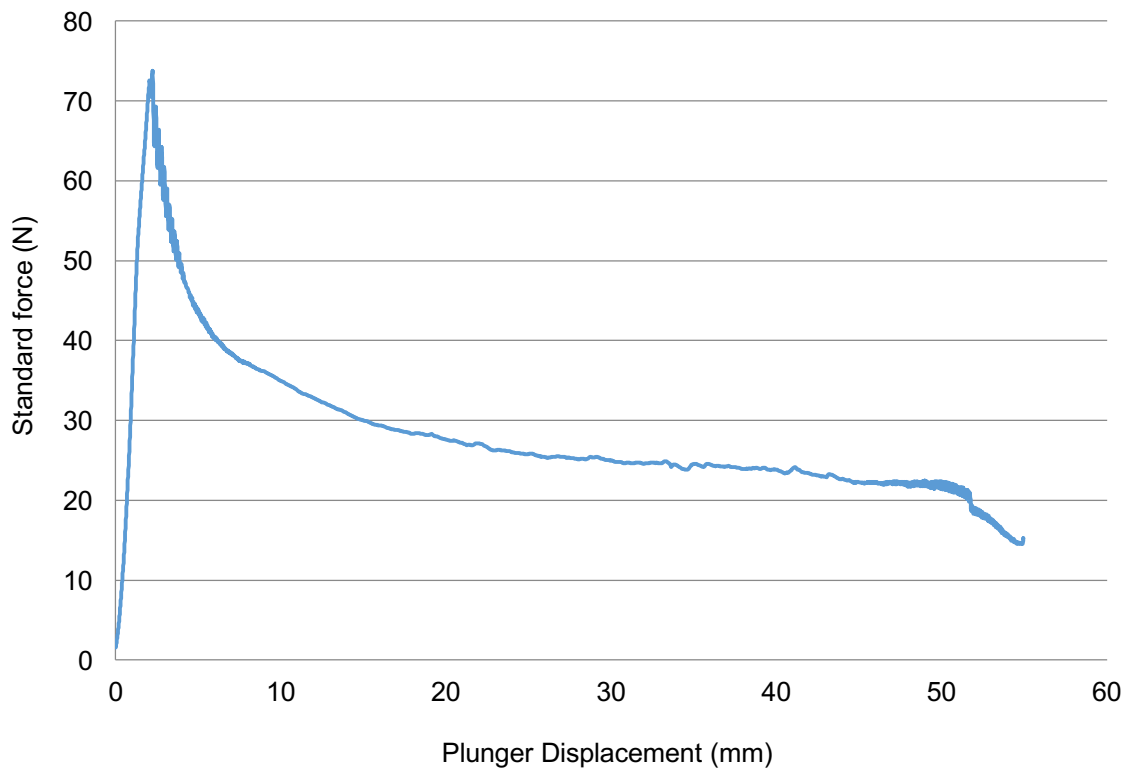


Figure 17. Representative graph (sample B11) graph of applied force vs plunger displacement

The average peak force obtained from all three replicates of each sample was calculated and graphed with the standard error of mean. Three research enquiries were designed for this experiment:

- does the amount of glycerol in the carrier impact injection force?
- does the use of less HMW PEG in the PEG phase of the carrier affect injection force?
- does gamma-sterilisation of samples affect injection force? More glycerol in the carrier is expected to have a lubricating effect for the IBS.

Lower high molecular weight polymer chains would also be expected to reduce the injection force required to expel the IBS. Gamma-irradiation of samples with large amounts of HMW PEG content would be expected to increase the injection force required by the IBS.

Figure 19 provides a graph of the average peak injection forces recorded for sterile IBS samples, with dotted columns representing compositions with LHMW content.

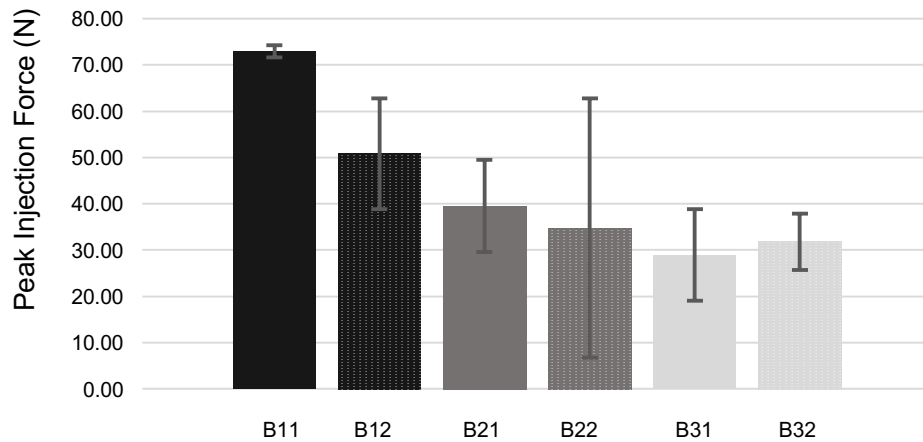


Figure 18. Average Peak Injection Forces for Sterile IBS Compositions. Dotted columns represent samples of LHMW PEG content

From the graph above we can see a general decrease in the average peak injection force as the amount of glycerol content increases in both groups with high HMW and low HMW PEG content. This finding is supported by the known industry application of glycerol in IBSs for the purposes of improving consistency and injectability of bone graft substitutes. The exception to this is B31 and B32, where B32 has a higher average peak injection force than B31. Conducting pair-wise comparisons, we found that the difference between B31 and B32 is not statistically significant ($p=1$), however, B32 is significantly ($p=0.04$) different to only group B11 samples. Looking at the average mean error of samples within each individual group, it can be seen that these errors are, particularly for group B22, noticeably large. It is speculated that varying degrees of agglomeration of bioceramic particles in IBS samples may have contributed to large mean errors.

Similarly, as hypothesised, lower HMW PEG content reduces injection force for IBS of the same PEG:glycerol ratio. This is due to the greater resistance to rearrangement of the longer HMW PEG chains in samples with high HMW PEG content compared to those samples with a larger content of low HMW content, when subjected to a force along a single axis. The difference between IBSs with more HMW PEG and less HMW PEG in their carrier was not found to be statistically

different between any two IBS groups, although IBS composition overall did have a significant impact on peak injection force.

Figure 20 also allows for the comparison of sterilised and non-sterilised samples and the impact of gamma radiation of IBS injectability. The variance of mean peak injection force between all tested samples was found to be statistically related mainly (38.4% partial Eta Squared) to IBS composition with IBS composition showing $p=0.031$. According to the graphical results, potentially cross-linked sterile compositions have a slightly higher peak injection force compared to non-sterile samples. Moreover, only in groups B21, B31, B22 and B32 have unsterile samples shown a greater resistance to injection than their sterile group members. Sterility alone, however, was not found to have a statistically significant ($p=0.861$) impact on the mean peak injection force recorded. There is a decrease in injection force proportional to the increase in glycerol content in the IBS in sterile samples, in both high and low HMW PEG containing groups. This is not seen for non-sterile samples with non-sterile B21 and B22 producing lower injection force values than other groups. In unsterile samples, when the glycerol content is kept constant and the amount of HMW PEG content is varied, as seen with the sterile samples as well, groups with higher HMW content displayed higher average peak injection forces than those with low HMW content. Although sterile samples also follow this relationship, the exception is B31 and B32 as previously mentioned.

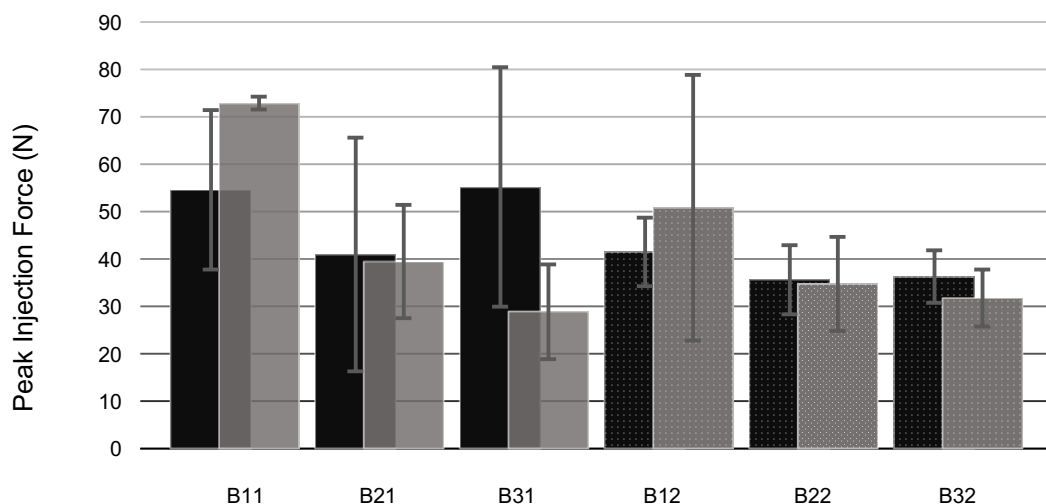


Figure 19. Peak injection forces for all groups. Light grey columns (including dotted-grey columns) represent gamma-sterilised samples of the same group.

Dotted columns represent samples of LHMW PEG content

A higher content of smaller ceramic particles may lead to filter-pressing issues. This is one fundamental reason as to why all samples of group 'A' (40:60 carrier to ceramic + BG) were discarded from rheological, and injectability analyses, as these samples were found to be completely non-injectable. Therefore, the use of larger ceramic particle size is one way in which filter-pressing can be avoided or reduced in injectable materials. Another method may be to ensure that the liquid phase of an injectable bone paste is chemically-engaged to smaller particles and of a viscosity capable of keeping smaller particles uniformly dispersed and moving together with the liquid phase throughout the injection process. The assumption that a higher glycerol content will lead to lower injection force seems applicable according to the injectability results from sterile samples, however, contradictory results seen for unsterile samples are counterintuitive to the expected lubricative effects expected for glycerol. The negative effects (higher average injection peak force) of higher glycerol than PEG content seen in unsterile samples, with the absence of the apparent order that gamma-sterilisation gives to IBS samples as seen in sterile samples, may be related to the fact that particles of β -TCP and bioglass move freely throughout the less viscous glycerol, however, under injection pressure, move slower compared to the glycerol itself, leading to a filter-pressing phenomenon. Gamma irradiation is known to cause changes in the polymer chains of PEG, either in the form of chain scission or, more likely, cross-linking. It appears that exposure to gamma irradiation has given putty compositions proportionality between injection force and glycerol and HMW content. The absence of this observable trend in the gamma-negative groups can be explained by a disruption of the fluid dynamics of the injectable putty when glycerol content exceeds a certain level, and a gamma induced cross-linked polymer network is not present to stabilise the IBS carrier matrix. The presence of a greater glycerol content in the liquid phase of the IBS, (shown to increase IBS viscosity, see Viscosity Study), may have led to issues such as filter-pressing as smaller particles moving at a slower speed to that of the carrier and build up in front of the plunger, creating resistance to its displacement. The most interesting phenomenon observed in the injectability study is the higher injection force for gamma-irradiated samples of B11 and B12, compared to untreated samples. B11 and B12 contain the least glycerol content and have a significantly increased average injection force (18.32 N for B11 and 9.33 N for B12), and the results hold true regardless of whether the amount of HMW is varied. For

the compositions with greater than 35 parts glycerol content in the carrier phase (B21, B32, B22, B32), the injection force in post-gamma samples compared to their pre-gamma counterparts is lower, regardless of whether higher molecular weight PEG is used. It is a known fact that exposure to gamma radiation can cause changes in PEG chains, either in the form of scission or in the form of cross-linking. As there is a reduction in injection force in post-gamma samples, except for B11 and B12, we can assume that some degree of chain scission has occurred in samples with decreasing PEG content. The reduction of complex viscosity in these samples also supports this theory. However, the effect of gamma irradiation has a completely opposite effect for B11 and B12, where the injectability of the force of the putty increases dramatically. In fact, as seen in the results and discussion for viscosity analysis, the opposite effect is also seen for the final complex viscosity of B11 compared to other groups. The presence of a greater amount of PEG chains lends availability to cross-linking in groups B11 and B12, whereas this is less likely when there is less than 65 parts PEG in the carrier phase.

We must also consider that although the same amount of putty was packed into the syringes, any accidental extrusion during handling whilst setting up the syringes in the mechanical tester apparatus would have resulted in lower average peak injection forces in such samples, as the plunger has less material to push against. Furthermore, any discrepancies between plungers such as amount of lubricant in each (as supplied by their manufacturer) may have also had an impact on the final results. Also, as the material was packed manually into the syringes, any gaps left within the material during compaction into the syringe barrel registered on the force vs plunger distance curve as a sudden drop in injection force. An automatic syringe-filling system should be employed in future studies of the material to ensure that such potential causes for discrepancies are avoided.

From the results of the injectability study, we determined that there is a critical threshold for both glycerol and PEG content, above or under which, counter-intuitive phenomena are observed for IBS injectability.

2.8. Viscosity Analysis

The viscosity of bone pastes is an important rheological property. Viscosity is closely linked to injectability, which also translates to the degree of ease with which the

material is handled. The change in IBS viscosity with varying liquid-to-powder ratios or in the presence of additives is usually examined during the development phase of an IBS. In the preliminary development phase of the IBS in this work, the 1:1 powder-to-liquid ratio was considered to have the most favourable consistency, injectability and viscosity, based on gross observation and handling. Therefore, for the purposes of the viscosity analysis, the effects of varying the concentration of carrier components, rather than the overall ceramic concentration in the IBS was analysed.

Materials may be considered elastic, viscous or viscoelastic, depending on their behaviour when subjected to applied strains and stresses. Polymeric fluids, whether solution or melt, may be considered as viscoelastic, particularly if its flow and mechanical properties change with changing temperature and/or time. Dynamic mechanical analysis is a method for testing such viscoelastic materials. This technique is used to measure the material's stress response to sinusoidal strain. It provides us with the viscoelastic property values of the material, such as its storage modulus (G') and loss modulus (G''). The elastic modulus is used to describe the ability of a material to return to its original shape when deformed. The loss modulus reveals how much of the applied energy to the material is dissipated or 'lost', as a result of permanent deformation. For comparing the viscoelasticity of polymers, a dimensionless factor, known as the dampening factor or the loss factor ($\tan \delta$), is used. $\tan \delta$ is the ratio of G''/G' . Therefore, it is >1 for purely viscous liquids, or <1 elastic solids. A $\tan \delta$ that is equal to one represents a perfectly viscoelastic material. It is also referred to as the or 'gel point' or 'sol-gel point' of a polymer, which is the point at which G' and G'' are equal, and a purely polymeric solution has achieved a viscoelastic gel-like status through the addition of plasticisers or due to cross-linking between polymeric chains. The complex viscosity (η^*) is another useful property that provides an overview of the viscoelastic profile of the polymeric material as it is fundamentally composed of both the elastic and viscous values of the material. In equation form, it is the ratio of shear-stress amplitude over the strain amplitude.

The different types of rheological tests for viscosity include oscillation, rotational and tension and relaxation experiments. Oscillatory rheology, used for the viscosity assessment of the IBS presented here, measures the stress response of a material subjected to sinusoidal shear deformation. A simple description of the apparatus is as follows: the material is placed between one rotating (at oscillation frequency ω)

bottom plate and one stationary top plate which subjects the material to a time-dependent strain, which is then imposed as a torque (stress) on the top plate. G' and G'' characterise the solid-like and fluid-like contributions to the measured stress response at ω , respectively.

Furthermore, there are different test modes in which a standard oscillatory rheometer can be operated, namely, the amplitude sweep or frequency sweep mode. The former varies ('sweeps') the amplitude of the applied stress in the non-destructive region for the material, is used to determine the upper limit of this region, and observes the changes in the material when this limit is exceeded. In a time-sweep mode, the time-dependent stress response of a material in the non-destructive region is analysed. The amplitude of the stress is kept constant whilst the oscillatory frequency of the applied stress is varied incrementally. High frequencies represent fast motion whilst low frequencies simulate slow motion experienced by the material. In temperature-dependent or time-dependent analysis amplitude and frequency is kept constant to analyse how time or temperature affects G' and G'' .

For the viscosity analysis, several prepared formulations of IBS were tested with an oscillatory rheometer used in a plate-plate configuration, appropriate to the nature of the IBS. Polymeric materials display different viscoelastic behaviour at different oscillatory frequencies, depending on a number of factors including the length of the polymer chain (molecular weight), its molecular structure (branching) and the orientation or network-forming ability of the polymer. The interplay between chain flexibility and number of molecular entanglements create the overall viscosity profile for a polymer-based material. For the IBS in this study, the effects of variable oscillatory frequency on the viscoelasticity of the IBS was investigated to ascertain the role of viscosity during ejection of the material from a syringe. As previously mentioned, when the liquid phase of an IBS moves relatively faster than the solid particles within an IBS, the solid particles may form a barrier to the motion of the plunger. This issue is known as filter pressing. Therefore, to explore the interrelationship between IBS viscosity and injection speed, a frequency sweep was used in the viscosity analysis. A frequency sweep between 1-100 Hz (100 Hz is typically the maximum frequency of commercial rheometers) was used in the oscillatory rheology experiment.

Figure 21 provides the rheogram for change in G' and G'' with increasing frequency for sample B11 (sterile) which was used as a representative sample for the purposes of this section of the discussion. From Figure 21, we can see that as oscillatory frequency increases, there is a rise in the values for both the storage modulus and loss modulus, indicating a weak gel behaviour for the IBS [269]. This shows that the viscoelasticity of the material is dependent on how fast it moves with applied strain, and is a typical profile for a viscoelastic polymer. In such analyses, the slopes of the G' and G'' curves are compared to determine whether elastic or viscous effects dominate. The equation for the fitted trendlines provide the extrapolated values for these slopes, however, it is clearly apparent that the G' curve is greater than G'' throughout the frequency scan. The increase of G' with frequency suggests that the number of effective junctions or 'entanglements' between polymer chains in the carrier of the IBS, increase with increasing frequency. An explanation for this is based on the timescales the measurements taken at each frequency. It can be deduced that the 'lifetimes' of the polymer chain entanglements formed with increasing frequency, are longer than the relatively short timescales of measurements taken at higher angular frequencies. More simply, there was less time for the entanglements to become disrupted during the higher frequency oscillation period, and thus the elastic behaviour increases monotonically, overriding the viscous contributions of the carrier. Conversely, even with larger timescale of measurement i.e. at lower ω , there are fewer effective junctions between polymer molecules, and thus G' decreases, as seen in the G' curve in Figure 21.

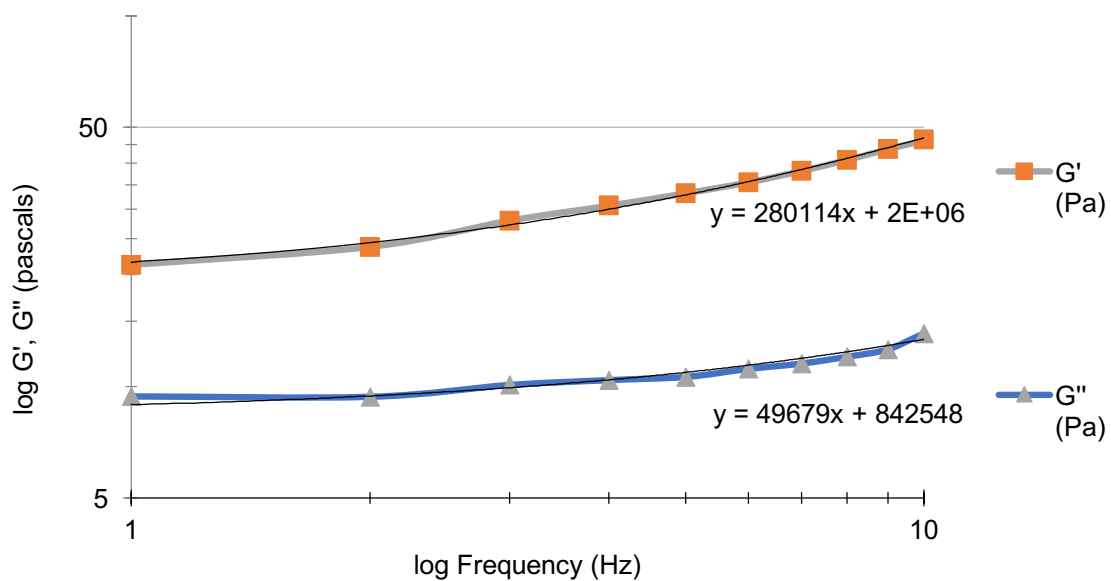


Figure 20. Change in G' , G'' with oscillatory frequency of representative IBS (B11)

This trend for G' is paralleled in all IBS compositions (Figure 22), albeit in different orders of magnitude. G'' , also increases with increasing angular frequency for the sterilised B11 sample (and all other gamma-sterilised IBS sample, see Figure 22). As we increase the amount of high molecular weight PEG concentration in the carrier, a more elastic solid-like behaviour, i.e. higher G' values obtained for the IBS, than those with less high molecular weight PEG content, is seen and expected. This is related to the higher number of molecular interactions possible within the carrier matrix. Comparing sterilised IBS groups B11 and B31, and B11 and B12, we can investigate the changes in G' (elasticity) of the IBS at less overall PEG content, and less HMW PEG content, respectively. B11 has a much higher G' value than B31 and B12 samples, as expected. This holds true for all IBS values at all oscillatory frequencies over the frequency range.

G'' also increases slightly as a function of ω (expected of viscoelastic samples), however, the condition $G' > G''$ never changes over the frequency scan range of the experiment. Firstly, G' and G'' never cross over between the 1-100 Hz, as may be seen with other hydrogels, signifying that for the IBS is no longer concerned with a 'gel point' (point at which the viscous solution has reached a gel or solid-like behaviour), by virtue of the physical bonds formed between the particles of the composition. These bonds give the IBS a network structure, pushing it towards a

solid-like state and eliminating the potential for any viscous dominance. The systematic increase in G' and G'' also indicate that phase separation between the solid and liquid components of the IBS has not occurred across the 1:1 powder:liquid concentration, and various carrier concentrations tested.

As the IBS is not purely solid, however, a frequency-dependency of G' (and G'') should still be, and is, observed. The initial plateau region seen for G'' can be attributed to the existence of strong network structures even at very low frequencies which take up more energy than dissipate it. With increasing HMW PEG concentration in the carrier, higher G'' values are recorded at each increase of oscillatory frequency. However, as this is only a slight increase, we can deduce that the relaxations or dissipations of the applied energy are only local. Interestingly, there is also a slight convergence of G'' magnitude across IBS formulations with increasing oscillatory frequency which implies that material structure loses significance at higher frequency oscillations. This is also reflected in the increase in the $\tan \delta$ value seen in Figure 24, indicating a rise in the viscosity of IBS with frequency. Nevertheless, the elastic effects of the IBS remain distinctly higher than the viscous effects at all frequencies tested - a behaviour that typically defines dispersions or gels [270].

It is noteworthy to mention that the linear viscoelastic response of materials may often times be confused for thixotropy, as G' appears to ever-increase with increasing frequency. In the linear viscoelastic region (determined by finding the maximum deformation or strain amplitude for the material by performing a strain sweep prior to a frequency sweep), the microstructure of the material over-responds within a small timescale, without changing entirely, whereas thixotropic materials undergo a breakdown (during shear) and rebuild (at standing) of microstructure, as a function of time. The IBS in question undergoes permanent deformation at even small amplitude shear strains and is therefore not considered to be thixotropic. However, it is also important to note that there is very little previous research into the viscoelasticity of ceramic suspensions, as suspensions with large amounts of solid content are difficult to both prepare and analyse [271]. Thus, literature from food and beverage materials research are relied on for scientific data comparisons.

Figure 22 presents the trends for G' , G'' and η^* for gamma-sterilised IBS formulations at each during a frequency sweep. It provides valuable insight into the effect of IBS composition on IBS rheology and is a commonly-encountered profile for thick polymeric gels or blends [272]. G' and G'' increase in a parallel fashion, however, with an apparent proportional decrease in these values with decreasing PEG, and decreasing HMW PEG content in the carrier. This additive effect is not unusual as polymeric fluids are not ideal elastic materials and viscoelastic materials display this relationship in the linear region. The continual rise is due to the effect of the sum of two small deformations being greater than the effect of each individual deformation. Oscillatory tests with small amplitude oscillatory motion are therefore commonly selected for studying the linear response of polymeric solutions or melts. Also, there is an incremental decrease in the complex viscosity of IBS compositions with frequency and IBS composition. Complex viscosity is a combined value of the contributions of the elastic and viscous parts of a material. IBSs with higher PEG and HMW PEG content in the IBS display higher complex viscosity at all frequencies. A higher complex viscosity signifies a greater degree of viscoelasticity of the sample. Fittingly, sample B32 with the least amount of overall PEG and HMW PEG content in the carrier, is the most viscous sample amongst the various IBS formulations.

With a frequency-dependent G' , G'' and η^* , the applicability of the Cox-Merz rule in rheology could be questioned. The Cox-Merz rule states that the apparent viscosity at a specific shear rate, is equal to the complex viscosity at a specific oscillatory frequency [273]. If this relationship is true for the material studied, it can combine information from both steady-state shear and viscoelastic analysis, creating a more detailed rheological profile. Due to the unavailability of steady-state shear data for comparison, this relationship was not investigated within the scope of this research. However, for future reference, the possibility of the Cox-Merz relationship and potential power modifications as previously performed for food-based materials [269] could be investigated.

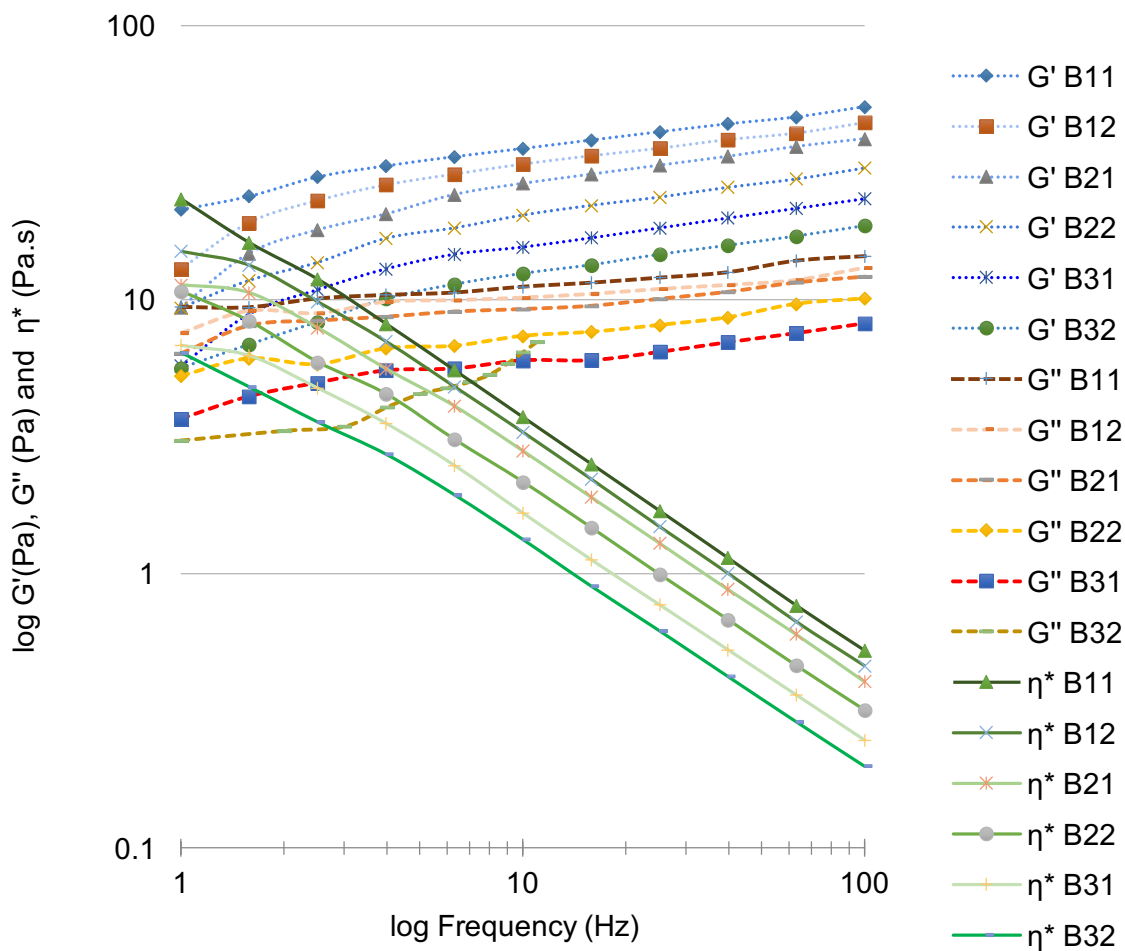


Figure 21. Oscillatory frequency-dependent change in G' , G'' and η^*

A decrease in $\tan \delta$ with increasing oscillatory frequency reflects the domination of the material's elastic component at faster shear motions (Figure 22). From physical observation, the difference between manual handling of the IBS immediately subsequent to ejection from the syringe compared to continued handling for approximately 10 seconds, can be described as the IBS becoming more mouldable or dough-like compared to its initial more viscous feel. A lower $\tan \delta$ value signifies a higher degree of cross-linking between polymeric molecules giving a more elastic nature to the IBS. The change in values of loss factor for IBS samples in the order of $B32 > B31 > B22 > B21 > B12 > B11$ toward 100 Hz, indicates that with a higher amount of glycerol in the carrier, the IBS approaches loses its solid state becomes more like a fluid. From Figure 23, it can be seen that at an angular frequency of 10 rad/s (chosen as a representative frequency), the $\tan \delta$ values are lower in IBS samples with more PEG and HMW PEG content, as the density of long chained

molecules in the carrier available for cross-linking is greater, as expected. Although the exception to this is B31 and B32, the difference is extremely small and could be statistically insignificant if a larger sample size was used. Furthermore, we can assume that this elastic dominance is linked to the creation of the peak injection force that must be initially overcome in order to completely expel the IBS from a syringe. The subsequent rapid drop in injection force observed in the injectability study can be related to the assumption of a more viscous nature of the IBS as it gains speed moving through the plunger (increase in $\tan \delta$).

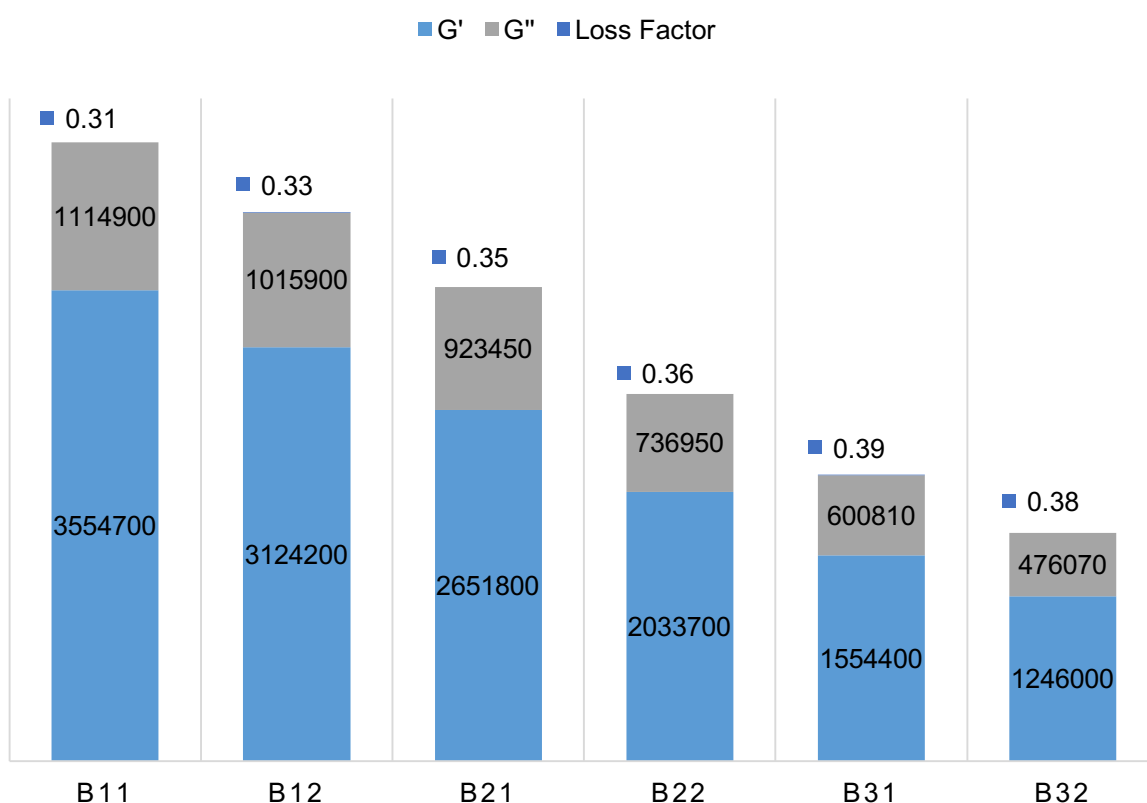


Figure 22. G' (Pa), G'' (Pa) and Loss Factor of sterile IBS at angular frequency of 10 rad/s

The effect of gamma sterilisation on the viscosity of the IBSs is displayed by the $\tan \delta$ vs angular frequency graph given in Figure 24. The lowest (1 rad/s), mid-range (10 rad/s) and highest (100 rad/s) oscillatory frequencies were chosen for display as representations of the changes across the frequency range tested. From this graph, it can be seen that at the lowest frequency, there is a randomness to the $\tan \delta$ values for both gamma-sterilised and non-sterile samples at lower frequencies

compared to $\tan \delta$ for these samples at higher frequencies. Therefore, a degree of order is gained with increased motion within the IBS, probably due to the alignment of polymer molecules with increased shear strain application. There is also a trend of decreasing $\tan \delta$ magnitude with higher oscillatory frequencies for all samples except for the non-sterile B11 sample. The magnitude of $\tan \delta$ does not appear to be overtly different between gamma-sterilised and non-sterile products.

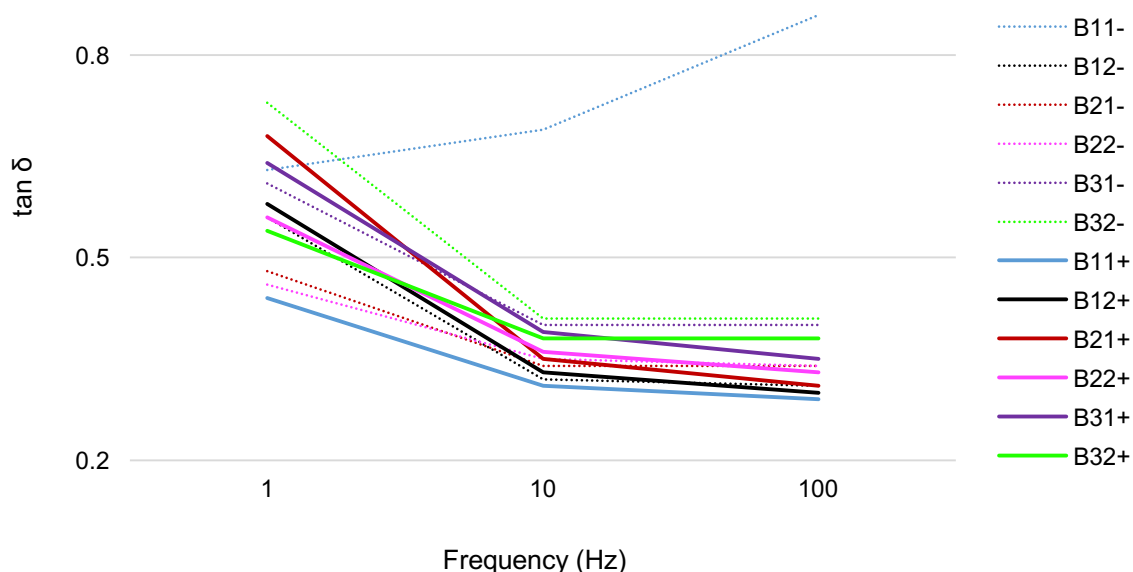


Figure 23. Change in $\tan \delta$ with oscillatory frequency. Dotted lines represent non-sterile IBS samples. '+' denotes sterilised sample, '-' denotes non-sterile sample

The change in $\tan \delta$ of various IBS samples upon exposure to gamma-irradiation is analysed more closely with the graph in Figure 25. Groups B11, B12 and B31 were used as representatives to compare in the observation of whether gamma-radiation increases the viscous nature of the IBS when PEG content is varied, and whether oscillation frequency has any impact on this. From the graph in Figure 26 it can be seen the respective paired samples of each IBS group, with the exception of group B11, follow the same trend of $\tan \delta$ reduction with increasing frequency. The $\tan \delta$ value for the non-sterile B11 sample increases with frequency, whilst also increasing the difference to its sterile counter-part. The viscous dominance with increasing glycerol content in the carrier is evident in the proportionally higher $\tan \delta$ values at all frequencies. The difference is more pronounced between B31 and sterile B11 and both B12 samples, with sterile B11 and both B12 samples exhibiting almost

overlapping curves across the frequency sweep. At higher frequencies gamma-sterilised B31 appears to lose its viscous behaviour and gain a more elastic nature, with $\tan \delta$ decreasing towards a frequency of 100 rad/s.

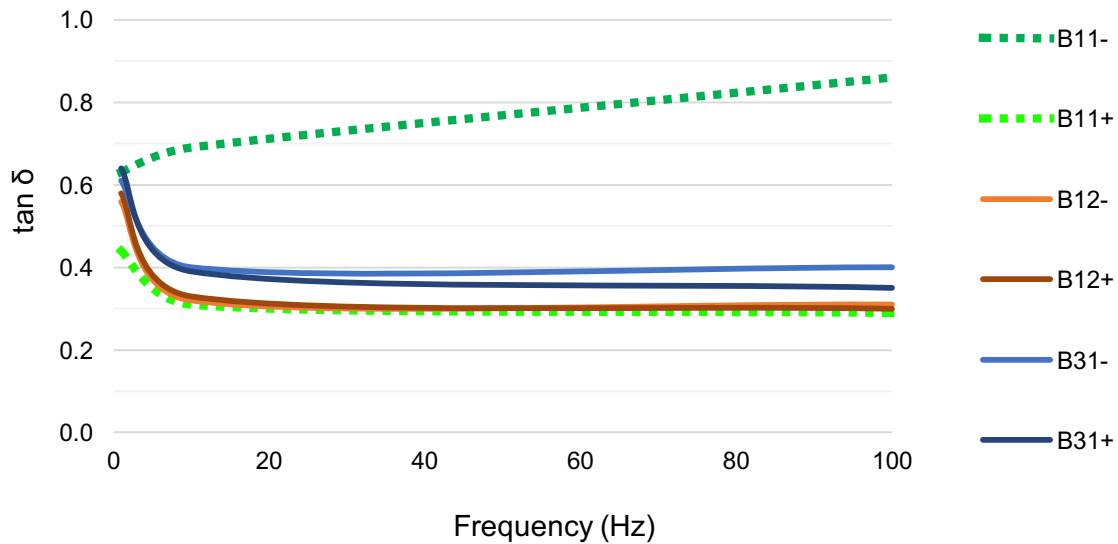


Figure 24. The effect of gamma sterilisation on the viscoelasticity of IBS samples.

In the legend ‘-’ denotes non-sterile samples and ‘+’ denotes gamma-sterilised samples

The divergence of the unsterile B11 sample from the general trends observed for all other IBS compositions over the frequency sweep does not have a scientific explanation at present. The impact of gamma sterilisation is not nearly as pronounced in all other IBS compositions. Furthermore, all other groups become less viscous as frequency increases, however, non-sterile B11 appears to become more viscous at higher frequencies. The results of the injectability study showed that sterile B11 had a larger peak injection force than non-sterile B11 implying a more elastic than viscous material. Therefore, a lower $\tan \delta$ for should be expected for sterile B11 than non-sterile B11. Although sterile B11 has a lower $\tan \delta$, the frequency-dependent increase in non-sterile B11 $\tan \delta$ values remain unexpected. Moreover, comparing injectability and viscosity test results for sterile and non-sterile B12 samples, sterile B12 has a larger peak injection force than non-sterile B12, however, the viscosities of the two samples are almost identical over the frequency scan. In fact, all samples show the same trend of reduction in $\tan \delta$ over frequency, even amongst the respective pairs of samples in each group. It is known that gamma-sterilisation does not necessarily always induce cross-linking in samples,

but may also cause polymer chain scissions. The higher viscoelasticity of sterile B11 compared to non-sterile B11 cannot be justified by any potential effects of gamma irradiation. This is because no remarkable difference between B11 and B12 was seen in the washout resistance and injectability study results of these two groups. Furthermore, all other groups, regardless of sterility status, follow the same trend of decreasing viscoelasticity with increasing glycerol content. Therefore, an error in material preparation or measurement may be the cause for such inexplicable discrepancy for B11 viscosity results.

For polymeric materials, low oscillation frequencies allow for enough time for relaxation between molecules which means energy storage is minimal. Higher oscillation frequencies do not permit for this sort of relaxation or stretching of the polymer chains and thus the material displays an increased elastic energy storage or shear modulus G' . It is also known that at lower angular frequencies, long polymer chains are in action, stretching along the axis of shear. At higher angular frequencies, shorter polymer chains account for the shear viscosity. The complex viscosity decreases proportional to glycerol and HMW PEG content in the composition.

2.9. *In Vitro* Study

The cytotoxic effects of the prepared IBS samples were investigated according to the protocol given in Materials and Methods. L929 fibroblasts were used to conduct the cell viability analysis as this cell line is commonly used in literature for the biocompatibility testing of synthetic biomaterials, as well as being a cell line that is recommended in the international standard ISO 10993 Biological Evaluation of Medical Devices. The guidance given in the standard was adapted to the IBS developed here, as with so many past examples in literature, as the IBS developed here does not conform to any of the general rules and conditions set out in ISO 10993-12: Sample Preparation and Reference Materials.

The data from the MTT analysis of cell viability for all prepared IBS samples according to the protocol described is summarised in the table below:

Table 5. L929 fibroblast cytotoxicity of IBSs

Cytotoxicity of IBS samples over time, containers and gamma doses						
Time (hours)	IBS Group	Container	Gamma Dose (kGy)	Cell Viability (%) / Extract Concentration (EC)		
				100 % (EC)	50 % (EC)	25 % (EC)
24	B11	Glass	25	19.65±0.36	36.73±1.01	68.34±0.70
24	B11	Syringe	25	22.94±0.43	52.49±0.75	92.05±0.80
48	B11	Glass	25	24.33±0.47	61.76±0.43	94.66±1.65
48	B11	Syringe	25	20.50±1.39	56.51±0.26	89.28±1.31
72	B11	Glass	25	19.82±0.53	33.7±0.47	78.79±0.71
72	B11	Syringe	25	22.47±0.22	39.6±0.41	83.19±0.55
24	B11	Glass	10	68.19±0.38	89.06±0.83	98.66±1.34
24	B11	Syringe	10	63.40±0.87	86.17±0.23	99.01±1.56
24	B12	Glass	10	68.12±0.71	91.47±0.94	98.43±1.27
24	B12	Syringe	10	56.53±0.59	83.75±0.67	92.64±1.63

The cell viability values for 10 kGy and 25 kGy samples are also provided graphically in Figure 26.

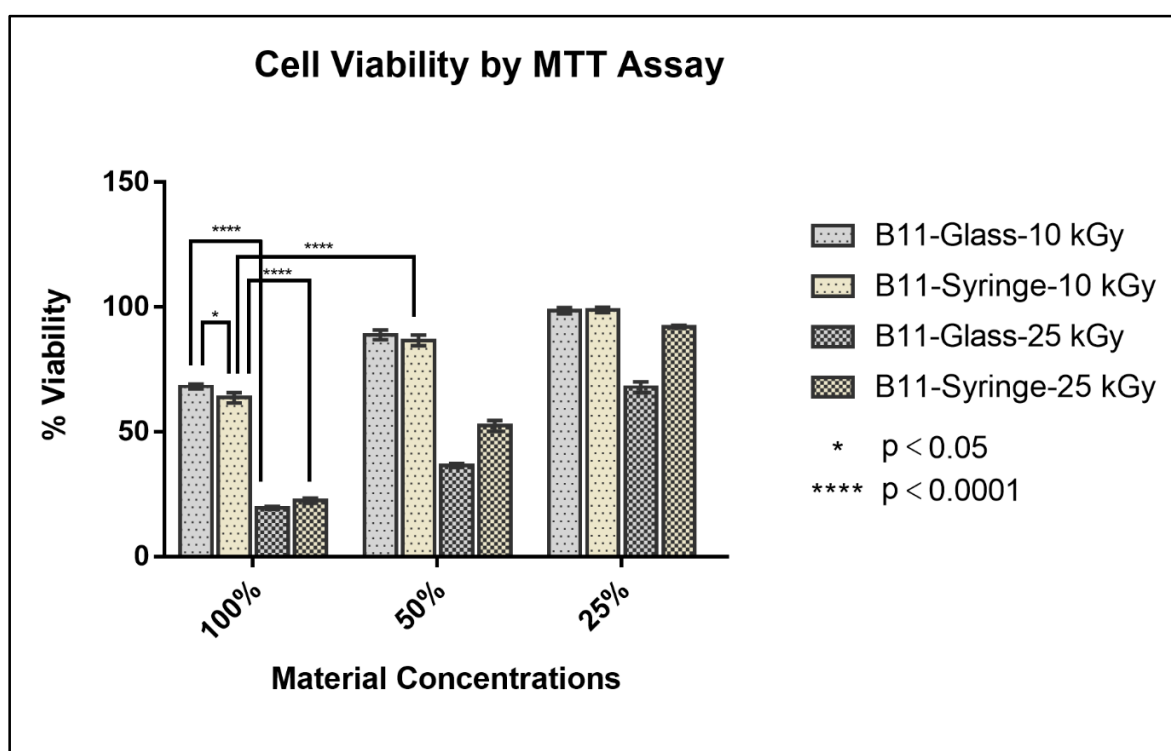


Figure 26. Cell viability by MTT assay

Looking at the cell viability results for samples treated at a gamma irradiation dose of 25 kGy with extract incubation for 24 hours, the maximum cell viability was 22.94%, with viability increasing with successive dilutions. The effect of extract incubation time on cell viability for samples treated at 25 kGy does not appear to have a notable effect on cell viability. There is also not notable difference in the cell

viability effects of samples that underwent 25 kGy gamma irradiation in glass tube containers or polypropylene syringes, over any of the extract incubation time points tested. The notion of syringe material toxicity can thus be disqualified with this comparison. There is, however, a significantly notable impact of sterilisation dose on the cytotoxicity measurements for B11 samples with 24 hours of extract incubation, with cell viability values increasing from 22.94 % to 63.40 % for syringe-contained samples, and 19.65 % to 68.19 % for glass container-contained samples. With a gamma dose of 10 kGy used, the difference between cell viability values between glass container- and syringe-contained IBS samples becomes greater than the difference between these samples at 25 kGy. This is the case for both B11 and B12 samples, thus the effect is the same irrespective of IBS composition. From this, it can be suggested that not only does gamma dose have an impact on the cytotoxicity of the IBS sample, but perhaps also the delivery materials itself as a lower gamma dose has revealed their susceptibility to gamma-induced toxic degradation products. Furthermore, for eluates taken at 24 hours of samples sterilised with a 10 kGy gamma dose, IBS composition does not produce a notable difference in cytotoxicity of samples retrieved from glass containers, but for those supplied in syringes, B11 and B12 cell viability values are 63.40 % and 56.53 %, respectively. Furthermore, cell viability increases from 63.40 % to 86.17% and from 56.53 % to 83.75 % for syringe-contained B11 and B12 samples, respectively.

Firstly, Tulyaganov *et al.* have presented a paper detailing the synthesis and assessment of *in vitro* bioactivity of a bioglass-PEG-glycerol composite paste for bone tissue engineering applications, in which all formulations of the three components demonstrated high rates of *in vitro* bioactivity after immersion in simulated body fluid [274]. Dissolution products such as calcium or silicon ion have been shown to increase proliferation of human osteoblasts and induce insulin-like growth factor II mRNA expression and protein synthesis [275] thus the small amount of 45S5 bioglass added to the IBS compositions is expected to promote *in vitro* activity in this manner. Silicon-supplemented cements have been shown to increase cell proliferation (three-fold) of MG-63 (human osteoblast-like cell line) more (threefold) over cements without this addition [276].

The *in vitro* characterisation of calcium phosphates is a challenging feat. This is due to the inherent bioactivity of bioceramics which produce controversial results relating to their effects on cell viability and proliferation. Results vary significantly not only

based on the type of cell used for cytotoxicity analysis, but also on the culture conditions and sample preparation and extraction methods used. Literature abounds with studies demonstrating how these elements impact the perceived biocompatibility of a bioceramic implant material. Across literature, there are reports of cytotoxicity results that have varied depending on ceramic surface reactivity, solubility, chemical composition, particle morphology, particle size, culture medium and sample extract concentration. This variability has been found to be especially true of β -TCP ceramics. Thus, cytocompatibility analysis should take into consideration fluid-mediated interactions, and note that in vitro results may not necessarily reflect in vivo outcomes, as encountered previously in bioceramics research. Moreover, the time dependent effects of bone bone graft substitutes on cell metabolism should also be considered when designing a cytocompatibility study. Zimmermann *et al.* [277] compared the effects of eluates from six commercially-available bone graft substitutes on the proliferation and metabolic activity of porcine mesenchymal multi-lineage stem cells. They found that not only was cell viability dependent on eluate concentration, but that with it increased with longer incubation times.

There are several reports for calcium phosphate-based bone graft substitute cytotoxicity test results that have shown strong dependency on the material extraction method used. Olkowski *et al.* [278] found that not only were the results of direct and indirect cytotoxicity tests for implant materials composed of calcium and magnesium phosphates and calcium sulphate hemihydrate significantly different, but also that the ratio of culture medium volume to the size of the material samples was crucial if release or uptake of calcium ions by the materials was involved. The authors cite and base their methods and results on other studies which investigate calcium ion toxicity in such systems. They also speculate that the sorption of ions by polymers in composite materials may also affect result - chitosan, for example, has chelating properties.

The reports of Sadowska *et al.* [279] also add valuable insight and future direction to the present study. This group demonstrated how changing the ratio of the volume of cell culture medium to the calcium phosphate ceramic, significantly changes the cytocompatibility observed for the ceramic. They found that when higher ratios (i.e. when a smaller amount of ceramic material is used in the same amount of cell

culture media) were used, cell (rat mesenchymal stem cells) shrinkage and apoptosis was mitigated. The authors base this on the attenuation of calcium and phosphate ion fluctuations in the medium that occur naturally due to the inherent bioactivity of the ceramics. The findings of our cohesion study for the prepared IBS samples provide supporting evidence for this notion. In fact, the impact of sample amount to cell culture medium ratio genotoxicity testing results for another well-known biomaterial, nano-active bioactive glass, has also been shown [280]. This group reports that in concentrations of extract above 4 mg/ml of sample to culture medium, the material shows genotoxic effects, attributable to the higher dissolution and degradation rate of nanoparticles compared to large particle sizes. Comparing these results to that observed for commercially-available bioglass, Novabone (NovaBone Products LLC, Alachua, FL), they found no significant difference for extract concentrations less than 5mg/ml, showing that even a commercially-available and successful product such as Novabone (NovaBone Products LLC, Alachua, FL) is sensitive to extraction ratios and test methods.

Other authors, such as Nakagawa *et al.* [281], present a very interesting study which relate in vitro performances of β -TCP to particle size. The researchers observed the mechanisms of micron (1-10 μ m) β -TCP particles in the calcification of human mesenchymal stem cell in vitro. They tested both the direct and indirect contact of β -TCP particles with these cells at 0, 0.01, 0.1, and 1.0 mg/mL concentrations (in cell culture medium), as well as the changes in calcium ion concentrations in the culture medium over days 2, 7, 14, and 21. A decreased cell viability for 1.0 mg/mL particle concentration in the direct contact condition was attributed to either a reduction of ions in the media due to cellular particle uptake (seen at day 2), a high cellular uptake of ceramic particles during stable extracellular ion concentrations (days 2-14), or the selective proliferation of cells only from the osteoblastic lineage in the selected cell culture medium. In the non-contact and media-only (no cells, just β -TCP particles) conditions, 0.1 mg/mL concentrations of β -TCP showed an increase of calcium in the media at 7 days and thereafter, as the particles has been taken up and dissolved by the cells at this stage. According to our cohesion study results, calcium release from IBS samples continued to increase over the 48 hours analysis period after an initial 'dip' for the first 4 hours of submersion in water. Thus, the results of cell viability for samples sterilised at 10

kGy gamma dose could be much higher at further time points such as at 7 days post-extract incubation. With such contrasting results for different particle concentrations and culture conditions, the study highlights the complex interplay of different factors when interpreting β -TCP cytocompatibility.

The inflammatory cell response to ceramic particles has been overviewed by Velard *et al.* [282] in their 2012 publication, which summarises the results of studies that have tested the relationship between different calcium phosphate parameters (particle sizes, sintering temperatures, solubilities) in animal or human models. Lange *et al.* [283] support this notion by documenting how β -TCP particle composition, size and morphology play a role in the induction of pro-inflammatory cytokines *in vitro*. Testing the effects of gamma-irradiated β -TCP particles of 1, 3, 13, 32 and 40 μm sizes on human peripheral blood mononuclear cells (PBMC) *in vitro*, they found that in fact smaller (1 μm) produced less pro-inflammatory cytokine production (although toxicity readings increased over time) than larger (32 μm and 40 μm) β -TCP particles. The authors state that only particles $<20 \mu\text{m}$ are phagocytosable, leaving larger particles to generate an inflammatory response, and also that phagocytosis is dictated by the geometry and surface roughness of the particulates.

The high solubility of β -TCP, particularly in comparison to the more stable HA, has caused concerns over whether it may invoke unwanted inflammatory responses in the body. Suzuki *et al.* [284] studied the effects of CaP ratio (1.50 (pure TCP), 1.55, 1.60, 1.64 and 1.67 (pure HA)) on solubility and further the viability of L929 cells. They found that at 6h of culturing 100% β -TCP with L929 cells, cell viability had reduced to 20%, observing rupture of anchored cells. However, upon pre-incubating TCP-HA (1:4) scaffolds in culture (MEM) containing 10% foetal bovine serum for 3 days, its surface stability and thus cell viability was greatly improved. The authors also speculate the disruption of adhesion and calcification of bone cells due to the precipitation of CO_3 apatite resulting from the combination of calcium ions present in the media and those released from the biomaterial.

The high dissolution rate of β -TCP particles *in vitro*, however, should not be translated to cytotoxicity or poor bone formation of β -TCP implants *in vivo*. As Lu *et al.* [285] have shown, on comparison of both *in vitro* and *in vivo* (placement of materials into rabbit femoral cavities for 12 weeks) performance of HA, β -TCP and

BCP, HA was the most stable *in vitro* whilst β -TCP was degraded the most, however, new bone formation was significantly higher for β -TCP *in vivo* compared to the other two materials which produced micro-particles that were phagocytosed. Additionally, Lange *et al.* [283] found that pure β -TCP and HA particles of the same size and dose cause similar effects on pro-inflammatory cytokines, but HA, which is known to be a more stable bioceramic, actually caused a greater increase in osteoclastogenic cytokines.

Hence these findings, in addition those presented in this work, indicate that *in vitro* cytotoxicity observed for β -TCP-based materials is variable depending on the method of extraction used, the particle types and sizes, and that *in vivo* bone formation may even be enhanced with β -TCP, in contrast to *in vitro* observations.

3.CONCLUSION

The IBS developed in this study is intended for use as a bone repair material in critical-sized defects or any non-load bearing bone void. A set of 'ideal' formulations were analysed in terms of chemical, morphological, rheological properties, and *in vitro* cytocompatibility. Results of various analyses reveal that there is a critical ratio of carrier content, above or below which rheological properties vary. Concurring data between washout-resistance and cohesion analysis, injectability and viscosity analysis, and cohesion and *in vitro* analysis demonstrate the clinical suitability profile of the IBS for the current formulations' tests. Results from the *in vitro* analysis have been discussed in light of the relevant data from literature regarding the impact of a number of factors such ionic fluctuations or ceramic particle sizes, the potential negative effects of which would most likely be accommodated and negated by cellular and other mechanisms *in vivo*. The results of this research, along with its discussion and recommendations, provides a strong basis for the design and execution of future investigations related to β -TCP/Bioglass –PEG-glycerol based injectable bone substitutes.

4. REFERENCES

1. de Pablos, J., C. Barrios, C. Alfaro, and J. Canadell, Large experimental segmental bone defects treated by bone transportation with monolateral external distractors, *Clinical Orthopaedics Related Research*, 259-65, **1994**.
2. Buckwalter, J.A., M.J. Glimcher, R.R. Cooper, and R. Recker, Bone biology. I: Structure, blood supply, cells, matrix, and mineralization, *Instructional Course Lecture*, 45, 371-86, **1996**.
3. Murphy, C.M., M.G. Haugh, and F.J. O'Brien, The effect of mean pore size on cell attachment, proliferation and migration in collagen-glycosaminoglycan scaffolds for bone tissue engineering, *Biomaterials*, 31, 461-6, **2010**.
4. Henkel, J., M.A. Woodruff, D.R. Epari, R. Steck, V. Glatt, I.C. Dickinson, P.F. Choong, M.A. Schuetz, and D.W. Hutmacher, Bone Regeneration Based on Tissue Engineering Conceptions - A 21st Century Perspective, *Bone Research*, 1, 216-48, **2013**.
5. Webster, T.J. and E.S. Ahn, Nanostructured biomaterials for tissue engineering bone, *Advances in Biochemical Engineering / Biotechnology*, 103, 275-308, **2007**.
6. DiGirolamo, D.J., T.L. Clemens, and S. Kousteni, The skeleton as an endocrine organ, *Nature Reviews Rheumatology*, 8, 674-83, **2012**.
7. Huggings, C., The composition of bone and the function of the bone cell, *Physiological Reviews*, 15, 119-143, **1937**.
8. Sommerfeldt, D.W. and C.T. Rubin, Biology of bone and how it orchestrates the form and function of the skeleton, *European Spine Journal*, 10 Suppl 2, S86-95, **2001**.
9. Hall, S.J., *Basic Biomechanics Fifth Edition*, 5, McGraw-Hill Higher Education, **2007**.
10. Ng, K.W., E. Romas, L. Donnan, and D.M. Findlay, Bone biology, *Baillière's Clinical Endocrinology and Metabolism*, 11, 1-22, **1997**.
11. Buckwalter, J.A., M.J. Glimcher, R.R. Cooper, and R. Recker, Bone biology. II: Formation, form, modeling, remodeling, and regulation of cell function, *Instructional Course Lectures*, 45, 387-99, **1996**.
12. Hill, P.A., Bone remodelling, *British Journal of Orthodontics*, 25, 101-7, **1998**.
13. Little, D.G., M. Ramachandran, and A. Schindeler, The anabolic and catabolic responses in bone repair, *The Journal of Bone and Joint Surgery British Volume*, 89, 425-33, **2007**.
14. Agata, H., I. Asahina, Y. Yamazaki, M. Uchida, Y. Shinohara, M.J. Honda, H. Kagami, and M. Ueda, Effective bone engineering with periosteum-derived cells, *Journal of Dental Research*, 86, 79-83, **2007**.
15. Teitelbaum, S.L. and F.P. Ross, Genetic regulation of osteoclast development and function, *Nature Reviews Genetics*, 4, 638-49, **2003**.
16. Rodan, G.A. and A.A. Reszka, Bisphosphonate mechanism of action, *Current Molecular Medicine*, 2, 571-7, **2002**.

17. Vaananen, K., Mechanism of osteoclast mediated bone resorption--rationale for the design of new therapeutics, *Advanced Drug Delivery Reviews*, 57, 959-71, **2005**.
18. Freundlich, M., E. Alonzo, E. Bellorin-Font, and J.R. Weisinger, Increased osteoblastic activity and expression of receptor activator of NF-kappaB ligand in nonuremic nephrotic syndrome, *Journal of the American Society of Nephrology*, 16, 2198-204, **2005**.
19. Payumo, F.C., H.D. Kim, M.A. Sherling, L.P. Smith, C. Powell, X. Wang, H.S. Keeping, R.F. Valentini, and H.H. Vandenberg, Tissue engineering skeletal muscle for orthopaedic applications, *Clinical Orthopaedics and Related Research*, S228-42, **2002**.
20. Gori, F., L.C. Hofbauer, C.R. Dunstan, T.C. Spelsberg, S. Khosla, and B.L. Riggs, The expression of osteoprotegerin and RANK ligand and the support of osteoclast formation by stromal-osteoblast lineage cells is developmentally regulated, *Endocrinology*, 141, 4768-76, **2000**.
21. Khosla, S., Minireview: the OPG/RANKL/RANK system, *Endocrinology*, 142, 5050-5, **2001**.
22. Giannoudis, P., C. Tzioupis, T. Almalki, and R. Buckley, Fracture healing in osteoporotic fractures: is it really different? A basic science perspective, *Injury*, 38 Suppl 1, S90-9, **2007**.
23. Chen, G. and Y. Lv, Decellularized Bone Matrix Scaffold for Bone Regeneration, *Methods in Molecular Biology*, **2017**.
24. Paduano, F., M. Marrelli, N. Alom, M. Amer, L.J. White, K.M. Shakesheff, and M. Tatullo, Decellularized bone extracellular matrix and human dental pulp stem cells as a construct for bone regeneration, *Journal of Biomaterials Science, Polymer Edition*, 28, 730-748, **2017**.
25. Kim, J.Y., G. Ahn, C. Kim, J.S. Lee, I.G. Lee, S.H. An, W.S. Yun, S.Y. Kim, and J.H. Shim, Synergistic Effects of Beta Tri-Calcium Phosphate and Porcine-Derived Decellularized Bone Extracellular Matrix in 3D-Printed Polycaprolactone Scaffold on Bone Regeneration, *Macromolecular Bioscience*, 18, e1800025, **2018**.
26. Dorati, R., C. Colonna, I. Genta, G. Bruni, L. Visai, and B. Conti, Preparation and characterization of an advanced medical device for bone regeneration, *American Association of Pharmaceutical Scientists Pharmaceutical Science and Technology*, 15, 75-82, **2014**.
27. Pilliar, R.M., H.U. Cameron, A.G. Binnington, J. Szivek, and I. Macnab, Bone ingrowth and stress shielding with a porous surface coated fracture fixation plate, *Journal of Biomedical Material Research*, 13, 799-810, **1979**.
28. Shibata, Y. and Y. Tanimoto, A review of improved fixation methods for dental implants. Part I: Surface optimization for rapid osseointegration, *Journal of Prosthodontic Research*, 59, 20-33, **2015**.
29. Stefani, R., G. Esposito, B. Zanotti, C. Iaccarino, M.M. Fontanella, and F. Servadei, Use of "custom made" porous hydroxyapatite implants for cranioplasty: postoperative analysis of complications in 1549 patients, *Surgical Neurology International*, 4, 12, **2013**.

30. Yu, N.Y., A. Schindeler, D.G. Little, and A.J. Ruys, Biodegradable poly(alpha-hydroxy acid) polymer scaffolds for bone tissue engineering, *Journal of Biomedical Materials Research Part B: Applied Biomaterials*, 93, 285-95, **2010**.
31. Ozdil, D. and H.M. Aydin, Polymers for medical and tissue engineering applications, *Chemical Technology and Biotechnology*, 89, 1793-1810, **2014**.
32. Sokolsky-Papkov, M., K. Agashi, A. Olaye, K. Shakesheff, and A.J. Domb, Polymer carriers for drug delivery in tissue engineering, *Advanced Drug Delivery Reviews*, 59, 187-206, **2007**.
33. Liu, X. and P.X. Ma, Polymeric scaffolds for bone tissue engineering, *Annals of Biomedical Engineering*, 32, 477-86, **2004**.
34. Swetha, M., K. Sahithi, A. Moorthi, N. Srinivasan, K. Ramasamy, and N. Selvamurugan, Biocomposites containing natural polymers and hydroxyapatite for bone tissue engineering, *International Journal of Biological Macromolecules*, 47, 1-4, **2010**.
35. Titorencu, I., M.G. Albu, M. Nemecz, and V.V. Jinga, Natural Polymer-Cell Bioconstructs for Bone Tissue Engineering, *Current Stem Cell Research & Therapy*, 12, 165-174, **2017**.
36. Kroeze, R.J., M.N. Helder, L.E. Govaert, and T.H. Smit, Biodegradable Polymers in Bone Tissue Engineering, *Materials*, 2, 833-856, **2009**.
37. BaoLin, G. and P.X. Ma, Synthetic biodegradable functional polymers for tissue engineering: a brief review, *Science China Chemistry*, 57, 490-500, **2014**.
38. Thadavirul, N., P. Pavasant, and P. Supaphol, Development of polycaprolactone porous scaffolds by combining solvent casting, particulate leaching, and polymer leaching techniques for bone tissue engineering, *Journal of Biomedical Material Research A*, 102, 3379-92, **2014**.
39. Bose, S., S. Vahabzadeh, and A. Bandyopadhyay, Bone tissue engineering using 3D printing, *Materials Today*, 16, 496-504, **2013**.
40. Lieberman, J.R., A. Daluiski, and T.A. Einhorn, The role of growth factors in the repair of bone. Biology and clinical applications, *The Journal of Bone and Joint Surgery American Volume*, 84-A, 1032-44, **2002**.
41. Pawlik, J., K. Chowela-Kowalska, K. Bramowska, M. Laczka, and E. Pamula, Effect of bioglass additives on the properties of ceramics and polymer composites, *Engineering of Biomaterials*, 24-31, **2009**.
42. Maiti, S.K. and G.R. Singh, Bone morphogenetic proteins--novel regulators of bone formation, *Indian Journal of Experimental Biology*, 36, 237-44, **1998**.
43. Lane, J.M., Bone morphogenic protein science and studies, *Journal of Orthopaedic Trauma*, 19, S17-22, **2005**.
44. Schmidmaier, G., P. Schwabe, B. Wildemann, and N.P. Haas, Use of bone morphogenetic proteins for treatment of non-unions and future perspectives, *Injury*, 38, S35-41, **2007**.
45. Meraw, S.J., C.M. Reeve, C.M. Lohse, and T.M. Sioussat, Treatment of peri-implant defects with combination growth factor cement, *Journal of Periodontology*, 71, 8-13, **2000**.

46. Janicki, P. and G. Schmidmaier, What should be the characteristics of the ideal bone graft substitute? Combining scaffolds with growth factors and/or stem cells, *International Journal of the Care of the Injured*, 42, S77–S81, **2011**.
47. Shen, H., X. Hu, F. Yang, J. Bei, and S. Wang, The bioactivity of rhBMP-2 immobilized poly(lactide-co-glycolide) scaffolds, *Biomaterials*, 30, 3150-7, **2009**.
48. Kempen, D.H., L. Lu, C. Kim, X. Zhu, W.J. Dhert, B.L. Currier, and M.J. Yaszemski, Controlled drug release from a novel injectable biodegradable microsphere/scaffold composite based on poly(propylene fumarate), *Journal of Biomedical Materials Research A*, 77, 103-11, **2006**.
49. Russell, R.G., R.C. Muhlbauer, S. Bisaz, D.A. Williams, and H. Fleisch, The influence of pyrophosphate, condensed phosphates, phosphonates and other phosphate compounds on the dissolution of hydroxyapatite in vitro and on bone resorption induced by parathyroid hormone in tissue culture and in thyroparathyroidectomised rats, *Calcified Tissue International*, 6, 183-96, **1970**.
50. Drake, M.T., B.L. Clarke, and S. Khosla, Bisphosphonates: mechanism of action and role in clinical practice, *Mayo Clinic Proceedings*, 83, 1032-45, **2008**.
51. Harrington, J.T., L.G. Ste-Marie, M.L. Brandi, R. Civitelli, P. Fardellone, A. Grauer, I. Barton, and S. Boonen, Risedronate rapidly reduces the risk for nonvertebral fractures in women with postmenopausal osteoporosis, *Calcified Tissue International*, 74, 129-35, **2004**.
52. Schlickewei, C.W., G. Laaff, A. Andresen, T.O. Klatter, J.M. Rueger, J. Ruesing, M. Epple, and W. Lehmann, Bone augmentation using a new injectable bone graft substitute by combining calcium phosphate and bisphosphonate as composite--an animal model, *Journal of Orthopaedic Surgery and Research*, 10, 116, **2015**.
53. Verron, E., M.L. Pissonnier, J. Lesoeur, V. Schnitzler, B.H. Fella, H. Pascal-Moussellard, P. Pilet, O. Gauthier, and J.M. Bouler, Vertebroplasty using bisphosphonate-loaded calcium phosphate cement in a standardized vertebral body bone defect in an osteoporotic sheep model, *Acta Biomaterialia*, 10, 4887-4895, **2014**.
54. Marx, R.E., E.R. Carlson, R.M. Eichstaedt, S.R. Schimmele, J.E. Strauss, and K.R. Georgeff, Platelet-rich plasma: Growth factor enhancement for bone grafts, *Oral Surgery, Oral Medicine, Oral Pathology, Oral Radiology*, 85, 638-46, **1998**.
55. Marx, R.E., Platelet-rich plasma (PRP): what is PRP and what is not PRP?, *International Journal of Implant Dentistry*, 10, 225-8, **2001**.
56. Foster, T.E., B.L. Puskas, B.R. Mandelbaum, M.B. Gerhardt, and S.A. Rodeo, Platelet-rich plasma: from basic science to clinical applications, *The American Journal of Sports Medicine*, 37, 2259-72, **2009**.
57. Rai, B., M.E. Oest, K.M. Dupont, K.H. Ho, S.H. Teoh, and R.E. Goldberg, Combination of platelet-rich plasma with polycaprolactone-tricalcium phosphate scaffolds for segmental bone defect repair, *Journal of Biomedical Material Research A*, 81, 888-99, **2007**.
58. Bi, L., W. Cheng, H. Fan, and G. Pei, Reconstruction of goat tibial defects using an injectable tricalcium phosphate/chitosan in combination with autologous platelet-rich plasma, *Biomaterials*, 31, 3201-11, **2010**.

59. Hasan, M.L., M. Taz, and B.T. Lee, Effects of platelet-rich plasma on biological activity and bone regeneration of brushite-based calcium phosphate cement, *Journal of Biomedical Materials Research B Applied Biomaterials*, **2017**.
60. Liu, Y., Y. Zhou, H. Feng, G.E. Ma, and Y. Ni, Injectable tissue-engineered bone composed of human adipose-derived stromal cells and platelet-rich plasma, *Biomaterials*, 29, 3338-45, **2008**.
61. Kutlu, B., R.S. Tigli Aydin, A.C. Akman, M. Gumusderelioglu, and R.M. Nohutcu, Platelet-rich plasma-loaded chitosan scaffolds: preparation and growth factor release kinetics, *Journal of Biomedical Materials Research B*, 101, 28-35, **2013**.
62. Calori, G.M., M. D'Avino, L. Tagliabue, W. Albisetti, M. d'Imporzano, and G. Peretti, An ongoing research for evaluation of treatment with BMPs or AGFs in long bone non-union: protocol description and preliminary results, *Injury*, 37 Suppl 3, S43-50, **2006**.
63. Yu, N.Y., A. Fathi, C.M. Murphy, K. Mikulec, L. Peacock, L.C. Cantrill, F. Dehghani, D.G. Little, and A. Schindeler, Local co-delivery of rhBMP-2 and cathepsin K inhibitor L006235 in poly(D,L-lactide-co-glycolide) nanospheres, *Journal of Biomedical Material Research B Applied Biomaterials*, 105, 136-144, **2017**.
64. Arnold, P.M., R.C. Sasso, M.E. Janssen, M.G. Fehlings, J.D. Smucker, A.R. Vaccaro, R.F. Heary, A.I. Patel, B. Goulet, I.H. Kalfas, and B. Kopjar, Efficacy of i-Factor Bone Graft versus Autograft in Anterior Cervical Discectomy and Fusion: Results of the Prospective, Randomized, Single-blinded Food and Drug Administration Investigational Device Exemption Study, *Spine (Phila Pa 1976)*, 41, 1075-83, **2016**.
65. Marie, P.J. and O. Fromigue, Osteogenic differentiation of human marrow-derived mesenchymal stem cells, *Regenerative Medicine*, 1, 539-48, **2006**.
66. Rickard, D.J., M. Kassem, T.E. Hefferan, G. Sarkar, T.C. Spelsberg, and B.L. Riggs, Isolation and characterization of osteoblast precursor cells from human bone marrow, *Journal of Bone and Mineral Research*, 11, 312-24, **1996**.
67. Hernigou, P., A. Poignard, F. Beaujean, and H. Rouard, Percutaneous autologous bone-marrow grafting for nonunions. Influence of the number and concentration of progenitor cells, *The Journal of bone and joint surgery American volume*, 87, 1430-7, **2005**.
68. Hernigou, P., G. Mathieu, A. Poignard, O. Manicom, F. Beaujean, and H. Rouard, Percutaneous autologous bone-marrow grafting for nonunions. Surgical technique, *The Journal of bone and joint surgery American volume*, 88 Suppl 1 Pt 2, 322-7, **2006**.
69. Quarto, R., M. Mastrogiacomo, R. Cancedda, S.M. Kutepov, V. Mukhachev, A. Lavroukov, E. Kon, and M. Marcacci, Repair of large bone defects with the use of autologous bone marrow stromal cells, *The New England Journal of Medicine*, 344, 385-6, **2001**.
70. Zhao, L., M.D. Weir, and H.H. Xu, An injectable calcium phosphate-alginate hydrogel-umbilical cord mesenchymal stem cell paste for bone tissue engineering, *Biomaterials*, 31, 6502-10, **2010**.
71. Hou, Q., P.A. De Bank, and K.M. Shakesheff, Injectable scaffolds for tissue regeneration, *Materials Chemistry*, 14, 1915, **2004**.

72. Nich, C. and M. Hamadouche, *1.120 – Synthetic Bone Grafts: Clinical Use*, 335–347, **2011**.
73. Gitelis, S., P. Piasecki, T. Turner, W. Haggard, J. Charters, and R. Urban, Use of a calcium sulfate-based bone graft substitute for benign bone lesions, *Orthopedics*, 24, 162-6, **2001**.
74. Kelly, C.M., R.M. Wilkins, S. Gitelis, C. Hartjen, J.T. Watson, and P.T. Kim, The use of a surgical grade calcium sulfate as a bone graft substitute: results of a multicenter trial, *Clinical Orthopaedics and Related Research*, 42-50, **2001**.
75. Ricci, J., *Material characteristics of calcium sulfate cement*, (eds: R.J. Pecora G), Elite Publishing, Pecora G, Ricci J.,, 13–77, **2001**.
76. Ambard, A.J. and L. Mueninghoff, Calcium phosphate cement: review of mechanical and biological properties, *Journal of Prosthodontics*, 15, 321-8, **2006**.
77. Magnan, B., M. Bondi, T. Maluta, E. Samaila, L. Schirru, and C. Dall'Oca, Acrylic bone cement: current concept review, *Musculoskeletal Surgery*, 97, 93-100, **2013**.
78. No, Y.J., S.I. Roohani-Esfahani, and H. Zreiqat, Nanomaterials: the next step in injectable bone cements, *Nanomedicine (Lond)*, 9, 1745-64, **2014**.
79. Lv, Y., A. Li, F. Zhou, X. Pan, F. Liang, X. Qu, D. Qiu, and Z. Yang, A Novel Composite PMMA-based Bone Cement with Reduced Potential for Thermal Necrosis, *ACS Applied Materials & Interfaces*, 7, 11280-5, **2015**.
80. Masala, S., G. Nano, S. Marcia, M. Muto, F.P. Fucci, and G. Simonetti, Osteoporotic vertebral compression fracture augmentation by injectable partly resorbable ceramic bone substitute (Cerament|SPINESUPPORT): a prospective nonrandomized study, *Neuroradiology*, 54, 1245-51, **2012**.
81. Pili, D. and P. Tranquilli Leali, Biomaterials and bone, *Aging Clinical and Experimental Research*, 23, 74-5, **2011**.
82. Low, K.L., S.H. Tan, S.H. Zein, J.A. Roether, V. Mourino, and A.R. Boccaccini, Calcium phosphate-based composites as injectable bone substitute materials, *Biomedical Materials Research Part B Applied Biomaterials*, 94, 273-86, **2010**.
83. Chow, L.C. and S. Takagi, A Natural Bone Cement-A Laboratory Novelty Led to the Development of Revolutionary New Biomaterials, *Journal of Research of the National Institute of Standards and Technology*, 106, 1029-33, **2001**.
84. Friedman, C.D., P.D. Costantino, K. Jones, L.C. Chow, H.J. Pelzer, and G.A. Sisson, Sr., Hydroxyapatite cement. II. Obliteration and reconstruction of the cat frontal sinus, *Archives of Otolaryngology - Head and Neck Surgery*, 117, 385-9, **1991**.
85. Costantino, P.D., C.D. Friedman, K. Jones, L.C. Chow, and G.A. Sisson, Experimental hydroxyapatite cement cranioplasty, *Plastic and Reconstructive Surgery*, 90, 174-85; discussion 186-91, **1992**.
86. Baroud, G., E. Cayer, and M. Bohner, Rheological characterization of concentrated aqueous beta-tricalcium phosphate suspensions: the effect of liquid-to-powder ratio, milling time, and additives, *Acta Biomaterialia*, 1, 357-63, **2005**.
87. Chow, L.C., Next generation calcium phosphate-based biomaterials, *Dental Materials Journal*, 28, 1-10, **2009**.

88. Xia, Z., L.M. Grover, Y. Huang, I.E. Adamopoulos, U. Gbureck, J.T. Triffitt, R.M. Shelton, and J.E. Barralet, In vitro biodegradation of three brushite calcium phosphate cements by a macrophage cell-line, *Biomaterials*, 27, 4557-65, **2006**.
89. Low, K.L., S.H. Tan, S.H. Zein, J.A. Roether, V. Mourino, and A.R. Boccaccini, Calcium phosphate-based composites as injectable bone substitute materials, *Biomedical Materials Research Part B Applied Biomaterials*, 94, 273-286, **2010**.
90. Vereecke, G. and J. Lemaitre, Calculation of the solubility diagrams in the system $\text{Ca}(\text{OH})_2\text{-H}_3\text{PO}_4\text{-KOH-HNO}_3\text{-CO}_2\text{-H}_2\text{O}$, *Crystal Growth*, 104, 820-832, **1990**.
91. Kuemmerle, J.M., A. Oberle, C. Oechslin, M. Bohner, C. Frei, I. Boecken, and B. von Rechenberg, Assessment of the suitability of a new brushite calcium phosphate cement for cranioplasty - an experimental study in sheep, *Journal of Craniomaxillofacial Surgery*, 33, 37-44, **2005**.
92. Yoshikawa, M., Y. Terada, and T. Toda, Setting time and sealing ability of alpha-tricalcium phosphate cement containing titanic oxide, *Journal of Osaka Dental University*, 32, 67-70, **1998**.
93. Doi, Y., Y. Shimizu, Y. Moriwaki, M. Aga, H. Iwanaga, T. Shibutani, K. Yamamoto, and Y. Iwayama, Development of a new calcium phosphate cement that contains sodium calcium phosphate, *Biomaterials*, 22, 847-54, **2001**.
94. Yokoyama, A., S. Yamamoto, T. Kawasaki, T. Kohgo, and M. Nakasu, Development of calcium phosphate cement using chitosan and citric acid for bone substitute materials, *Biomaterials*, 23, 1091-1101, **2002**.
95. Tao, J., H. Pan, Y. Zeng, X. Xu, and R. Tang, Roles of amorphous calcium phosphate and biological additives in the assembly of hydroxyapatite nanoparticles, *The Journal of Physical Chemistry B*, 111, 13410-8, **2007**.
96. Sarkar, M.R., N. Wachter, P. Patka, and L. Kinzl, First histological observations on the incorporation of a novel calcium phosphate bone substitute material in human cancellous bone, *Journal of Biomedical Material Research*, 58, 329-34, **2001**.
97. Krebs, J., N. Aebli, B.G. Goss, S. Sugiyama, T. Bardyn, I. Boecken, P.J. Leamy, and S.J. Ferguson, Cardiovascular changes after pulmonary embolism from injecting calcium phosphate cement, *Journal of Biomedical Materials Research B Applied Biomaterials*, 82, 526-32, **2007**.
98. Ito, M., A. Miyazaki, T. Yamagishi, H. Yagasaki, A. Hashem, and Y. Oshida, Experimental development of a chitosan-bonded beta-tricalcium phosphate bone filling paste, *Bio-Medical Materials and Engineering*, 4, 439-49, **1994**.
99. Hanker, J.S., B.C. Terry, W.W. Ambrose, and C.R. Lupton, Plaster of Paris as a bioresorbable scaffold in implants for bone repair, **1986**.
100. Klein, C.P., H.B. van der Lubbe, and K. de Groot, A plastic composite of alginate with calcium phosphate granulate as implant material: an in vivo study, *Biomaterials*, 8, 308-10, **1987**.
101. Gerhart, T.N., R.L. Miller, S.J. Kleshinski, and W.C. Hayes, In vitro characterization and biomechanical optimization of a biodegradable particulate composite bone cement, *Journal of Biomedical Materials Research*, 22, 1071-82, **1988**.

102. Takagi, S., L.C. Chow, S. Hirayama, and F.C. Eichmiller, Properties of elastomeric calcium phosphate cement-chitosan composites, *Dental Materials Journal*, 19, 797-804, **2003**.
103. Xu, H.H., J.B. Quinn, S. Takagi, and L.C. Chow, Processing and properties of strong and non-rigid calcium phosphate cement, *Journal of Dental Research*, 81, 219-24, **2002**.
104. Xu, H.H., J.B. Quinn, S. Takagi, and L.C. Chow, Synergistic reinforcement of in situ hardening calcium phosphate composite scaffold for bone tissue engineering, *Biomaterials*, 25, 1029-37, **2004**.
105. Brauer, G.M., D.R. Steinberger, and J.W. Stansbury, Dependence of curing time, peak temperature, and mechanical properties on the composition of bone cement, *Journal of Biomedical Materials Research*, 20, 839-52, **1986**.
106. King, K.P., *Chapter 217 - Methylmethacrylate*, (eds: J.L. Atlee), Elsevier Inc., 865-866, **2007**.
107. Sodhi, N., S.E. Dalton, A. Khlopas, A.A. Sultan, G.L. Curtis, M.A. Harb, Q. Naziri, J.M. Newman, J.W. Barrington, and M.A. Mont, Does a simple syringe applicator enhance bone cement set up time in knee arthroplasty?, *Annals of Translational Medicine*, 5, S25, **2017**.
108. Koh, B.T., J.H. Tan, A.K. Ramruttun, and W. Wang, Effect of storage temperature and equilibration time on polymethyl methacrylate (PMMA) bone cement polymerization in joint replacement surgery, *Journal of Orthopaedic Surgery and Research*, 10, 178, **2015**.
109. Prieto, E.M., J.M. Page, A.J. Harmata, and S.A. Guelcher, Injectable foams for regenerative medicine, *Wiley Interdisciplinary Reviews: Nanomedicine and Nanobiotechnology*, 6, 136-54, **2014**.
110. Goldberg, C.S., O. Antonyshyn, R. Midha, and J.A. Fialkov, Measuring pulsatile forces on the human cranium, *Journal of Craniofacial Surgery*, 16, 134-9, **2005**.
111. Sugawara, A., K. Fujikawa, S. Hirayama, T. Mori, T. Ikemi, S. Takagi, and L. Chow, Histopathological Reactions of Macroporous Premixed Calcium Phosphates Cement for Bone Defects Repair, International Association for Dental Research, **2004**.
112. Ghosh, I., J. Snyder, R. Vippagunta, M. Alvine, R. Vakil, W.Q. Tong, and S. Vippagunta, Comparison of HPMC based polymers performance as carriers for manufacture of solid dispersions using the melt extruder, *International Journal of Pharmaceutics*, 419, 12-9, **2011**.
113. Krebs, M.D., E. Salter, E. Chen, K.A. Sutter, and E. Alsberg, Calcium phosphate-DNA nanoparticle gene delivery from alginate hydrogels induces in vivo osteogenesis, *Journal of Biomedical Materials Research A*, 92, 1131-8, **2010**.
114. Lee, K.Y., E. Alsberg, and D.J. Mooney, Degradable and injectable poly(aldehyde guluronate) hydrogels for bone tissue engineering, *Journal of Biomedical Materials Research*, 56, 228-33, **2001**.
115. Martinez-Sanz, E., D.A. Ossipov, J. Hilborn, S. Larsson, K.B. Jonsson, and O.P. Varghese, Bone reservoir: Injectable hyaluronic acid hydrogel for minimal invasive bone augmentation, *Journal of Controlled Release*, 152, 232-40, **2011**.

116. Cai, L., J. Chen, A.J. Rondinone, and S. Wang, Injectable and Biodegradable Nanohybrid Polymers with Simultaneously Enhanced Stiffness and Toughness for Bone Repair, *Advanced Functional Materials*, 22, 3181-3190, **2012**.
117. Tarasevich, B.J., A. Gutowska, X.S. Li, and B.M. Jeong, The effect of polymer composition on the gelation behavior of PLGA-g-PEG biodegradable thermoreversible gels, *Journal of Biomedical Material Research A*, 89, 248-54, **2009**.
118. Bakhach, J., The cryopreservation of composite tissues: Principles and recent advancement on cryopreservation of different type of tissues, *Organogenesis*, 5, 119-26, **2009**.
119. Liu, C. and H. He, Springer Series in Biomaterials Science and Engineering, *Developments and Applications of Calcium Phosphate Bone Cements*, Springer, **2018**.
120. Rajzer, I., O. Castano, E. Engel, and J.A. Planell, Injectable and fast resorbable calcium phosphate cement for body-setting bone grafts, *Journal of Materials Science: Materials in Medicine*, 21, 2049-56, **2010**.
121. Aberg, J., H.B. Henriksson, H. Engqvist, A. Palmquist, C. Brantsing, A. Lindahl, P. Thomsen, and H. Brisby, Biocompatibility and resorption of a radiopaque premixed calcium phosphate cement, *Journal of Biomedical Materials Research A*, 100, 1269-78, **2012**.
122. Irbe, Z., G. Krieke, K. Salma-Ancane, and L. Berzina-Cimdina *Fast Setting Pre-Mixed Calcium Phosphate Bone Cements Based on α -Tricalcium Phosphate*. Key Engineering Materials, **604**, 204-207, **2014**.
123. Leroux, L., Z. Hatim, M. Freche, and J.L. Lacout, Effects of various adjuvants (lactic acid, glycerol, and chitosan) on the injectability of a calcium phosphate cement, *Bone*, 25, 31S-34S, **1999**.
124. Feighan, J.E., D. Davy, A.B. Prewett, and S. Stevenson, Induction of bone by a demineralized bone matrix gel: a study in a rat femoral defect model, *Journal of Orthopaedic Research*, 13, 881-91, **1995**.
125. Wang, T., L. Chen, T. Shen, and D. Wu, Preparation and properties of a novel thermo-sensitive hydrogel based on chitosan/hydroxypropyl methylcellulose/glycerol, *International Journal of Biological Macromolecules*, 93, 775-782, **2016**.
126. Pagliaro, M. and M. Rossi, *CHAPTER 1 Glycerol: Properties and Production*, (eds: M. Pagliaro and M. Rossi), RSC Green Chemistry Book Series, **2008**.
127. Dreifke, M.B., N.A. Ebraheim, and A.C. Jayasuriya, Investigation of potential injectable polymeric biomaterials for bone regeneration, *Journal of Biomedical Materials Research A*, 101, 2436-47, **2013**.
128. Perez, R.A., H.-W. Kim, and M.-P. Ginebra, Polymeric additives to enhance the functional properties of calcium phosphate cements, *Tissue Engineering*, 3, **2012**.
129. Lutolf, M.P., F.E. Weber, H.G. Schmoekel, J.C. Schense, T. Kohler, R. Muller, and J.A. Hubbell, Repair of bone defects using synthetic mimetics of collagenous extracellular matrices, *Nature Biotechnology*, 21, 513-8, **2003**.

130. Peled, E., J. Boss, J. Bejar, C. Zinman, and D. Seliktar, A novel poly(ethylene glycol)-fibrinogen hydrogel for tibial segmental defect repair in a rat model, *Journal of Biomedical Material Research A*, 80, 874-84, **2007**.
131. Kaihara, S., S. Matsumura, and J.P. Fisher, Cellular responses to degradable cyclic acetal modified PEG hydrogels, *Journal of Biomedical Materials Research A*, 90, 863-73, **2009**.
132. Shin, H., S. Jo, and A.G. Mikos, Modulation of marrow stromal osteoblast adhesion on biomimetic oligo[poly(ethylene glycol) fumarate] hydrogels modified with Arg-Gly-Asp peptides and a poly(ethyleneglycol) spacer, *Journal of Biomedical Material Research*, 61, 169-79, **2002**.
133. Kim, J., T.E. Hefferan, M.J. Yaszemski, and L. Lu, Potential of hydrogels based on poly(ethylene glycol) and sebacic acid as orthopedic tissue engineering scaffolds, *Tissue Engineering Part A*, 15, 2299-307, **2009**.
134. Suggs, L.J., E.Y. Kao, L.L. Palombo, R.S. Krishnan, M.S. Widmer, and A.G. Mikos, Preparation and characterization of poly(propylene fumarate-co-ethylene glycol) hydrogels, *Journal of Biomaterial Science Polymer Edition*, 9, 653-66, **1998**.
135. Cai, L., K. Wang, and S. Wang, Poly(ethylene glycol)-grafted poly(propylene fumarate) networks and parabolic dependence of MC3T3 cell behavior on the network composition, *Biomaterials*, 31, 4457-66, **2010**.
136. Briggs, T., M.D. Treiser, P.F. Holmes, J. Kohn, P.V. Moghe, and T.L. Arinze, Osteogenic differentiation of human mesenchymal stem cells on poly(ethylene glycol)-variant biomaterials, *Journal of Biomedical Materials Research A*, 91, 975-84, **2009**.
137. Nicodemus, G.D., I. Villanueva, and S.J. Bryant, Mechanical stimulation of TMJ condylar chondrocytes encapsulated in PEG hydrogels, *Journal of Biomedical Materials Research A*, 83, 323-31, **2007**.
138. Kaihara, S., S. Matsumura, and J.P. Fisher, Synthesis and characterization of cyclic acetal based degradable hydrogels, *European Journal of Pharmaceutics and Biopharmaceutics*, 68, 67-73, **2008**.
139. Lynn, A.D., T.R. Kyriakides, and S.J. Bryant, Characterization of the in vitro macrophage response and in vivo host response to poly(ethylene glycol)-based hydrogels, *Journal of Biomedical Materials Research Part A*, 93, 941-53, **2010**.
140. Saikia, K.C., T.D. Bhattacharya, S.K. Bhuyan, D.J. Talukdar, S.P. Saikia, and P. Jitesh, Calcium phosphate ceramics as bone graft substitutes in filling bone tumor defects, *Indian Journal of Orthopaedics*, 42, 169-172, **2008**.
141. Lu, J., M. Descamps, J. Dejou, G. Koubi, P. Hardouin, J. Lemaitre, and J.P. Proust, The biodegradation mechanism of calcium phosphate biomaterials in bone, *Journal of Biomedical Materials Research*, 63, 408-12, **2002**.
142. Le Huec, J.C., D. Clement, B. Brouillaud, N. Barthe, B. Dupuy, B. Foliguet, and B. Basse-Cathalinat, Evolution of the local calcium content around irradiated beta-tricalcium phosphate ceramic implants: in vivo study in the rabbit, *Biomaterials*, 19, 733-8, **1998**.
143. Le Huec, J.C., T. Schaefferbeke, D. Clement, J. Faber, and A. Le Rebeller, Influence of porosity on the mechanical resistance of hydroxyapatite ceramics under compressive stress, *Biomaterials*, 16, 113-8, **1995**.

144. Koerten, H.K. and J. van der Meulen, Degradation of calcium phosphate ceramics, *Journal of Biomedical Materials Research*, 44, 78-86, **1999**.
145. Ray, R.D. and A.A. Ward, Jr., A preliminary report on studies of basic calcium phosphate in bone replacement, *Surgical forum*, 429-34, **1951**.
146. Uchida A, N.S., McCartney ER, Ching W, The use of ceramics for bone replacement. A comparative study of three different porous ceramics, *The Journal of Bone and Joint Surgery. British Volume*, 66, 269-275, **1984**.
147. Greenwald, A.S., S.D. Boden, V.M. Goldberg, Y. Khan, C.T. Laurencin, R.N. Rosier, and I. American Academy of Orthopaedic Surgeons. The Committee on Biological, Bone-graft substitutes: facts, fictions, and applications, *The Journal of bone and joint surgery American volume*, 83-A Suppl 2 Pt 2, 98-103, **2001**.
148. LeGeros, R.Z., S. Lin, R. Rohanizadeh, D. Mijares, and J.P. LeGeros, Biphasic calcium phosphate bioceramics: preparation, properties and applications, *Journal of Materials Science: Materials in Medicine*, 14, 201-9, **2003**.
149. Lu, J.X., B. Flautre, K. Anselme, P. Hardouin, A. Gallur, M. Descamps, and B. Thierry, Role of interconnections in porous bioceramics on bone recolonization in vitro and in vivo, *Journal of Materials Science: Materials in Medicine*, 10, 111-20, **1999**.
150. Fujibayashi, S., J. Shikata, C. Tanaka, M. Matsushita, and T. Nakamura, Lumbar posterolateral fusion with biphasic calcium phosphate ceramic, *Journal of Spinal Disorders & Techniques*, 14, 214-21, **2001**.
151. Gbureck, U., J.E. Barralet, K. Spatz, L.M. Grover, and R. Thull, Ionic modification of calcium phosphate cement viscosity. Part I: hypodermic injection and strength improvement of apatite cement, *Biomaterials*, 25, 2187-95, **2004**.
152. Suzuki, O., M. Nakamura, Y. Miyasaka, M. Kagayama, and M. Sakurai, Bone formation on synthetic precursors of hydroxyapatite, *The Tohoku Journal of Experimental Medicine*, 164, 37-50, **1991**.
153. Kamakura, S., Y. Sasano, H. Homma, O. Suzuki, M. Kagayama, and K. Motegi, Implantation of octacalcium phosphate nucleates isolated bone formation in rat skull defects, *Oral Diseases*, 7, 259-65, **2001**.
154. Samavedi, S., A.R. Whittington, and A.S. Goldstein, Calcium phosphate ceramics in bone tissue engineering: a review of properties and their influence on cell behavior, *Acta Biomaterialia*, 9, 8037-45, **2013**.
155. Chang, B.S., C.K. Lee, K.S. Hong, H.J. Youn, H.S. Ryu, S.S. Chung, and K.W. Park, Osteoconduction at porous hydroxyapatite with various pore configurations, *Biomaterials*, 21, 1291-8, **2000**.
156. Champion, E., Sintering of calcium phosphate bioceramics, *Acta Biomaterialia*, 9, 5855-75, **2013**.
157. Mangkonsu, C., I. Kunio, L. Bunhan, R. Otman, and A.M. Noor, The Effect of Microwave Sintering on the Microstructure and Properties of Calcium Phosphate Ceramic, *Procedia Chemistry*, 19, 498-504, **2006**.
158. Veljović, D., E. Palcevskis, A. Dindune, S. Putić, I. Balać, R. Petrović, and D. Janačković, Microwave sintering improves the mechanical properties of biphasic

- calcium phosphates from hydroxyapatite microspheres produced from hydrothermal processing, *Journal of Materials Science*, 45, 3175-3183, **2010**.
159. Wagner, D.E., A.D. Jones, H. Zhou, and S.B. Bhaduri, Cytocompatibility evaluation of microwave sintered biphasic calcium phosphate scaffolds synthesized using pH control, *Materials Science and Engineering: C*, 33, 1710-9, **2013**.
 160. Bose, S., S. Dasgupta, S. Tarafder, and A. Bandyopadhyay, Microwave-processed nanocrystalline hydroxyapatite: simultaneous enhancement of mechanical and biological properties, *Acta Biomaterialia*, 6, 3782-90, **2010**.
 161. Yin, Y., F. Ye, J. Cui, F. Zhang, X. Li, and K. Yao, Preparation and characterization of macroporous chitosan-gelatin/beta-tricalcium phosphate composite scaffolds for bone tissue engineering, *Journal of Biomedical Material Research A*, 67, 844-55, **2003**.
 162. Ding, S.J., Preparation and properties of chitosan/calcium phosphate composites for bone repair, *Dental Materials Journal*, 25, 706-12, **2006**.
 163. Laasri, S., M. Taha, E.K. Hlil, A. Laghzizil, and A. Hajjaji, Manufacturing and mechanical properties of calcium phosphate biomaterials, *Comptes Rendus Mécanique*, 340, 715-720, **2012**.
 164. Hench, L.L., R.J. Splinter, W.C. Allen, and T.K. Greenlee, Bonding mechanisms at the interface of ceramic prosthetic materials, *Journal of Biomedical Materials Research Symp*, 5, 117-141, **1971**.
 165. Hench, L.L. and H.A. Paschall, Direct chemical bonding of bioactive glass-ceramic materials and bone, *Journal of Biomedical Materials Research Symp*, 4, 25-42, **1973**.
 166. Jones, J.R., Reprint of: Review of bioactive glass: From Hench to hybrids, *Acta Biomaterialia*, 23 Suppl, S53-82, **2015**.
 167. Wilson, J. and S.B. Low, Bioactive ceramics for periodontal treatment: comparative studies in the Patus monkey, *Journal of Applied Biomaterials*, 3, 123-9, **1992**.
 168. Hench, L.L. and J.M. Polak, Third-generation biomedical materials, *Science*, 295, 1014-7, **2002**.
 169. Stoor, P., E. Soderling, and J.I. Salonen, Antibacterial effects of a bioactive glass paste on oral microorganisms, *Acta Odontologica Scandinavica*, 56, 161-5, **1998**.
 170. Bellantone, M., H.D. Williams, and L.L. Hench, Broad-spectrum bactericidal activity of Ag(2)O-doped bioactive glass, *Antimicrobial Agents and Chemotherapy*, 46, 1940-5, **2002**.
 171. Gentleman, E., Y.C. Fredholm, G. Jell, N. Lotfibakhshaiesh, M.D. O'Donnell, R.G. Hill, and M.M. Stevens, The effects of strontium-substituted bioactive glasses on osteoblasts and osteoclasts in vitro, *Biomaterials*, 31, 3949-56, **2010**.
 172. Leach, J.K., D. Kaigler, Z. Wang, P.H. Krebsbach, and D.J. Mooney, Coating of VEGF-releasing scaffolds with bioactive glass for angiogenesis and bone regeneration, *Biomaterials*, 27, 3249-55, **2006**.
 173. Rust, K.R., G.T. Singleton, J. Wilson, and P.J. Antonelli, Bioglass middle ear prosthesis: long-term results, *American Journal of Otolaryngology*, 17, 371-4, **1996**.

174. Stanley, H.R., M.B. Hall, A.E. Clark, C.J. King, L.L. Hench, and J.J. Berte, Using 45S5 bioglass cones as endosseous ridge maintenance implants to prevent alveolar ridge resorption: a 5-year evaluation. , *International Journal of Oral Maxillofacial Implants*, 12, 95–105, **1997**.
175. Thompson, I.D., *Clinical applications of bioactive glasses for maxillofacial repair*, (eds: F.M. Hench LL, Jones JR), World Scientific, Singapore, 77–96, **2011**.
176. Rosenberg, E.S., S.C. Cho, N. Elian, Z.N. Jalbout, S. Froum, and C.I. Evian, A comparison of characteristics of implant failure and survival in periodontally compromised and periodontally healthy patients: a clinical report, *The International Journal of Oral & Maxillofacial Implants*, 19, 873-9, **2004**.
177. Yukna, R.A., G.H. Evans, M.B. Aichelmann-Reidy, and E.T. Mayer, Clinical comparison of bioactive glass bone replacement graft material and expanded polytetrafluoroethylene barrier membrane in treating human mandibular molar class II furcations, *Journal of Periodontology*, 72, 125-33, **2001**.
178. Norton, M.R. and J. Wilson, Dental implants placed in extraction sites implanted with bioactive glass: human histology and clinical outcome, *International Journal of Oral Maxillofacial Implants*, 17, 249-57, **2002**.
179. Sculean, A., P. Windisch, T. Keglevich, and I. Gera, Clinical and histologic evaluation of an enamel matrix protein derivative combined with a bioactive glass for the treatment of intrabony periodontal defects in humans, *The International Journal of Periodontics and Restorative Dentistry*, 25, 139-47, **2005**.
180. Ilharreborde, B., E. Morel, F. Fitoussi, A. Presedo, P. Souchet, G.F. Penneçot, and K. Mazda, Bioactive glass as a bone substitute for spinal fusion in adolescent idiopathic scoliosis a comparative study with iliac crest autograft, *Journal of Pediatric Orthopaedics*, 28, 347–351, **2008**.
181. Gillam, D.G., J.Y. Tang, N.J. Mordan, and H.N. Newman, The effects of a novel Bioglass dentifrice on dentine sensitivity: a scanning electron microscopy investigation, *Journal of Oral Rehabilitation*, 29, 305-13, **2002**.
182. Pradeep, A.R. and A. Sharma, Comparison of clinical efficacy of a dentifrice containing calcium sodium phosphosilicate to a dentifrice containing potassium nitrate and to a placebo on dentinal hypersensitivity: a randomized clinical trial, *Journal of Periodontology*, 81, 1167-73, **2010**.
183. Earl, J.S., R.K. Leary, K.H. Muller, R.M. Langford, and D.C. Greenspan, Physical and chemical characterization of dentin surface following treatment with NovaMin technology, *The Journal of Clinical Dentistry*, 22, 62-7, **2011**.
184. Bretcanu, O., X. Chatzistavrou, K. Paraskevopoulos, R. Conradt, I. Thompson, and A.R. Boccaccini, Sintering and crystallisation of 45S5 Bioglass (R) powder, *Journal of the European Ceramic Society*, 29, 3299 - 3306, **2009**.
185. Bellucci, D., A. Anesi, R. Salvatori, L. Chiarini, and V. Cannillo, A comparative in vivo evaluation of bioactive glasses and bioactive glass-based composites for bone tissue repair, *Journal of Materials Science and Engineering C*, 79, 286–295, **2017**.
186. Gomez-Vega , J.M., E. Saiz, A.P. Tomsia, T. Oku, K. Suganuma, G.W. Marshall, and S.J. Marshall, Novel Bioactive Functionally Graded Coatings on Ti6Al4V, *Advanced Materials*, 12, 894 - 898, **2000**.

187. Schepers, E.J. and P. Ducheyne, Bioactive glass particles of narrow size range for the treatment of oral bone defects: a 1-24 month experiment with several materials and particle sizes and size ranges, *Journal of Oral Rehabilitation*, 24, 171-81, **1997**.
188. Oonishi, H., S. Kushitani, E. Yasukawa, H. Iwaki, L.L. Hench, J. Wilson, E. Tsuji, and T. Sugihara, Particulate bioglass compared with hydroxyapatite as a bone graft substitute, *Clinical Orthopaedics and Related Research*, 316-25, **1997**.
189. Schmitt, J.M., D.C. Buck, S.P. Joh, S.E. Lynch, and J.O. Hollinger, Comparison of porous bone mineral and biologically active glass in critical-sized defects, *Journal of Periodontology*, 68, 1043-53, **1997**.
190. Vogel, M., C. Voigt, U.M. Gross, and C.M. Muller-Mai, In vivo comparison of bioactive glass particles in rabbits, *Biomaterials*, 22, 357-62, **2001**.
191. Vogel, M., C. Voigt, C. Knabe, R.J. Radlanski, U.M. Gross, and C.M. Muller-Mai, Development of multinuclear giant cells during the degradation of Bioglass particles in rabbits, *Journal of Biomedical Material Research A*, 70, 370-9, **2004**.
192. Lai, W., J. Garino, C. Flaitz, and P. Ducheyne, Excretion of resorption products from bioactive glass implanted in rabbit muscle, *Journal of Biomedical Materials Research A*, 75, 398-407, **2005**.
193. Lai, W., J. Garino, and P. Ducheyne, Silicon excretion from bioactive glass implanted in rabbit bone, *Biomaterials*, 23, 213-7, **2002**.
194. Pedone A, C.T., Malavasi G, Menziani MC, New insights into the atomic structure of 45S5 bioglass by means of solid-state NMR spectroscopy and accurate first-principles simulations, *Chemistry of Materials*, 22, 5644–5652, **2010**.
195. Hulbert, S.F., F.W. Cooke, J.J. Klawitter, R.B. Leonard, B.W. Sauer, D.D. Moyle, and H.B. Skinner, Attachment of prostheses to the musculoskeletal system by tissue ingrowth and mechanical interlocking, *Journal of Biomedical Materials Research*, 7, 1-23, **1973**.
196. Skedros, J.G., G.C. Clark, S.M. Sorenson, K.W. Taylor, and S. Qiu, Analysis of the effect of osteon diameter on the potential relationship of osteocyte lacuna density and osteon wall thickness, *The Anatomical Record*, 294, 1472-85, **2011**.
197. Khairoun, I., M.G. Boltong, F.C. Driessens, and J.A. Planell, Some factors controlling the injectability of calcium phosphate bone cements, *Journal of Materials Science: Materials in Medicine*, 9, 425-8, **1998**.
198. Nilsson, M., E. Liden, C. Ehrenborg, J. Forsgren, and S.A. Jönsson, What is injectability? A new injectability method for hydraulic cements developed for minimally invasive surgery, *Montreal*, 51, **2008**.
199. Bohner, M., Design of ceramic-based cements and putties for bone graft substitution, *European Cells and Materials*, 20, 1-12, **2010**.
200. Liu, J., J. Li, J. Ye, and F. He, Setting behavior, mechanical property and biocompatibility of anti-washout wollastonite/calcium phosphate composite cement, *Ceramics International*, 42, **2016**.
201. Bohner, M. and G. Baroud, Injectability of calcium phosphate pastes, *Biomaterials*, 26, 1553-63, **2005**.

202. Habib, M., G. Baroud, F. Gitzhofer, and M. Bohner, Mechanisms underlying the limited injectability of hydraulic calcium phosphate paste. Part II: particle separation study, *Acta Biomaterialia*, 6, 250-6, **2010**.
203. Habib, M., G. Baroud, F. Gitzhofer, and M. Bohner, Mechanisms underlying the limited injectability of hydraulic calcium phosphate paste, *Acta Biomaterialia*, 4, 1465-71, **2008**.
204. Ishikawa, K., Effects of spherical tetracalcium phosphate on injectability and basic properties of apatitic cement, *Key Engineering Materials*, 240, 369-372, **2003**.
205. Burguera, E.F., H.H. Xu, and L. Sun, Injectable calcium phosphate cement: effects of powder-to-liquid ratio and needle size, *Journal of Biomedical Materials Research B Applied Biomaterials*, 84, 493-502, **2008**.
206. Barralet, J.E., L.M. Grover, and U. Gbureck, Ionic modification of calcium phosphate cement viscosity. Part II: hypodermic injection and strength improvement of brushite cement, *Biomaterials*, 25, 2197-203, **2004**.
207. Gbureck, U., K. Spatz, R. Thull, and J.E. Barralet, Rheological enhancement of mechanically activated alpha-tricalcium phosphate cements, *Journal of Biomedical Materials Research B Applied Biomaterials*, 73, 1-6, **2005**.
208. Knowles, J.C., S. Callcut, and G. Georgiou, Characterisation of the rheological properties and zeta potential of a range of hydroxyapatite powders, *Biomaterials*, 21, 1387-92, **2000**.
209. Bujake, J.E.J., Rheology of concentrated dicalcium phosphate suspensions, *Journal of Pharmaceutical Sciences*, 54, 1599-1604, **1965**.
210. Tian, J.M., Y. Zhang, X.M. Guo, and L.M. Dong, Preparation and characterization of hydroxyapatite suspensions for solid freeform fabrication, *Ceramics International*, 28, 299-302, **2002**.
211. Olhero, S.M. and J.M.F. Ferreira, Influence of particle size distribution on rheology and particle packing of silica-based suspensions, *Powder Technology*, 139, 69-75, **2004**.
212. Kim, B.C., K. Ku, K.S. Kim, and Y.S. Kim, Effect of filler particulate size on the rheological properties of suspension CaCo₃ suspended in a aqueous HEC solution, *Polymer Korea*, 11, 158-162, **1987**.
213. Rao, R.R. and T.S. Kannan, Dispersion and slip casting of hydroxyapatite, *Journal of the American Ceramic Society*, 84, 1710-1716, **2001**.
214. Chen, Y., W. Xu, G. Zeng, and W. Liu, Shear-thickening behavior of precipitated Calcium Carbonate particles suspensions in glycerine, *Applied Rheology*, 25, 1-8, **2015**.
215. Garcia, F., N. LeBolay, and C. Frances, Rheological behaviour and related granulometric properties of dense aggregated suspensions during an ultrafine comminution process *Powder Technology*, 130, 407-414, **2003**.
216. Miyamoto, Y., K. Ishikawa, M. Takechi, T. Toh, T. Yuasa, M. Nagayama, and K. Suzuki, Histological and compositional evaluations of three types of calcium phosphate cements when implanted in subcutaneous tissue immediately after mixing, *Journal of Biomedical Materials Research*, 48, 36-42, **1999**.

217. Pioletti, D.P., H. Takei, T. Lin, P. Van Landuyt, Q.J. Ma, S.Y. Kwon, and K.L. Sung, The effects of calcium phosphate cement particles on osteoblast functions, *Biomaterials*, 21, 1103-14, **2000**.
218. Bohner, M., N. Doebelin, and G. Baroud, Theoretical and experimental approach to test the cohesion of calcium phosphate pastes, *European Cells and Materials*, 12, 26-35, **2006**.
219. Cherg, A., S. Takagi, and L.C. Chow, Effects of hydroxypropyl methylcellulose and other gelling agents on the handling properties of calcium phosphate cement, *Journal of Biomedical Materials Research*, 35, 273-7, **1997**.
220. An, J., J.G. Wolke, J.A. Jansen, and S.C. Leeuwenburgh, Influence of polymeric additives on the cohesion and mechanical properties of calcium phosphate cements, *Journal of Materials Science: Materials in Medicine*, 27, 58, **2016**.
221. Moreau, J.L., M.D. Weir, and H.H. Xu, Self-setting collagen-calcium phosphate bone cement: mechanical and cellular properties, *Journal of Biomedical Materials Research A*, 91, 605-13, **2009**.
222. Salama, A., R.E. Abou-Zeid, M. El-Sakhawy, and A. El-Gendy, Carboxymethyl cellulose/silica hybrids as templates for calcium phosphate biomimetic mineralization, *International Journal of Biological Macromolecules*, 74, 155-61, **2015**.
223. Muzzarelli, R., Biochemical significance of exogenous chitins and chitosans in animals and patients, *Carbohydrate Polymers*, 20, 7-16, **1993**.
224. Reynolds, M.A., M.E. Aichelmann-Reidy, J.D. Kassolis, H.S. Prasad, and M.D. Rohrer, Calcium sulfate-carboxymethylcellulose bone graft binder: Histologic and morphometric evaluation in a critical size defect, *Journal of Biomedical Material Research B Applied Biomaterials*, 83, 451-8, **2007**.
225. Schwartz, Z., M. Goldstein, E. Raviv, A. Hirsch, D.M. Ranly, and B.D. Boyan, Clinical evaluation of demineralized bone allograft in a hyaluronic acid carrier for sinus lift augmentation in humans: a computed tomography and histomorphometric study, *Clinical Oral Implants Research*, 18, 204-11, **2007**.
226. Sato, T., M. Kikuchi, and M. Aizawa, Preparation of hydroxyapatite/collagen injectable bone paste with an anti-washout property utilizing sodium alginate. Part 1: influences of excess supplementation of calcium compounds, *Journal of Materials Science: Materials in Medicine*, 28, 49, **2017**.
227. Maulida, H.N., D. Hikmawati, and A.S. Budiadin, Injectable Bone Substitute Paste Based on Hydroxyapatite, Gelatin and Streptomycin for Spinal Tuberculosis, *Journal of Spine*, 4, **2015**.
228. Xu, H.H., L.E. Carey, C.G. Simon, Jr., S. Takagi, and L.C. Chow, Premixed calcium phosphate cements: synthesis, physical properties, and cell cytotoxicity, *Dental Materials Journal*, 23, 433-41, **2007**.
229. Grover, L.M., M.P. Hofmann, U. Gbureck, B. Kumarasami, and J.E. Barralet, Frozen delivery of brushite calcium phosphate cements, *Acta Biomaterialia*, 4, 1916-23, **2008**.
230. Jacques, L., P. Christian, and B. David, Pasty or liquid multiple constituent compositions for injectable calcium phosphate cements, Ecole Polytechnique Federale de Lausanne (EPFL) U.S., **2008**.

231. Chow, L.C. and S. Takagi, Premixed self-hardening bone graft pastes, ADA Foundation, USA, **2002**.
232. Pekkan, G., A. Aktas, and K. Pekkan, Comparative radiopacity of bone graft materials, *Journal of Craniomaxillofacial Surgery*, 40, e1-4, **2012**.
233. Bucchi, C., E. Borie, A. Arias, F.J. Dias, and R. Fuentes, Radiopacity of alloplastic bone grafts measured with cone beam computed tomography: An analysis in rabbit calvaria, *Bosnian Journal of Basic Medical Sciences*, 17, 61-66, **2016**.
234. Ajeesh, M., B.F. Francis, J. Annie, and P.R. Harikrishna Varma, Nano iron oxide-hydroxyapatite composite ceramics with enhanced radiopacity, *Journal of Materials Science: Materials in Medicine*, 21, 1427-34, **2010**.
235. Kanjickal, D., S. Lopina, M.M. Evancho-Chapman, S. Schmidt, and D. Donovan, Effects of sterilization on poly(ethylene glycol) hydrogels, *Journal of Biomedical Materials Research*, 87, 608-17, **2008**.
236. Valente, T.A., D.M. Silva, P.S. Gomes, M.H. Fernandes, J.D. Santos, and V. Sencadas, Effect of Sterilization Methods on Electrospun Poly(lactic acid) (PLA) Fiber Alignment for Biomedical Applications, *ACS Applied Materials & Interfaces*, 8, 3241-9, **2016**.
237. Rnjak-Kovacina, J., T.M. DesRochers, K.A. Burke, and D.L. Kaplan, The effect of sterilization on silk fibroin biomaterial properties, *Macromolecular Bioscience*, 15, 861-74, **2015**.
238. Bliley, J.M.S., W.N. ; Minter, D.M. ; Tompkins-Rhoades, C. ; Day, J. ; Williamson, G. ; Liao, H.T. ; Marra, K.G., Ethylene Oxide Sterilization Preserves Bioactivity and Attenuates Burst Release of Encapsulated Glial Cell Line Derived Neurotrophic Factor from Tissue Engineered Nerve Guides for Long Gap Peripheral Nerve Repair, *ACS Biomaterials Science and Engineering*, 1, 504-512, **2015**.
239. Bertoldi, S., S. Fare, H.J. Haugen, and M.C. Tanzi, Exploiting novel sterilization techniques for porous polyurethane scaffolds, *Journal of Materials Science: Materials in Medicine*, 26, 182, **2015**.
240. Lerouge, S., M. Tabrizian, M.R. Wertheimer, R. Marchand, and L. Yahia, Safety of plasma-based sterilization: surface modifications of polymeric medical devices induced by Sterrad and Plazlyte processes, *Biomedical Materials Engineering*, 12, 3-13, **2002**.
241. Nuutinen, J.P., C. Clerc, T. Virta, and P. Tormala, Effect of gamma, ethylene oxide, electron beam, and plasma sterilization on the behaviour of SR-PLLA fibres in vitro, *Journal of Biomaterials Science, Polymer Edition*, 13, 1325-36, **2002**.
242. Dai, Z., J. Ronholm, Y. Tian, B. Sethi, and X. Cao, Sterilization techniques for biodegradable scaffolds in tissue engineering applications, *Journal of Tissue Engineering*, 7, 2041731416648810, **2016**.
243. Lleixa Calvet, J., D. Grafahrend, D. Klee, and M. Moller, Sterilization effects on starPEG coated polymer surfaces: characterization and cell viability, *Journal of Materials Science: Materials in Medicine*, 19, 1631-6, **2008**.
244. Iqbal, Z., W. Moses, S. Kim, E.J. Kim, W.H. Fissell, and S. Roy, Sterilization effects on ultrathin film polymer coatings for silicon-based implantable medical devices, *Journal of Biomedical Materials Research B Applied Biomaterials*, **2017**.

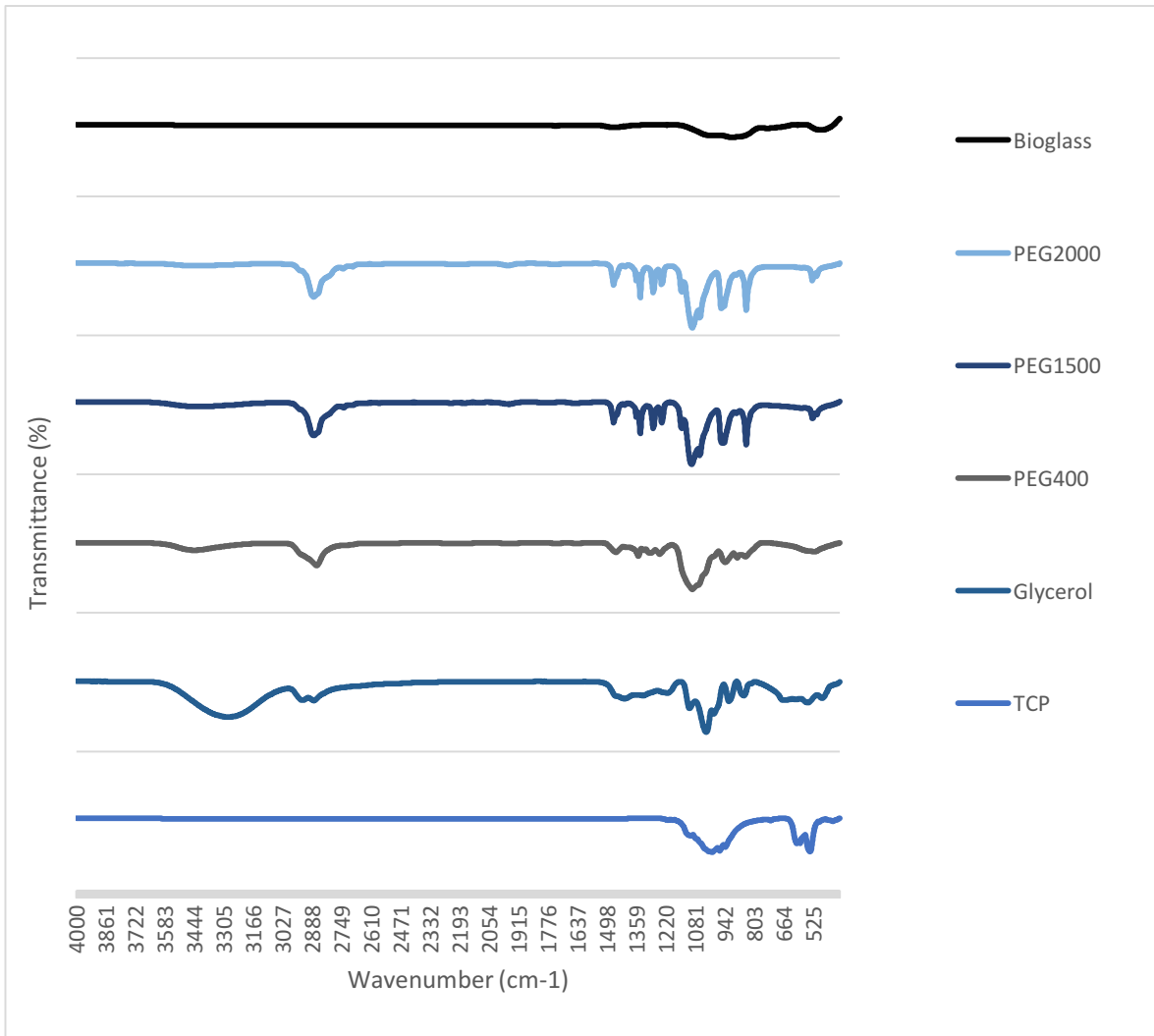
245. DePaula, C.A., Ceramic composition for filling bone defects, Musculoskeletal Transplant Foundation, USA, **2007**.
246. El-Tablawy, S.Y., W.M. Abd-Allah, and E. Araby, Efficacy of Irradiated Bioactive Glass 45S5 on Attenuation of Microbial Growth and Eradication of Biofilm from AISI 316 L Discs: In-vitro Study, *Silicon*, 1-12, **2017**.
247. Farag, M.M., W.M. Abd-Allah, and A.M. Ibrahim, Effect of gamma irradiation on drug releasing from nano-bioactive glass, *Drug Delivery and Translational Research*, 5, 63-73, **2015**.
248. Farag, M.M., W.M. Abd-Allah, and H.Y.A. Ahmed, Study of the dual effect of gamma irradiation and strontium substitution on bioactivity, cytotoxicity, and antimicrobial properties of 45S5 bioglass, *Journal of Biomedical Materials Research A*, 105, 1646-1655, **2017**.
249. Türker, S., A.Y. Özer, B. Kutlu, R. Nohutcu, H. Bilgili, D. Öztürk, M. Özalp, and A. Sungur, Gamma Irradiation Studies I. Dental Grafts, *Journal of Medical Devices*, 5, 031011-031011-11, **2011**.
250. Sarikaya, B. and H.M. Aydin, Collagen/Beta-Tricalcium Phosphate Based Synthetic Bone Grafts via Dehydrothermal Processing, *BioMed Research International*, 2015, 576532, **2015**.
251. Burdick, J.A. and K.S. Anseth, Photoencapsulation of osteoblasts in injectable RGD-modified PEG hydrogels for bone tissue engineering, *Biomaterials*, 23, 4315-23, **2002**.
252. Lin, C.C. and K.S. Anseth, PEG hydrogels for the controlled release of biomolecules in regenerative medicine, *Pharmaceutical Research*, 26, 631-43, **2009**.
253. Gaharwar, A.K., S.A. Dammu, J.M. Canter, C.J. Wu, and G. Schmidt, Highly extensible, tough, and elastomeric nanocomposite hydrogels from poly(ethylene glycol) and hydroxyapatite nanoparticles, *Biomacromolecules*, 12, 1641-50, **2011**.
254. Xianmiao, C., L. Yubao, Z. Yi, Z. Li, L. Jidong, and W. Huanan, Properties and in vitro biological evaluation of nano-hydroxyapatite/chitosan membranes for bone guided regeneration., *Material Science Engineering C*, 29, 29-35, **2009**.
255. Sanjeeva Rao, B., T. Venkatappa Rao, K. Madhukar, B. Chandra Mouli, S. Kalahast, and K. Gopala Kishan Rao, ESR and FTIR study of gamma irradiated poly (ethylene glycol), *Internation Journal of Chemical Sciences* 7, 2434-2440, **2009**.
256. Guimaraes, J.L., A.C. Trindade Cursino, C. Ketzer Saul, M.R. Sierrakowski, L.P. Ramos, and K.G. Satyanarayana, Evaluation of Castor Oil Cake Starch and Recovered Glycerol and Development of "Green" Composites Based on Those with Plant Fibers, *Materials (Basel)*, 9, **2016**.
257. Marcos, M.A., D. Cabaleiro, M.J.G. Guimarey, M.J.P. Comunas, L. Fedele, J. Fernandez, and L. Lugo, PEG 400-Based Phase Change Materials Nano-Enhanced with Functionalized Graphene Nanoplatelets, *Nanomaterials (Basel)*, 8, **2017**.
258. Yunos, M.Z.B. and W.A.W.A. Rahman, Effect of Glycerol on Performance Rice Straw/Starch Based Polymer, *Journal of Applied Sciences*, 11, 2456-2459, **2011**.
259. Zhang, J., H. Zhou, K. Yang, Y. Yuan, and C. Liu, RhBMP-2-loaded calcium silicate/calcium phosphate cement scaffold with hierarchically porous structure for enhanced bone tissue regeneration, *Biomaterials*, 34, 9381-92, **2013**.

260. Wei, J., J. Jia, F. Wu, S. Wei, H. Zhou, H. Zhang, J.W. Shin, and C. Liu, Hierarchically microporous/macroporous scaffold of magnesium-calcium phosphate for bone tissue regeneration, *Biomaterials*, 31, 1260-9, **2010**.
261. An, J., J.G. Wolke, J.A. Jansen, and S.C. Leeuwenburgh, Influence of polymeric additives on the cohesion and mechanical properties of calcium phosphate cements, *J Mater Sci Mater Med*, 27, 58, **2016**.
262. Farahnaky, A., B. Saberi, and M. Majzoubi, Effect of Glycerol on Physical and Mechanical Properties of Wheat Starch Edible Films, *Journal of Texture Studies*, 44, 176-186, **2013**.
263. Bohner, M., N. Doebelin, and G. Baroud, Theoretical and experimental approach to test the cohesion of calcium phosphate pastes, *Eur Cell Mater*, 12, 26-35, **2006**.
264. Aronson, H., Correction factor for dissolution profile calculations, *Journal of Pharmaceutical Sciences*, 82, 1190, **1993**.
265. Bilanovic, D., J. Starosvetsky, and R.H. Armon, Preparation of biodegradable xanthan-glycerol hydrogel, foam, film, aerogel and xerogel at room temperature, *Carbohydrate Polymers*, 148, 243-50, **2016**.
266. Carlisle, B.J., G. Craft, J.P. Harmon, A. Ilkevitch, J. Nicoghossian, I. Sheyner, and J.T. Stewart, PEG and Thickeners: A Critical Interaction Between Polyethylene Glycol Laxative and Starch-Based Thickeners, *Journal of the American Medical Directors Association*, 17, 860-1, **2016**.
267. Chethana, S., N.K. Rastogi, and K.S. Raghavarao, New aqueous two phase system comprising polyethylene glycol and xanthan, *Biotechnology Letters*, 28, 25-8, **2006**.
268. Ghahremankhani, A.A., F. Dorkoosh, and R. Dinarvand, PLGA-PEG-PLGA tri-block copolymers as in situ gel-forming peptide delivery system: effect of formulation properties on peptide release, *Pharmaceutical Development and Technology*, 13, 49-55, **2008**.
269. Augusto, P.E.D., M. Cristianini, and A. Ibarz, Effect of temperature on dynamic and steady-state shear rheological properties of siriguela (*Spondias purpurea* L.) pulp, *Journal of Food Engineering*, 108, 283-289, **2012**.
270. Correa, D.A., P.M.M. Castillo, and R.J. Martelo, Rheology of a Traditional Dairy Beverage from Colombian Caribbean *Contemporary Engineering Sciences*, 11, 1103 - 1110, **2018**.
271. Setz, L.F.G., A.C. Silva, S.C. Santos, S.R.H. Mello-Castanho, and M.R. Morelli, A viscoelastic approach from alpha-Al₂O₃ suspensions with high solids content, *Journal of the European Ceramic Society*, 33, 3211–3219, **2013**.
272. Ahmad, N.H., J. Ahmed, D.M. Hashim, Y.A. Manap, and S. Mustafa, Oscillatory and steady shear rheology of gellan/dextran blends, *Journal of Food Science and Technology*, 52, 2902-9, **2015**.
273. Rao, M.A., Engineering Properties of Foods., *Rheological Properties of Fluid Foods*, 3, CRC Press, Boca Raton **2005**.
274. Tulyaganov, D.U., S. Agathopoulos, P. Valerio, A. Balamurugan, A. Saranti, M.A. Karakassides, and J.M. Ferreira, Synthesis, bioactivity and preliminary biocompatibility studies of glasses in the system CaO-MgO-SiO₂-Na₂O-P₂O₅-CaF₂, *Journal of Materials Science: Materials in Medicine*, 22, 217-27, **2011**.

275. Xynos, I.D., A.J. Edgar, L.D. Buttery, L.L. Hench, and J.M. Polak, Ionic products of bioactive glass dissolution increase proliferation of human osteoblasts and induce insulin-like growth factor II mRNA expression and protein synthesis, *Biochemical and Biophysical Research Communications*, 276, 461-5, **2000**.
276. Aparicio, J.L., C. Rueda, A. Manchon, A. Ewald, U. Gbureck, M.H. Alkhraisat, L.B. Jerez, and E.L. Cabarcos, Effect of physicochemical properties of a cement based on silicocarnotite/calcium silicate on in vitro cell adhesion and in vivo cement degradation, *Biomedical Materials*, 11, 045005, **2016**.
277. Zimmermann, C.E., M. Gierloff, J. Hedderich, Y. Acil, J. Wiltfang, and H. Terheyden, Biocompatibility of bone graft substitutes: effects on survival and proliferation of porcine multilineage stem cells in vitro, *Folia Morphologica (Warsz)*, 70, 154-60, **2011**.
278. Olkowski, R., P. Kaszczewski, J. Czechowska, D. Siek, D. Pijocha, A. Zima, A. Slosarczyk, and M. Lewandowska-Szumiel, Cytocompatibility of the selected calcium phosphate based bone cements: comparative study in human cell culture, *Journal of Material Science: Materials in Medicine*, 26, 270, **2015**.
279. Maria Sadowska, J., J. Guillem-Marti, M. Espanol, C. Stahli, N. Dobelin, and M.P. Ginebra, In vitro response of mesenchymal stem cells to biomimetic hydroxyapatite substrates: a new strategy to assess the effect of ion exchange, *Acta Biomaterialia*, **2018**.
280. Tavakoli, M., E. Bateni, M. Rismanchian, M. Fathi, A. Doostmohammadi, A. Rabiei, H. Sadeghi, M. Etebari, and M. Mirian, Genotoxicity effects of nano bioactive glass and Novabone bioglass on gingival fibroblasts using single cell gel electrophoresis (comet assay): An in vitro study, *Dental Research Journal (Isfahan)*, 9, 314-20, **2012**.
281. Nakagawa, Y., T. Muneta, K. Tsuji, S. Ichinose, Y. Hakamatsuka, H. Koga, and I. Sekiya, β -Tricalcium Phosphate Micron Particles Enhance Calcification of Human Mesenchymal Stem Cells In Vitro, *Journal of Nanomaterials*, 2013, 13, **2013**.
282. Velard, F., J. Braux, J. Amedee, and P. Laquerriere, Inflammatory cell response to calcium phosphate biomaterial particles: an overview, *Acta Biomaterialia*, 9, 4956-63, **2013**.
283. Lange, T., A.F. Schilling, F. Peters, F. Haag, M.M. Morlock, J.M. Rueger, and M. Amling, Proinflammatory and osteoclastogenic effects of beta-tricalciumphosphate and hydroxyapatite particles on human mononuclear cells in vitro, *Biomaterials*, 30, 5312-8, **2009**.
284. Suzuki, T., R. Ohashi, Y. Yokogawa, K. Nishizawa, F. Nagata, Y. Kawamoto, T. Kameyama, and M. Toriyama, Initial anchoring and proliferation of fibroblast L-929 cells on unstable surface of calcium phosphate ceramics, *Journal of Bioscience and Bioengineering*, 87, 320-7, **1999**.
285. Lu, J., T. Tang, H. Ding, and K. Dai, Micro-particles of bioceramics could cause cell and tissue damage, *Sheng wu yi xue gong cheng xue za zhi = Journal of biomedical engineering*, 23, 85-89, **2006**.

5. APPENDIX

ATR – FT-IR SPECTROGRAMS FOR IBS CONSTITUENTS



STATISTICAL ANALYSES REPORTS

T-TEST PAIRS=SterileB21@24hour SterileB22@24hr SterileB11@24hour WITH SterileB31@24hour
 SterileB32@24hr SterileB31@24hour (PAIRED)
 /CRITERIA=CI(.9500)
 /MISSING=ANALYSIS.

T-Test

		Notes
Output Created		25-AUG-2018 20:25:53
Comments		
Input	Data	C:\Users\Leica\Desktop\WAS HOUTfinal.sav
	Active Dataset	DataSet1

	Filter	<none>
	Weight	<none>
	Split File	<none>
	N of Rows in Working Data File	1048468
Missing Value Handling	Definition of Missing	User defined missing values are treated as missing.
	Cases Used	Statistics for each analysis are based on the cases with no missing or out-of-range data for any variable in the analysis.
Syntax		T-TEST PAIRS=SterileB21@24hour SterileB22@24hr SterileB11@24hour WITH SterileB31@24hour SterileB32@24hr SterileB31@24hour (PAIRED) /CRITERIA=CI(.9500) /MISSING=ANALYSIS.
Resources	Processor Time	00:00:02,41
	Elapsed Time	00:00:02,43

Paired Samples Statistics

		Mean	N	Std. Deviation	Std. Error Mean
Pair 1	SterileB21@24hour	,4043	3	,08880	,05127
	SterileB31@24hour	,4117	3	,04038	,02331
Pair 2	SterileB22@24hr	,4040	3	,06222	,03592
	SterileB32@24hr	,4037	3	,08318	,04802
Pair 3	SterileB11@24hour	,3903	3	,04664	,02693
	SterileB31@24hour	,4117	3	,04038	,02331

Paired Samples Correlations

		N	Correlation	Sig.
Pair 1	SterileB21@24hour & SterileB31@24hour	3	-,548	,631
Pair 2	SterileB22@24hr & SterileB32@24hr	3	,621	,573

Pair 3	SterileB11@24hour & SterileB31@24hour	3	,415	,727
--------	--	---	------	------

Paired Samples Test

		Paired Differences			95% Confidence Interval of the Difference
		Mean	Std. Deviation	Std. Error Mean	Lower
Pair 1	SterileB21@24hour - SterileB31@24hour	-,00740	,11596	,06695	-,29546
Pair 2	SterileB22@24hr - SterileB32@24hr	,00033	,06603	,03812	-,16370
Pair 3	SterileB11@24hour - SterileB31@24hour	-,02137	,04735	,02734	-,13898

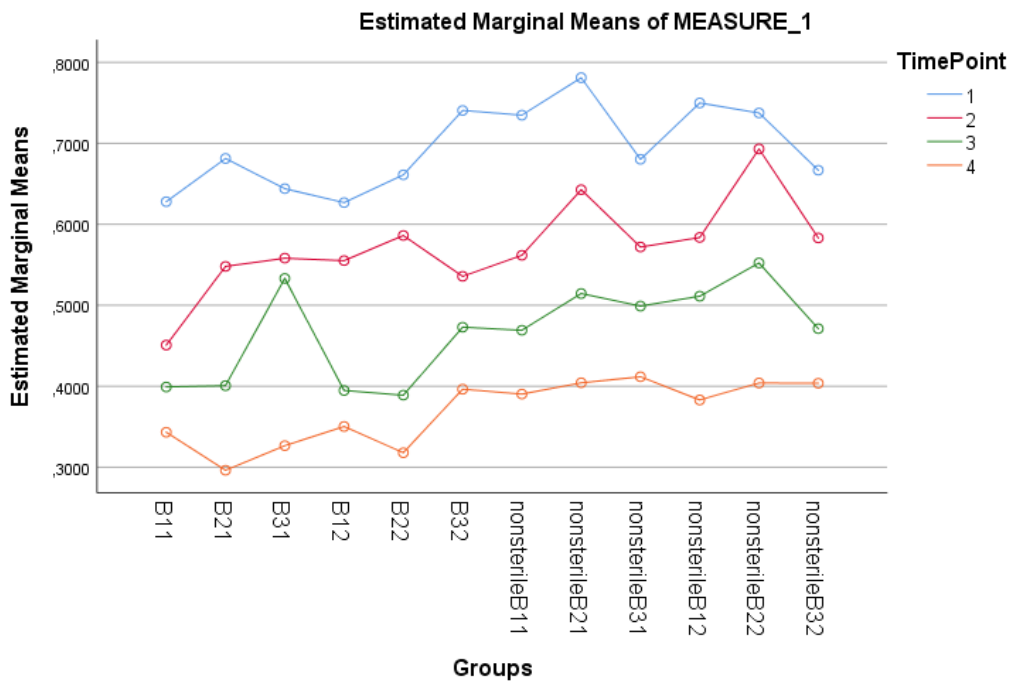
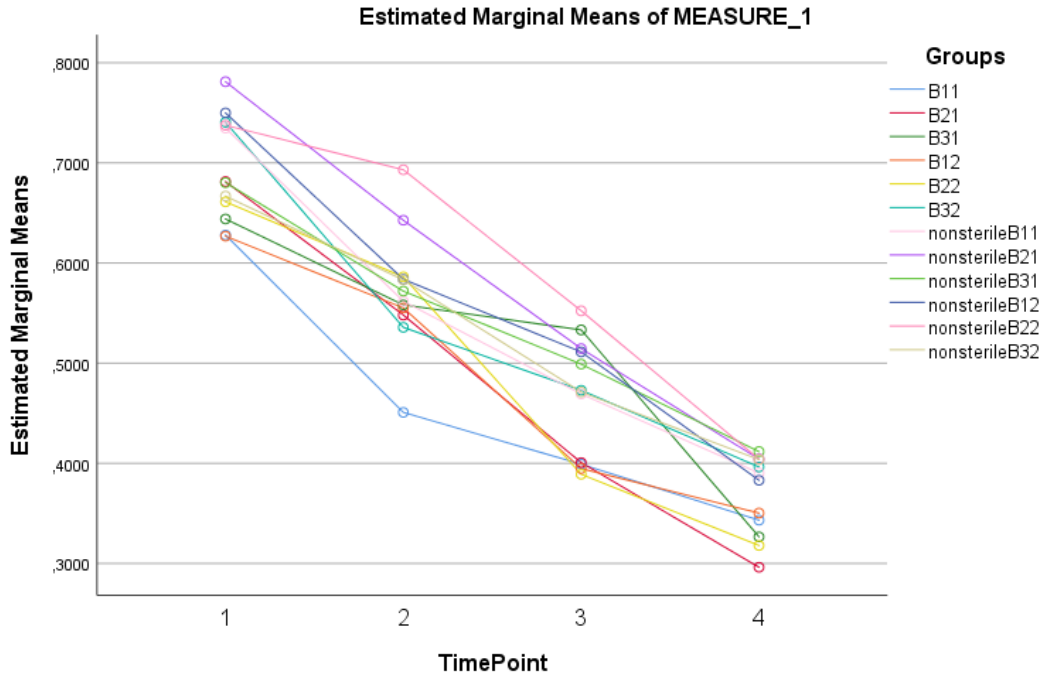
Paired Samples Test

		Paired Differences 95% Confidence Interval of the Difference Upper	t	df	Sig. (2-tailed)
Pair 1	SterileB21@24hour - SterileB31@24hour	,28066	-,111	2	,922
Pair 2	SterileB22@24hr - SterileB32@24hr	,16437	,009	2	,994
Pair 3	SterileB11@24hour - SterileB31@24hour	,09625	-,782	2	,516

WASHOUT STUDY STATISTICAL ANALYSIS REPORT

```
GLM Weight@1h Weight@8h Weight@12h Weight@24h BY Groups
/WSFACTOR=TimePoint 4 Polynomial
/METHOD=SSTYPE(3)
/PLOT=PROFILE(TimePoint*Groups Groups*TimePoint) TYPE=LINE
ERRORBAR=NO MEANREFERENCE=NO YAXIS=AUTO
/EMMEANS=TABLES(Groups) COMPARE ADJ(BONFERRONI)
/EMMEANS=TABLES(TimePoint) COMPARE ADJ(BONFERRONI)
/PRINT=DESCRIPTIVE ETASQ HOMOGENEITY
/CRITERIA=ALPHA(.05)
/WSDESIGN=TimePoint
/DESIGN=Groups.
```

Profile Plots



General Linear Model

Notes

Output Created	25-AUG-2018 19:28:23	
Comments		
Input	Data	C:\Users\Leica\Desktop\WAS HOUTfinal.sav
	Active Dataset	DataSet1
	Filter	<none>
	Weight	<none>
	Split File	<none>

	N of Rows in Working Data File	1048468
Missing Value Handling	Definition of Missing	User-defined missing values are treated as missing.
	Cases Used	Statistics are based on all cases with valid data for all variables in the model.
Syntax		<pre> GLM Weight@1h Weight@8h Weight@12h Weight@24h BY Groups /WSFACTOR=TimePoint 4 Polynomial /METHOD=SSTYPE(3) /PLOT=PROFILE(TimePoint* Groups Groups*TimePoint) TYPE=LINE ERRORBAR=NO MEANREFERENCE=NO YAXIS=AUTO /EMMEANS=TABLES(Group s) COMPARE ADJ(BONFERRONI) /EMMEANS=TABLES(TimeP oint) COMPARE ADJ(BONFERRONI) /PRINT=DESCRIPTIVE ETASQ HOMOGENEITY /CRITERIA=ALPHA(.05) /WSDESIGN=TimePoint /DESIGN=Groups. </pre>
Resources	Processor Time	00:00:07,59
	Elapsed Time	00:00:07,59

Warnings

Box's Test of Equality of Covariance Matrices is not computed because there are fewer than two nonsingular cell covariance matrices.

Within-Subjects Factors

Measure: MEASURE_1

TimePoint	Dependent Variable
1	Weight@1h
2	Weight@8h
3	Weight@12h
4	Weight@24h

Between-Subjects Factors

Groups	Value Label	N
1,00	B11	3
2,00	B21	3
3,00	B31	1
4,00	B12	3
5,00	B22	3
6,00	B32	3
7,00	nonsterileB11	3
8,00	nonsterileB21	3
9,00	nonsterileB31	3
10,00	nonsterileB12	3
11,00	nonsterileB22	3
12,00	nonsterileB32	3

Descriptive Statistics

	Groups	Mean	Std. Deviation	N
Weight@1h	B11	,627933	,0963113	3
	B21	,681300	,0513555	3
	B31	,644000	.	1
	B12	,626800	,0519504	3
	B22	,661100	,0070449	3
	B32	,740567	,0828518	3
	nonsterileB11	,734800	,0265955	3
	nonsterileB21	,781033	,0927608	3
	nonsterileB31	,680267	,0406503	3
	nonsterileB12	,749867	,0078749	3
	nonsterileB22	,737533	,0251170	3
	nonsterileB32	,666800	,1061868	3
	Total		,697294	,0725049
Weight@8h	B11	,450833	,0650269	3
	B21	,548000	,1888401	3

	B31	,558200	.	1
	B12	,555133	,0598761	3
	B22	,586133	,0745408	3
	B32	,535733	,0372218	3
	nonsterileB11	,561733	,0351543	3
	nonsterileB21	,642700	,0361017	3
	nonsterileB31	,571960	,0818396	3
	nonsterileB12	,583733	,0924533	3
	nonsterileB22	,693100	,0380000	3
	nonsterileB32	,583133	,1640190	3
	Total	,573376	,0960559	34
Weight@12h	B11	,399100	,0363443	3
	B21	,400700	,1324303	3
	B31	,533200	.	1
	B12	,394733	,0076166	3
	B22	,389000	,0641526	3
	B32	,472900	,0544649	3
	nonsterileB11	,469167	,0158140	3
	nonsterileB21	,514500	,1350632	3
	nonsterileB31	,498967	,0478871	3
	nonsterileB12	,511167	,0495424	3
	nonsterileB22	,552267	,1164616	3
	nonsterileB32	,471133	,1179045	3
	Total	,463356	,0880672	34
Weight@24h	B11	,343200	,0496051	3
	B21	,296200	,0842283	3
	B31	,326600	.	1
	B12	,350300	,0271860	3
	B22	,317933	,0122623	3
	B32	,396333	,0528602	3
	nonsterileB11	,390333	,0466376	3
	nonsterileB21	,404300	,0887966	3
	nonsterileB31	,411700	,0403796	3
	nonsterileB12	,383067	,0318114	3
	nonsterileB22	,404033	,0622220	3
	nonsterileB32	,403700	,0831807	3
	Total	,371468	,0609336	34

Multivariate Tests^a

Effect		Value	F	Hypothesis df	Error df
TimePoint	Pillai's Trace	,987	498,577 ^b	3,000	20,000

	Wilks' Lambda	,013	498,577 ^b	3,000	20,000
	Hotelling's Trace	74,787	498,577 ^b	3,000	20,000
	Roy's Largest Root	74,787	498,577 ^b	3,000	20,000
TimePoint * Groups	Pillai's Trace	1,248	1,424	33,000	66,000
	Wilks' Lambda	,171	1,482	33,000	59,628
	Hotelling's Trace	2,728	1,543	33,000	56,000
	Roy's Largest Root	1,881	3,763 ^c	11,000	22,000

Multivariate Tests^a

Effect		Sig.	Partial Eta Squared
TimePoint	Pillai's Trace	,00000	,987
	Wilks' Lambda	,00000	,987
	Hotelling's Trace	,00000	,987
	Roy's Largest Root	,00000	,987
TimePoint * Groups	Pillai's Trace	,11129	,416
	Wilks' Lambda	,09277	,445
	Hotelling's Trace	,07524	,476
	Roy's Largest Root	,00395	,653

a. Design: Intercept + Groups

Within Subjects Design: TimePoint

b. Exact statistic

c. The statistic is an upper bound on F that yields a lower bound on the significance level.

Mauchly's Test of Sphericity^a

Measure: MEASURE_1

Within Subjects Effect	Mauchly's W	Approx. Chi-Square	df	Sig.	Epsilon ^b Greenhouse-Geisser
TimePoint	,453	16,431	5	,006	,749

Mauchly's Test of Sphericity^a

Measure: MEASURE_1

Within Subjects Effect	Huynh-Feldt	Epsilon	Lower-bound
TimePoint		1,000	,333

Tests the null hypothesis that the error covariance matrix of the orthonormalized transformed dependent variables is proportional to an identity matrix.^a

a. Design: Intercept + Groups

Within Subjects Design: TimePoint

b. May be used to adjust the degrees of freedom for the averaged tests of significance. Corrected tests are displayed in the Tests of Within-Subjects Effects table.

Tests of Within-Subjects Effects

Measure: MEASURE_1

Source		Type III Sum of Squares	df	Mean Square	F
TimePoint	Sphericity Assumed	1,809	3	,603	223,190
	Greenhouse-Geisser	1,809	2,247	,805	223,190
	Huynh-Feldt	1,809	3,000	,603	223,190
	Lower-bound	1,809	1,000	1,809	223,190
TimePoint * Groups	Sphericity Assumed	,103	33	,003	1,151
	Greenhouse-Geisser	,103	24,716	,004	1,151
	Huynh-Feldt	,103	33,000	,003	1,151
	Lower-bound	,103	11,000	,009	1,151
Error(TimePoint)	Sphericity Assumed	,178	66	,003	
	Greenhouse-Geisser	,178	49,432	,004	
	Huynh-Feldt	,178	66,000	,003	
	Lower-bound	,178	22,000	,008	

Tests of Within-Subjects Effects

Measure: MEASURE_1

Source		Sig.	Partial Eta Squared
TimePoint	Sphericity Assumed	,000	,910
	Greenhouse-Geisser	,000	,910
	Huynh-Feldt	,000	,910
	Lower-bound	,000	,910
TimePoint * Groups	Sphericity Assumed	,308	,365
	Greenhouse-Geisser	,329	,365
	Huynh-Feldt	,308	,365
	Lower-bound	,373	,365
Error(TimePoint)	Sphericity Assumed		
	Greenhouse-Geisser		
	Huynh-Feldt		
	Lower-bound		

Tests of Within-Subjects Contrasts

Measure: MEASURE_1

Source		Type III Sum of Squares	df	Mean Square	F	Sig.
TimePoint	Linear	1,804	1	1,804	1035,574	,000
	Quadratic	,004	1	,004	1,362	,256
	Cubic	,000	1	,000	,043	,838

TimePoint * Groups	Linear	,035	11	,003	1,811	,114
	Quadratic	,036	11	,003	1,055	,436
	Cubic	,031	11	,003	,887	,566
Error(TimePoint)	Linear	,038	22	,002		
	Quadratic	,069	22	,003		
	Cubic	,071	22	,003		

Tests of Within-Subjects Contrasts

Measure: MEASURE_1

Source	TimePoint	Partial Eta Squared
TimePoint	Linear	,979
	Quadratic	,058
	Cubic	,002
TimePoint * Groups	Linear	,475
	Quadratic	,345
	Cubic	,307
Error(TimePoint)	Linear	
	Quadratic	
	Cubic	

Levene's Test of Equality of Error Variances^a

		Levene Statistic	df1	df2	Sig.
Weight@1h	Based on Mean	2,999	10	22	,015
	Based on Median	,753	10	22	,670
	Based on Median and with adjusted df	,753	10	11,830	,669
	Based on trimmed mean	2,757	10	22	,023
Weight@8h	Based on Mean	2,711	10	22	,025
	Based on Median	,804	10	22	,627
	Based on Median and with adjusted df	,804	10	7,684	,635
	Based on trimmed mean	2,525	10	22	,034
Weight@12h	Based on Mean	2,575	10	22	,031
	Based on Median	,702	10	22	,713
	Based on Median and with adjusted df	,702	10	10,393	,707
	Based on trimmed mean	2,386	10	22	,043
Weight@24h	Based on Mean	1,658	10	22	,155
	Based on Median	,430	10	22	,916
	Based on Median and with adjusted df	,430	10	13,582	,907

Based on trimmed mean	1,526	10	22	,196
-----------------------	-------	----	----	------

Tests the null hypothesis that the error variance of the dependent variable is equal across groups.^a

a. Design: Intercept + Groups

Within Subjects Design: TimePoint

Tests of Between-Subjects Effects

Measure: MEASURE_1

Transformed Variable: Average

Source	Type III Sum of Squares	df	Mean Square	F	Sig.	Partial Eta Squared
Intercept	34,120	1	34,120	2270,465	,000	,990
Groups	,245	11	,022	1,482	,208	,426
Error	,331	22	,015			

Estimated Marginal Means

1. Groups

Estimates

Measure: MEASURE_1

Groups	Mean	Std. Error	95% Confidence Interval	
			Lower Bound	Upper Bound
B11	,455	,035	,382	,529
B21	,482	,035	,408	,555
B31	,516	,061	,388	,643
B12	,482	,035	,408	,555
B22	,489	,035	,415	,562
B32	,536	,035	,463	,610
nonsterileB11	,539	,035	,466	,612
nonsterileB21	,586	,035	,512	,659
nonsterileB31	,541	,035	,467	,614
nonsterileB12	,557	,035	,484	,630
nonsterileB22	,597	,035	,523	,670
nonsterileB32	,531	,035	,458	,605

Pairwise Comparisons

Measure: MEASURE_1

(I) Groups	(J) Groups	Mean Difference (I-J)	Std. Error	Sig. ^a	95% Confidence Interval for Difference ^a	
					Lower Bound	Upper Bound
B11	B21	-,026	,050	1,000	-,222	,169
	B31	-,060	,071	1,000	-,337	,216

	B12	-,026	,050	1,000	-,222	,169
	B22	-,033	,050	1,000	-,229	,162
	B32	-,081	,050	1,000	-,277	,114
	nonsterileB11	-,084	,050	1,000	-,279	,112
	nonsterileB21	-,130	,050	1,000	-,326	,065
	nonsterileB31	-,085	,050	1,000	-,281	,110
	nonsterileB12	-,102	,050	1,000	-,297	,094
	nonsterileB22	-,141	,050	,648	-,337	,054
	nonsterileB32	-,076	,050	1,000	-,271	,120
B21	B11	,026	,050	1,000	-,169	,222
	B31	-,034	,071	1,000	-,310	,243
	B12	,000	,050	1,000	-,196	,195
	B22	-,007	,050	1,000	-,202	,189
	B32	-,055	,050	1,000	-,250	,141
	nonsterileB11	-,057	,050	1,000	-,253	,138
	nonsterileB21	-,104	,050	1,000	-,300	,091
	nonsterileB31	-,059	,050	1,000	-,255	,136
	nonsterileB12	-,075	,050	1,000	-,271	,120
	nonsterileB22	-,115	,050	1,000	-,311	,080
	nonsterileB32	-,050	,050	1,000	-,245	,146
B31	B11	,060	,071	1,000	-,216	,337
	B21	,034	,071	1,000	-,243	,310
	B12	,034	,071	1,000	-,243	,310
	B22	,027	,071	1,000	-,250	,303
	B32	-,021	,071	1,000	-,297	,256
	nonsterileB11	-,024	,071	1,000	-,300	,253
	nonsterileB21	-,070	,071	1,000	-,347	,206
	nonsterileB31	-,025	,071	1,000	-,302	,251
	nonsterileB12	-,041	,071	1,000	-,318	,235
	nonsterileB22	-,081	,071	1,000	-,358	,195
	nonsterileB32	-,016	,071	1,000	-,292	,261
B12	B11	,026	,050	1,000	-,169	,222
	B21	,000	,050	1,000	-,195	,196
	B31	-,034	,071	1,000	-,310	,243
	B22	-,007	,050	1,000	-,202	,189
	B32	-,055	,050	1,000	-,250	,141
	nonsterileB11	-,057	,050	1,000	-,253	,138
	nonsterileB21	-,104	,050	1,000	-,299	,092
	nonsterileB31	-,059	,050	1,000	-,254	,137
	nonsterileB12	-,075	,050	1,000	-,271	,120
	nonsterileB22	-,115	,050	1,000	-,310	,081

	nonsterileB32	-,049	,050	1,000	-,245	,146
B22	B11	,033	,050	1,000	-,162	,229
	B21	,007	,050	1,000	-,189	,202
	B31	-,027	,071	1,000	-,303	,250
	B12	,007	,050	1,000	-,189	,202
	B32	-,048	,050	1,000	-,243	,148
	nonsterileB11	-,050	,050	1,000	-,246	,145
	nonsterileB21	-,097	,050	1,000	-,293	,098
	nonsterileB31	-,052	,050	1,000	-,248	,143
	nonsterileB12	-,068	,050	1,000	-,264	,127
	nonsterileB22	-,108	,050	1,000	-,304	,087
	nonsterileB32	-,043	,050	1,000	-,238	,153
B32	B11	,081	,050	1,000	-,114	,277
	B21	,055	,050	1,000	-,141	,250
	B31	,021	,071	1,000	-,256	,297
	B12	,055	,050	1,000	-,141	,250
	B22	,048	,050	1,000	-,148	,243
	nonsterileB11	-,003	,050	1,000	-,198	,193
	nonsterileB21	-,049	,050	1,000	-,245	,146
	nonsterileB31	-,004	,050	1,000	-,200	,191
	nonsterileB12	-,021	,050	1,000	-,216	,175
	nonsterileB22	-,060	,050	1,000	-,256	,135
	nonsterileB32	,005	,050	1,000	-,190	,201
nonsterileB11	B11	,084	,050	1,000	-,112	,279
	B21	,057	,050	1,000	-,138	,253
	B31	,024	,071	1,000	-,253	,300
	B12	,057	,050	1,000	-,138	,253
	B22	,050	,050	1,000	-,145	,246
	B32	,003	,050	1,000	-,193	,198
	nonsterileB21	-,047	,050	1,000	-,242	,149
	nonsterileB31	-,002	,050	1,000	-,197	,194
	nonsterileB12	-,018	,050	1,000	-,213	,178
	nonsterileB22	-,058	,050	1,000	-,253	,138
	nonsterileB32	,008	,050	1,000	-,188	,203
nonsterileB21	B11	,130	,050	1,000	-,065	,326
	B21	,104	,050	1,000	-,091	,300
	B31	,070	,071	1,000	-,206	,347
	B12	,104	,050	1,000	-,092	,299
	B22	,097	,050	1,000	-,098	,293
	B32	,049	,050	1,000	-,146	,245
	nonsterileB11	,047	,050	1,000	-,149	,242

	nonsterileB31	,045	,050	1,000	-,151	,240
	nonsterileB12	,029	,050	1,000	-,167	,224
	nonsterileB22	-,011	,050	1,000	-,207	,184
	nonsterileB32	,054	,050	1,000	-,141	,250
nonsterileB31	B11	,085	,050	1,000	-,110	,281
	B21	,059	,050	1,000	-,136	,255
	B31	,025	,071	1,000	-,251	,302
	B12	,059	,050	1,000	-,137	,254
	B22	,052	,050	1,000	-,143	,248
	B32	,004	,050	1,000	-,191	,200
	nonsterileB11	,002	,050	1,000	-,194	,197
	nonsterileB21	-,045	,050	1,000	-,240	,151
	nonsterileB12	-,016	,050	1,000	-,212	,179
	nonsterileB22	-,056	,050	1,000	-,252	,139
	nonsterileB32	,010	,050	1,000	-,186	,205
	nonsterileB12	B11	,102	,050	1,000	-,094
B21		,075	,050	1,000	-,120	,271
B31		,041	,071	1,000	-,235	,318
B12		,075	,050	1,000	-,120	,271
B22		,068	,050	1,000	-,127	,264
B32		,021	,050	1,000	-,175	,216
nonsterileB11		,018	,050	1,000	-,178	,213
nonsterileB21		-,029	,050	1,000	-,224	,167
nonsterileB31		,016	,050	1,000	-,179	,212
nonsterileB22		-,040	,050	1,000	-,235	,156
nonsterileB32		,026	,050	1,000	-,170	,221
nonsterileB22		B11	,141	,050	,648	-,054
	B21	,115	,050	1,000	-,080	,311
	B31	,081	,071	1,000	-,195	,358
	B12	,115	,050	1,000	-,081	,310
	B22	,108	,050	1,000	-,087	,304
	B32	,060	,050	1,000	-,135	,256
	nonsterileB11	,058	,050	1,000	-,138	,253
	nonsterileB21	,011	,050	1,000	-,184	,207
	nonsterileB31	,056	,050	1,000	-,139	,252
	nonsterileB12	,040	,050	1,000	-,156	,235
	nonsterileB32	,066	,050	1,000	-,130	,261
	nonsterileB32	B11	,076	,050	1,000	-,120
B21		,050	,050	1,000	-,146	,245
B31		,016	,071	1,000	-,261	,292
B12		,049	,050	1,000	-,146	,245

B22	,043	,050	1,000	-,153	,238
B32	-,005	,050	1,000	-,201	,190
nonsterileB11	-,008	,050	1,000	-,203	,188
nonsterileB21	-,054	,050	1,000	-,250	,141
nonsterileB31	-,010	,050	1,000	-,205	,186
nonsterileB12	-,026	,050	1,000	-,221	,170
nonsterileB22	-,066	,050	1,000	-,261	,130

Based on estimated marginal means

a. Adjustment for multiple comparisons: Bonferroni.

Univariate Tests

Measure: MEASURE_1

	Sum of Squares	df	Mean Square	F	Sig.	Partial Eta Squared
Contrast	,061	11	,006	1,482	,208	,426
Error	,083	22	,004			

The F tests the effect of Groups. This test is based on the linearly independent pairwise comparisons among the estimated marginal means.

2. TimePoint

Estimates

Measure: MEASURE_1

TimePoint	Mean	Std. Error	95% Confidence Interval	
			Lower Bound	Upper Bound
1	,694	,011	,671	,718
2	,573	,017	,538	,608
3	,467	,015	,436	,498
4	,369	,010	,347	,391

Pairwise Comparisons

Measure: MEASURE_1

(I) TimePoint	(J) TimePoint	Mean Difference (I-J)	Std. Error	Sig. ^b	95% Confidence Interval for Difference ^b Lower Bound
1	2	,122*	,017	,000	,073
	3	,227*	,014	,000	,186
	4	,325*	,010	,000	,297
2	1	-,122*	,017	,000	-,170
	3	,105*	,015	,000	,062

	4		,204*	,013	,000	,165
3	1		-,227*	,014	,000	-,268
	2		-,105*	,015	,000	-,149
	4		,098*	,009	,000	,073
4	1		-,325*	,010	,000	-,353
	2		-,204*	,013	,000	-,242
	3		-,098*	,009	,000	-,124

Pairwise Comparisons

Measure: MEASURE_1

(I) TimePoint	(J) TimePoint	95% Confidence Interval for Difference	
			Upper Bound
1	2		,170
	3		,268
	4		,353
2	1		-,073
	3		,149
	4		,242
3	1		-,186
	2		-,062
	4		,124
4	1		-,297
	2		-,165
	3		-,073

Based on estimated marginal means

*. The mean difference is significant at the ,05 level.

b. Adjustment for multiple comparisons: Bonferroni.

Multivariate Tests

	Value	F	Hypothesis df	Error df	Sig.	Partial Eta Squared
Pillai's trace	,987	498,577 ^a	3,000	20,000	,000	,987
Wilks' lambda	,013	498,577 ^a	3,000	20,000	,000	,987
Hotelling's trace	74,787	498,577 ^a	3,000	20,000	,000	,987
Roy's largest root	74,787	498,577 ^a	3,000	20,000	,000	,987

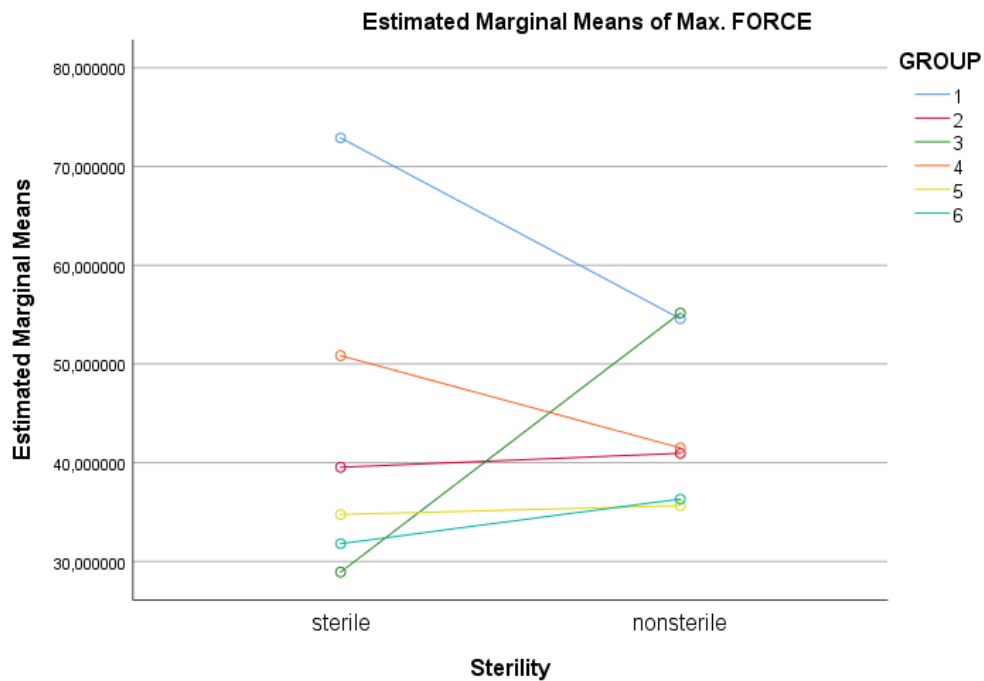
Each F tests the multivariate effect of TimePoint. These tests are based on the linearly independent pairwise comparisons among the estimated marginal means.

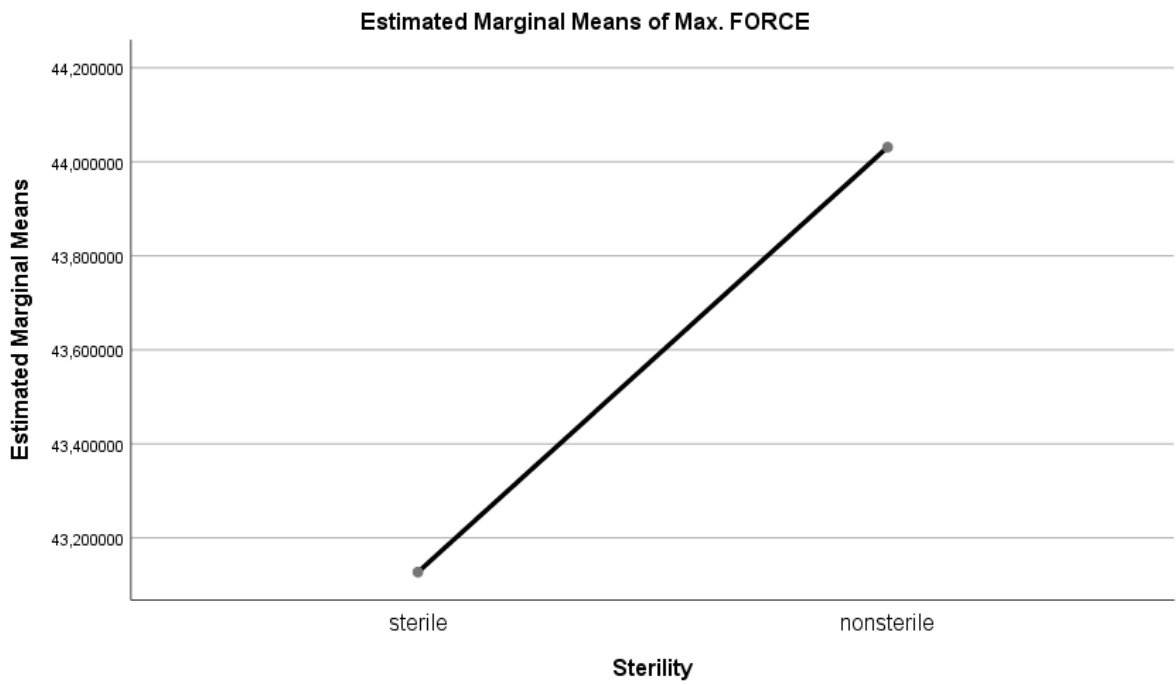
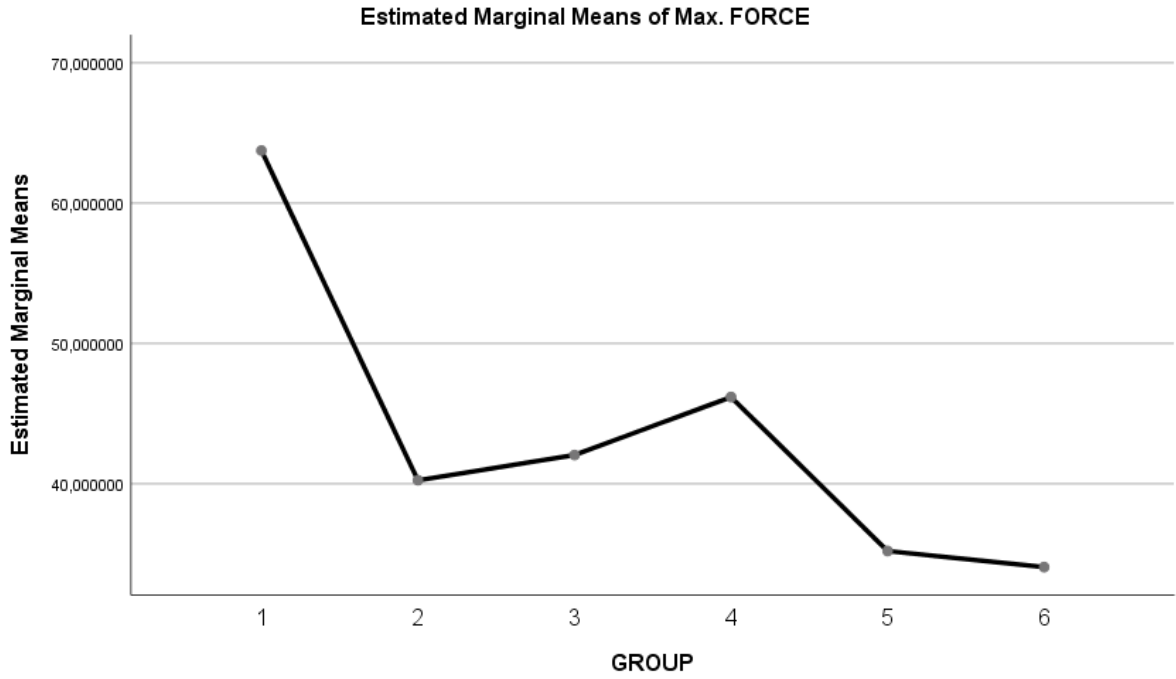
a. Exact statistic

INJECTABILITY STUDY STATISTICAL ANALYSIS REPORT

```
UNIANOVA Peak_Injection_Force BY GROUP Sterility
/METHOD=SSTYPE(3)
/INTERCEPT=INCLUDE
/POSTHOC=GROUP(QREGW)
/PLOT=PROFILE(Sterility*GROUP GROUP Sterility) TYPE=LINE
ERRORBAR=NO MEANREFERENCE=NO YAXIS=AUTO
/EMMEANS=TABLES(GROUP) COMPARE ADJ(BONFERRONI)
/EMMEANS=TABLES(GROUP*Sterility)
/EMMEANS=TABLES(Sterility) COMPARE ADJ(BONFERRONI)
/PRINT ETASQ DESCRIPTIVE HOMOGENEITY
/CRITERIA=ALPHA(.05)
/DESIGN=GROUP Sterility GROUP*Sterility.
```

Profile Plots





Univariate Analysis of Variance

Notes

Output Created	26-AUG-2018 21:28:10
Comments	
Input	Data
	C:\Users\Leica\Desktop\deni z tez statistics\INJECTABILITYfina l.sav
	Active Dataset
	DataSet2

	Filter	<none>
	Weight	<none>
	Split File	<none>
	N of Rows in Working Data File	37
Missing Value Handling	Definition of Missing	User-defined missing values are treated as missing.
	Cases Used	Statistics are based on all cases with valid data for all variables in the model.
Syntax		<pre> UNIANOVA Peak_Injection_Force BY GROUP Sterility /METHOD=SSTYPE(3) /INTERCEPT=INCLUDE /POSTHOC=GROUP(QREG W) /PLOT=PROFILE(Sterility*G ROUP GROUP Sterility) TYPE=LINE ERRORBAR=NO MEANREFERENCE=NO YAXIS=AUTO /EMMEANS=TABLES(GROU P) COMPARE ADJ(BONFERRONI) /EMMEANS=TABLES(GROU P*Sterility) /EMMEANS=TABLES(Sterilit y) COMPARE ADJ(BONFERRONI) /PRINT ETASQ DESCRIPTIVE HOMOGENEITY /CRITERIA=ALPHA(.05) /DESIGN=GROUP Sterility GROUP*Sterility. </pre>
Resources	Processor Time	00:00:00,80

Between-Subjects Factors

		Value Label	N
GROUP	1		6
	2		6
	3		6
	4		6
	5		6
	6		6
Sterility	1	sterile	18
	2	nonsterile	18

Descriptive Statistics

Dependent Variable: Max. FORCE

GROUP	Sterility	Mean	Std. Deviation	N
1	sterile	72,90333333	1,339937810	3
	nonsterile	54,58333333	16,836122871	3
	Total	63,74333333	14,655610075	6
2	sterile	39,54000000	11,965466978	3
	nonsterile	40,95333333	24,645454618	3
	Total	40,24666667	17,344381991	6
3	sterile	28,92333333	9,963635548	3
	nonsterile	55,16333333	25,248949153	3
	Total	42,04333333	22,389164046	6
4	sterile	50,84333333	27,972576451	3
	nonsterile	41,51000000	7,242209608	3
	Total	46,17666667	18,976279579	6
5	sterile	34,75333333	9,887721342	3
	nonsterile	35,65666667	7,318089459	3
	Total	35,20500000	7,795728959	6
6	sterile	31,80000000	6,024275890	3
	nonsterile	36,32000000	5,582320306	3
	Total	34,06000000	5,754198467	6
Total	sterile	43,12722222	19,401541723	18
	nonsterile	44,03111111	16,221172761	18
	Total	43,57916667	17,630849323	36

Levene's Test of Equality of Error Variances^{a,b}

Levene Statistic	df1	df2	Sig.
------------------	-----	-----	------

Max. FORCE	Based on Mean	2,711	11	24	,020
	Based on Median	,859	11	24	,588
	Based on Median and with adjusted df	,859	11	10,843	,597
	Based on trimmed mean	2,535	11	24	,027

Tests the null hypothesis that the error variance of the dependent variable is equal across groups.^{a,b}

a. Dependent variable: Max. FORCE

b. Design: Intercept + GROUP + Sterility + GROUP * Sterility

Tests of Between-Subjects Effects

Dependent Variable: Max. FORCE

Source	Type III Sum of Squares	df	Mean Square	F	Sig.
Corrected Model	5227,050 ^a	11	475,186	2,018	,073
Intercept	68369,176	1	68369,176	290,285	,000
GROUP	3525,277	5	705,055	2,994	,031
Sterility	7,353	1	7,353	,031	,861
GROUP * Sterility	1694,419	5	338,884	1,439	,247
Error	5652,590	24	235,525		
Total	79248,815	36			
Corrected Total	10879,640	35			

Tests of Between-Subjects Effects

Dependent Variable: Max. FORCE

Source	Partial Eta Squared
Corrected Model	,480
Intercept	,924
GROUP	,384
Sterility	,001
GROUP * Sterility	,231
Error	
Total	
Corrected Total	

a. R Squared = ,480 (Adjusted R Squared = ,242)

Estimated Marginal Means

1. GROUP

Estimates

Dependent Variable: Max. FORCE

GROUP	Mean	Std. Error	95% Confidence Interval	
			Lower Bound	Upper Bound
1	63,743	6,265	50,812	76,674
2	40,247	6,265	27,316	53,178
3	42,043	6,265	29,112	54,974
4	46,177	6,265	33,246	59,108
5	35,205	6,265	22,274	48,136
6	34,060	6,265	21,129	46,991

Pairwise Comparisons

Dependent Variable: Max. FORCE

(I) GROUP	(J) GROUP	Mean Difference (I-J)	Std. Error	Sig. ^b	95% Confidence Interval for Difference ^b	
					Lower Bound	Upper Bound
1	2	23,497	8,860	,209	-5,374	52,368
	3	21,700	8,860	,330	-7,171	50,571
	4	17,567	8,860	,885	-11,304	46,438
	5	28,538	8,860	,055	-,333	57,409
	6	29,683*	8,860	,040	,812	58,554
2	1	-23,497	8,860	,209	-52,368	5,374
	3	-1,797	8,860	1,000	-30,668	27,074
	4	-5,930	8,860	1,000	-34,801	22,941
	5	5,042	8,860	1,000	-23,829	33,913
	6	6,187	8,860	1,000	-22,684	35,058
3	1	-21,700	8,860	,330	-50,571	7,171
	2	1,797	8,860	1,000	-27,074	30,668
	4	-4,133	8,860	1,000	-33,004	24,738
	5	6,838	8,860	1,000	-22,033	35,709
	6	7,983	8,860	1,000	-20,888	36,854
4	1	-17,567	8,860	,885	-46,438	11,304
	2	5,930	8,860	1,000	-22,941	34,801
	3	4,133	8,860	1,000	-24,738	33,004
	5	10,972	8,860	1,000	-17,899	39,843
	6	12,117	8,860	1,000	-16,754	40,988
5	1	-28,538	8,860	,055	-57,409	,333
	2	-5,042	8,860	1,000	-33,913	23,829
	3	-6,838	8,860	1,000	-35,709	22,033
	4	-10,972	8,860	1,000	-39,843	17,899

	6	1,145	8,860	1,000	-27,726	30,016
6	1	-29,683*	8,860	,040	-58,554	-,812
	2	-6,187	8,860	1,000	-35,058	22,684
	3	-7,983	8,860	1,000	-36,854	20,888
	4	-12,117	8,860	1,000	-40,988	16,754
	5	-1,145	8,860	1,000	-30,016	27,726

Based on estimated marginal means

*. The mean difference is significant at the ,05 level.

b. Adjustment for multiple comparisons: Bonferroni.

Univariate Tests

Dependent Variable: Max. FORCE

	Sum of Squares	df	Mean Square	F	Sig.	Partial Eta Squared
Contrast	3525,277	5	705,055	2,994	,031	,384
Error	5652,590	24	235,525			

The F tests the effect of GROUP. This test is based on the linearly independent pairwise comparisons among the estimated marginal means.

2. GROUP * Sterility

Dependent Variable: Max. FORCE

GROUP	Sterility	Mean	Std. Error	95% Confidence Interval	
				Lower Bound	Upper Bound
1	sterile	72,903	8,860	54,616	91,190
	nonsterile	54,583	8,860	36,296	72,870
2	sterile	39,540	8,860	21,253	57,827
	nonsterile	40,953	8,860	22,666	59,240
3	sterile	28,923	8,860	10,636	47,210
	nonsterile	55,163	8,860	36,876	73,450
4	sterile	50,843	8,860	32,556	69,130
	nonsterile	41,510	8,860	23,223	59,797
5	sterile	34,753	8,860	16,466	53,040
	nonsterile	35,657	8,860	17,370	53,944
6	sterile	31,800	8,860	13,513	50,087
	nonsterile	36,320	8,860	18,033	54,607

3. Sterility

Estimates

Dependent Variable: Max. FORCE

Sterility	Mean	Std. Error	95% Confidence Interval	
			Lower Bound	Upper Bound
sterile	43,127	3,617	35,662	50,593
nonsterile	44,031	3,617	36,565	51,497

Pairwise Comparisons

Dependent Variable: Max. FORCE

(I) Sterility	(J) Sterility	Mean Difference (I-J)	Std. Error	Sig. ^a	95% Confidence Interval for Difference ^a	
					Lower Bound	Upper Bound
sterile	nonsterile	-,904	5,116	,861	-11,462	9,654
nonsterile	sterile	,904	5,116	,861	-9,654	11,462

Based on estimated marginal means

a. Adjustment for multiple comparisons: Bonferroni.

Univariate Tests

Dependent Variable: Max. FORCE

	Sum of Squares	df	Mean Square	F	Sig.	Partial Eta Squared
Contrast	7,353	1	7,353	,031	,861	,001
Error	5652,590	24	235,525			

The F tests the effect of Sterility. This test is based on the linearly independent pairwise comparisons among the estimated marginal means.

Post Hoc Tests

GROUP

Homogeneous Subsets

Max. FORCE

Ryan-Einot-Gabriel-Welsch Range^a

GROUP	N	Subset	
		1	2
6	6	34,06000000	
5	6	35,20500000	
2	6	40,24666667	40,24666667
3	6	42,04333333	42,04333333

4	6	46,17666667	46,17666667
1	6		63,74333333
Sig.		,653	,092

Means for groups in homogeneous subsets are displayed.

Based on observed means.

The error term is Mean Square(Error) = 235,525.

a. Alpha = ,05.

6. CURRICULUM VITAE

Credentials

Name, Surname: Deniz Sarp

Place of Birth: Ankara, Turkey

Marital Status: Married

E-mail: deniz.ozdil1@gmail.com

Address: Dodurga Mahallesi, Tepe Çalışanları Sitesi, 11/5 no.13 Çankaya Ankara

Education

B: Bachelors: B Mechanical Engineering (Bioengineering) Hons II / B Medical Science (2011)

MsC.: Masters: MSc Bioengineering (2018)

Foreign Languages

English

Work Experience

1. Biomedical Design Engineer – IonCorp Pty Ltd 06/2011-02/2012
2. Biomedical Design Engineer – Cryptych Pty Ltd 02/2012-08/2013
3. Technical Director – BMT Calsis Sağlık Teknolojileri Ticaret A.Ş 11/2013 – 03/2017
4. Company Director - Mekoptronik Mekanik Elektronik ve Optik Sistemleri Ltd Şti 3/2017 – 3/2018
5. Regulatory Affairs Specialist - Inofab Health Technologies Pty Ltd 3/2018 – current

Areas of Experience

Biomedical product design and manufacturing, project management, intellectual property, 3D modelling and analysis of orthopaedic implants.

Projects and Budgets

-

Publications

Book Chapters

1. Ozdil D, Aydin HM, Stem Cell Based Medicinal Products: Regulatory Perspectives (Chapter 11, page 321-340). In Advanced Surfaces in Stem Cell Research, WileyScrivener Publishing LLC, USA, ISBN: 978-1-119-24250-5, 2016.
2. Ozdil D, Wimpenny I, Aydin HM, Yang Y, Biocompatibility of Biodegradable Medical Polymers (Chapter 13, page 379-414). In Science and Principles of Biodegradable and Bioresorbable Medical Polymers: Materials and Properties, Elsevier Inc., UK, ISBN: 9780081003725, 2016.

Articles

1. Ozdil D & Aydin HM, Polymers for Tissue Engineering Applications, Review, 2014, Journal of Chemical Technology and Biotechnology – DOI: 10.1002/jctb.45.
2. Sahan S et al., Polyurethane-Ceramic Matrices as Orbital Implants, 2017, International Journal of Artificial Organs
3. Sahan S et al., Polyurethane/Tricalcium Phosphate Bone Adhesives and Substitutes for Load Bearing Applications, 2017, Journal of Biomaterials and Tissue Engineering, DOI: 10.1166/jbt.2017.1585.
4. Yucekul A et al., Tri-Layered Composite Plug for the Repair of Osteochondral Defects, 2017, Journal of Tissue Engineering

Patents

1. COMPOSITIONS AND METHODS FOR DETECTING ANASTOMOSIS LEAKAGE - WO2014007821 (A1) – 09.01.2014
2. ULTRASOUND BASED ANTIGEN BINDING DETECTION - WO2014003709 (A1) – 03.01.2014
3. DIVERTICULUM TREATING DEVICE - WO/2014/178869 - 06.11.2014
4. ORTHOPEDIC STIFFENING DEVICE - WO/2015/142320 - 24.09.2015
5. MENISCUS HORN RELOCATION DEVICE AND METHOD - US 2016/0174962 A1 – 23.06.2016

Oral and Poster Presentations

-



HACETTEPE UNIVERSITY
GRADUATE SCHOOL OF SCIENCE AND ENGINEERING
THESIS ORIGINALITY REPORT

HACETTEPE UNIVERSITY
GRADUATE SCHOOL OF SCIENCE AND ENGINEERING
TO THE DEPARTMENT OF BIOENGINEERING

Date 6/9/18

Thesis Title / Topic: DEVELOPMENT OF BETA-TRICALCIUM PHOSPHATE BASED INJECTABLE SYNTHETIC BONE GRAFT MATERIALS

According to the originality report obtained by my thesis advisor by using the *Turnitin* plagiarism detection software and by applying the filtering options stated below on 1/9/18 for the total of 120 pages including the a) Title Page, b) Introduction, c) Main Chapters, d) Conclusion sections of my thesis entitled as above, the similarity index of my thesis is 10 %.

Filtering options applied:

1. Bibliography/Works Cited excluded
2. Quotes excluded
3. Match size up to 5 words excluded

I declare that I have carefully read Hacettepe University Graduate School of Science and Engineering Guidelines for Obtaining and Using Thesis Originality Reports; that according to the maximum similarity index values specified in the Guidelines, my thesis does not include any form of plagiarism; that in any future detection of possible infringement of the regulations I accept all legal responsibility; and that all the information I have provided is correct to the best of my knowledge.

I respectfully submit this for approval.

06.09.2018

Name Surname: DENİZ SARP

Student No: N14327364

Department: BIOENGINEERING

Program: POST GRADUATE

Status: Masters Ph.D. Integrated Ph.D.

ADVISOR APPROVAL

APPROVED.

ASSOC. PROF. HALİL MURAT AYDIN